






Universitat Autònoma de Barcelona

ADVERTIMENT. L'accés als continguts d'aquesta tesi queda condicionat a l'acceptació de les condicions d'ús establertes per la següent llicència Creative Commons:  http://cat.creativecommons.org/?page_id=184

ADVERTENCIA. El acceso a los contenidos de esta tesis queda condicionado a la aceptación de las condiciones de uso establecidas por la siguiente licencia Creative Commons:  <http://es.creativecommons.org/blog/licencias/>

WARNING. The access to the contents of this doctoral thesis it is limited to the acceptance of the use conditions set by the following Creative Commons license:  <https://creativecommons.org/licenses/?lang=en>



Universitat Autònoma de Barcelona

Improved and efficient therapy of acromegaly by implementation of a personalized and predictive algorithm including molecular and clinical information

PhD thesis by:

Joan Gil Ortega

Thesis supervisors:

Prof. Manel Puig Domingo

Dr. Mireia Jordà Ramos

Tutor:

Prof. Manel Puig Domingo

Doctoral Program in Medicine. Department of Medicine.

2020



Acknowledgments

M'agradaria agrair amb aquestes línies a les persones que han fet possible aquesta tesi, tant directament com indirectament. D'aquest període de la meva vida m'emporto moltes i bones experiències, grans aprenentatges i fins i tot, alguna nova habilitat. Però les persones que he trobat i m'han acompanyat durant aquests anys han estat el més important al·licient i el principal record que m'enduc d'aquests anys.

I si parlem de persones no puc evitar anomenar, per contradictori que sembli, una institució, l'IGTP i l'antic IMPPC. On la primera persona que vaig conèixer va ser la meva directora de tesi Mireia Jordà que m'ha guiat durant tot aquest procés amb passió i dedicació. També vull agrair al Prof. Manel Puig per deixar-me participar en aquesta recerca tant captivadora en una malaltia tan interessant. A més a més, al IGTP he fet grans amics que sé que m'acompanyaran durant uns quants anys després d'aquesta experiència. He d'agrar a la gent del EiN les hores compartides a la Núria, la meva mestra en el laboratori, a la Bea, la Mireia, l'Helena, la Irene i tota la resta d'estudiants que han anat desfilant i que espero que els he ensenyat hagi estat profitós (especialment les minions Anna i Melania). A la gent del MAPLab i aniling, en especial a la Júlia, la Mar i la Berta per l'ajuda en moments crítics. També a les persones que he conegut durant i que hem compartit molts dies i moltes històries, en Roberto, l'Emili, l'Izaskun, la Natàlia... Els qui m'han transmès l'amor per la bicicleta: l'Iñaki, en Sergio, en Lloyd i la Tanya amb el seu taller. I com no agrair als tres mosqueters: Edu, Laura i Marc els bons moments viscuts, molts que s'han gaudit i patit alhora. A la gent d'escalada: la Carme i la Marta.

I fora de la recerca he d'agrar a la gent de la música també el suportar-me en molts moments. A les nenes del conservatori: la Vero, la Luisa, l'Ana i la Glòria. A l'Òria per fer-me de psicòloga de tant en tant. I a la meva estimada JOC que ha vegades m'ha fet anar més de cul que una altra cosa però que molts cops ha estat necessària.

També voldria agrair a la meva família el seu suport en tot moment malgrat les vicissituds viscudes, en especial a la meva mare ja que aguantar a un fill fent el doctorat no és fàcil i els meus avis. Als meus professors de tots aquests anys, especialment a en Pep Lloreta, i a la gent del PRBB. I finalment, als amics de la UPF que alguns ja han passat pel tràngol del doctorat en especial a la Natàlia i a la Mònica.

Moltes gràcies a tots.

Abbreviations

ACC	accuracy
ACTH	adrenocorticotrop hormone; also adrenocorticotropin or corticotropin
AIP	aryl hydrocarbon receptor interacting protein
ARRB1	arrestin-beta 1
ARRB2	arrestin-beta 2
ATG	autogel
AUC	area under the curve
BMI	body mass index
cAMP	cyclic adenosine monophosphate
CDH1	E-cadherin; cadherin 1
CDH2	N-cadherin; cadherin 2
cDNA	complementary DNA
CI	confidence interval
CpG	cytosine nucleotide is followed by a guanine nucleotide in the linear sequence
CR	complete responders to SRLs chorionic somatomammotropin hormone 1; also known as human placental
CSH1	lactogen
CSH2	chorionic somatomammotropin hormone 2
CSHL1	chorionic somatomammotropin hormone like 1
CV	coefficient of variation
DA	dopamine agonists
DNA	deoxyribonucleic acid
DRD1	dopamine receptor D1
DRD2	dopamine receptor D2
DRD5	dopamine receptor D5
EMT	epithelial-mesenchymal transition
ERK1	mitogen-activated protein kinase 3, extracellular signal-regulated kinase 1
ERK2	mitogen-activated protein kinase 1, extracellular signal-regulated kinase 2
ESRP1	epithelial splicing regulator 1
FC	fold change

FFAs	free fatty acids
FIPA	familial isolated pituitary adenoma
FSH	follicle-stimulating hormone
GH	growth hormone or somatotropin
GH1	growth hormone 1; pituitary growth hormone
GH2	growth hormone 2
GHR	growth hormone receptor
GHRH	growth hormone-releasing hormone, also known as somatocrinin
GHRHR	growth-hormone-releasing hormone receptor
GHRL	ghrelin
GHSR1a	growth hormone secretagogue receptor 1A
	guanine nucleotide binding protein (G protein), alpha stimulating activity
GNAS	polypeptide 1
GUSB	glucuronidase beta
HBP	high blood pressure
HPRT1	hypoxanthine phosphoribosyl transferase 1
IGF-1	insulin-like growth factor 1, also called somatomedin C
IHC	immunohistochemistry
In1-GHRL	intron 1 ghrelin
IRS-1	insulin receptor substrate 1
JAK2	Janus kinase 2
KLK10	kallikrein 10
LAR	long acting release
LH	luteinizing hormone, also known as lutropin
MAPK	Mitogen-Activated Protein Kinases
MEK	Dual specificity mitogen-activated protein kinase kinase
miRNA	micro RNAs
MRI	magnetic resonance imaging
MRPL19	mitochondrial ribosomal protein L19
MSH	melanocyte stimulating hormone
NeuroD4	neuronal differentiation 4
NR	non-responders to SRLs
OGTT	oral glucose tolerance test
OR	odds ratio

PCR	polymerase chain reaction
	phosphatidylethanolamine binding protein 1, also known as raf kinase inhibitory protein
PEBPB1	protein
PEG	polyethylene glycol
PGK1	phosphoglycerate kinase 1
	pituitary-specific positive transcription factor 1; POU domain, class 1, transcription factor 1
Pit1	factor 1
PLAGL1	pleiomorphic adenoma gene-like 1, also known as zinc finger 1 (ZAC1)
PR	partial responders to SRLs
PRL	prolactin, also known as lactotropin
PSMC4	proteasome 26S subunit ATPase 4
qPCR	quantitative polymerase chain reactions, also known as real time PCR
REMAH	Registro Molecular de Adenomas Hipofisarios
	phosphatidylethanolamine binding protein 1, also known as raf kinase inhibitory protein
RKIP	protein
RNA	ribonucleic acid
ROC	receiver operating characteristic
RORC	retinoic acid-related orphan receptor C
RT-qPCR	reverse transcription Qpcr
SD	standard deviation
SDS	standard deviation score
SLRs	somatostatin receptor ligands
SNAI1	snail family transcriptional repressor 1
SNAI2	snail family transcriptional repressor 2
SRIF	somatostatin; somatotropin release-inhibiting factor
SST	somatostatin
sst5TMD4	splicing variant of SSTR5 with 4 transmembrane domains
sst5TMD5	splicing variant of SSTR5 with 5 transmembrane domains
SSTR1	somatostatin receptor 1
SSTR2	somatostatin receptor 2
SSTR3	somatostatin receptor 3
SSTR4	somatostatin receptor 4
SSTR5	somatostatin receptor 5
SSTRs	somatostatin receptors

STAT1	signal transducer and activator of transcription 1
STAT5	signal transducer and activator of transcription 5
TBP	TATA-Box Binding Protein
TGF- β	transforming growth factor beta
TSH	thyroid-stimulating hormone, also known as thyrotropin
TWIST1	twist family bHLH transcription factor 1
VIM	vimentin
VIP	secretin; vasoactive intestinal peptide

Contents

Section	Page
Acknowledgments	1
Abbreviations	2
Abstract	8
Resum	9
1. Introduction	10
1.1 The Pituitary Gland	10
1.1.1 Anatomy and histology	10
1.1.2 Somatotroph cells and growth hormone	11
1.1.3 GH regulation	11
1.1.4 Peripheral GH actions	13
1.2 Acromegaly	14
1.2.1 History of acromegaly	14
1.2.2 Epidemiology	14
1.2.3 Pathogenesis	15
1.2.4 Diagnosis	16
1.2.5 Clinical Manifestations	17
1.3 Treatment of Acromegaly	18
1.3.1 Surgery	18
1.3.2 Radiation treatment	19
1.3.3 Dopamine agonist	19
1.3.4 Somatostatin receptor ligands (SRLs)	19
1.3.5 Pegvisomant	21
1.3.6 Choice of therapy	22
1.4 Clinical and molecular predictors to medical therapy response	23
1.5 Personalized medicine in acromegaly	27
2. Hypotheses	29
3. Objectives	30
4. Material and methods	31
4.1 Patients	32
4.2 Biochemical and hormonal assays	32
4.3 Bioethical statement	33
4.4 DNA and RNA isolation	33
4.5 Retrotranscription	33
4.6 Quantitative polymerase chain reaction	33
4.6 <i>GNAS</i> sequencing	35
4.7 E-cadherin promoter methylation assessment	35
4.8 Standard Statistical Analysis	38
4.9 Data mining analyses	39
5. Results	45
5.1 Study 1: Molecular profiling for acromegaly treatment: a validation study	46
5.2 Study 2: Association of Epithelial-mensenchymal transition (EMT) markers with response to somatostatin receptor ligands	

in GH-secreting tumors	58
5.3 Study 3: Molecular determinants of enhanced response to somatostatin receptor ligands after debulking in large GH producing adenomas	66
5.4 Study 4: Data mining analyses for precision medicine in acromegaly	72
6. Discussion	81
7. Conclusions	91
8. Future perspective	92
9. Bibliography	95
10. Annex	118
10.1 Supplementary Tables	118
10.2 Supplementary Figures	122

Abstract

Actual pharmacologic treatment in acromegaly is currently based upon assay-error strategy. The prompt biochemical control of the disease is essential to reduce comorbidities and mortality. Fortunately, several drugs have been developed over the years to treat acromegaly being first generation somatostatin receptor ligands (SRLs), the first-line treatment. However, up to 50% of patients do not respond adequately to SRLs, which delays biochemical control for months or even a year. The main objective of this thesis was to evaluate the potential usefulness of different molecular markers as predictors of response to SRLs and elaborate a new treatment algorithm accordingly. We took advantage of the REMAH cohort of several nodes in Spain to collect 100 acromegaly samples and performed molecular analysis. We measured molecular expression by RT-qPCR, measured protein by IHC and; quantified CpG methylation and evaluated mutations by sanger sequencing. Furthermore, we were able to stratify the SRLs respond in the majority of the cases and collected clinical associated data too. Taking all that into account, we have been able to validate reported biomarkers (*SSTR2*, Ki-67, E-cadherin and *RORC*) associated to SRLs response, describe the association of the epithelial-mesenchymal transition and SRLs in somatotropinomas, molecularly characterize the SRLs improvement after tumor debulking in large GH-producing tumors and define treatment algorithm based on molecular expression through data mining approaches. We conclude presenting treatment algorithms for new diagnosed acromegaly patients that will benefit from personalized medicine using IHC or more complex RNA quantification approaches to overcome the assay-error strategy in acromegaly treatment.

Resum

El tractament farmacològic actual de l'acromegàlia està basat en el mètode de prova i error. En aquesta malaltia, un control bioquímic ràpid és decisiu per evitar comorbiditats i reduir la mortalitat. Afortunadament, avui en dia tenim diversos tractaments farmacològics amb els lligands del receptor de la somatostatina (LRS) de primera generació com a primera línia farmacològica. Tanmateix més del 50% dels pacients no aconsegueixen controlar els nivells hormonals amb els LRS la qual cosa pot arribar a endarrerir el control bioquímic de la malaltia durant mesos o fins i tot més d'un any. El principal objectiu d'aquesta tesis és l'avaluació de la potencial utilitat dels diferents marcadors de resposta a LRS i la consegüent elaboració d'un nou algoritme de tractament amb aquests marcadors. Fent ús de diversos nodes de la cohort REMAH arreu d'Espanya, vam obtenir 100 mostres tumorals d'acromegàlia en les quals vam realitzar anàlisis moleculars. A més a més, vam caracteritzar la resposta a LRS en la majoria dels casos i les dades clíniques associades a aquests pacients. Amb tot això vam ser capaços de validar biomarcadors prèviament reportats (*SSTR2*, Ki-67, E-cadherin i *RORC*), descriure l'associació entre el fenomen de transició epiteli-mesènquima i la resposta a LRS en aquests tumors productors d'hormona del creixement, caracteritzar molecularment la millora de l'efecte dels LRS després de cirurgia parcial en tumors grans i invasius, i finalment, definir algoritmes de tractament personalitzats en funció de l'expressió de diversos gens i situacions clíniques. Concloem aquest estudi doncs proposant nous algoritmes de tractament basats en la medicina predictiva i personalitzada per a nous casos d'acromegàlia utilitzant tècniques de quantificació del RNA o immunohistoquímica per tal superar l'estratègia de tractament de prova i error.

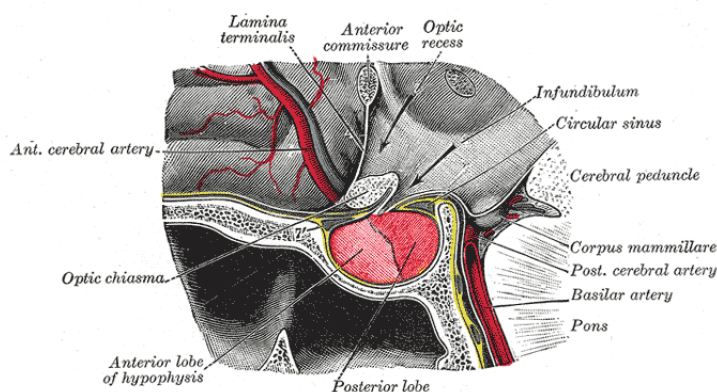
1. Introduction

1.1 The pituitary gland

1.1.1 Anatomy and histology

The pituitary gland, also called hypophysis, can be considered a master regulator of the endocrine system due to its central role in many physiological and essential functions such as growth, blood pressure, metabolism, stress response and all functions of sex organs (1). The pituitary gland possesses a bean-shaped structure and lies within the sella turcica, a saddle-shaped depression in the sphenoid bone, close to the optic chiasm (Figure 1). The gland is connected to the hypothalamus through the pituitary stalk, a portal system. The pituitary weighs 0.5 gram approximately and consists of three lobes that are functionally and anatomically distinct (2). The posterior lobe or neurohypophysis contains a large collection of hypothalamic axonal projections and secretes oxytocin and vasopressin directly to the blood (3). The intermediate lobe or pars intermedia is the border between the anterior and posterior lobes of the pituitary and produces melanocyte stimulating hormone (*MSH*). However, the pars intermedia regresses at the 15th week of gestation and is either very small or absent in adults (4). Finally, the anterior lobe or adenohypophysis contains five types of endocrine cells which produce and secrete the following hormones: the gonadotrophs secrete the gonadotrophins luteinizing hormone (*LH*) and follicle-stimulating hormone (*FSH*); the corticotrophs, adrenocorticotrophin (*ACTH*); the lactotrophs, prolactin (*PRL*); the thyrotrophs, thyroid-stimulating hormone (*TSH*); and the somatotrophs produce growth hormone (*GH*) and eventually prolactin (*PRL*) as well (1).

Figure 1.



Anatomical localization of the pituitary gland. Henry Gray (1918) *Anatomy of the Human Body*

The different cell lineages of the adenohypophysis may give rise to different types of adenomas, often associated with distinct hypersecretory syndromes (5): ACTH-secreting corticotroph adenomas result in Cushing's disease, GH-secreting somatotroph adenomas result in acromegaly, PRL-secreting lactotroph adenomas result in hyperprolactinemia, and TSH-secreting thyrotroph adenomas result in hyperthyroidism. Gonadotroph adenomas, most of them hormonally silent, lead to hypogonadism in most of the cases.

As the studies described in this thesis focus on acromegaly which is mostly caused by a GH-secreting somatotroph adenoma (also known as somatotropinoma), I will firstly introduce somatotroph cells and GH.

1.1.2 Somatotroph cells and growth hormone

Somatotroph cells constitute the predominant cell type in the anterior pituitary (about 45% of cell population) and synthesizing, storing and secreting *GH* are the defining functions of these cells. Somatotroph cells, together with lactotrophs and thyrotrophs, require Pituitary-specific positive transcription factor 1 (*Pit1*), also known as *POU1F1*, for final differentiation and the maintenance of *Pit1* expression in those cells through adulthood. *Pit1* is necessary for transcription of *GH* and growth hormone releasing hormone receptor (*GHRHR*) (6) and its expression is positively autoregulated by a distal enhancer (7). *GH* and *GHRHR* are also regulated indirectly by *Pit1* through *NeuroD4* expression (8).

The human GH gene is located in a locus containing five homologous genes, the so-called human growth hormone locus, on the long arm of chromosome 17. The genes in the cluster are growth hormone 1 (*GH1*), corresponding to the pituitary growth hormone or simply as *GH*, chorionic somatomammotropin hormone like 1 (*CSHL1*), chorionic somatomammotropin hormone 1 (*CSH1*), growth hormone 2 (*GH2*) and chorionic somatomammotropin hormone 2 (*CSH2*), from 3' to 5', respectively. The structure of these genes comprises five exons and four introns (Miller and Eberhardt, 1983). *GH* is transcribed in the adenohypophysis while the others are expressed during the gestation (10). GH circulates mainly as a 22-kDa protein consisting of 191 amino acids; however, some other spliced-variants can be found (11).

1.1.3 GH regulation

The regulation of GH is a very complex issue with several players acting at different levels. The most convoluted and unknown network of GH regulators is the neuroendocrine layer of regulation that comprises: ghrelin, kisspeptin neuropeptidases, leptin, dopamine, orexin, gastrointestinal neuropeptides, among others (12).

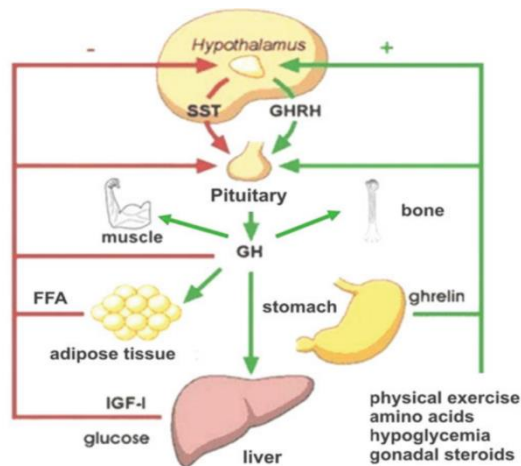
Ghrelin is mainly secreted to the blood by neuroendocrine cells of the gastrointestinal tract, and it has been called the "hunger hormone" because it stimulates appetite (13). It is also expressed in the arcuate nucleus of the hypothalamus and the pituitary (14). It is an endogenous ligand of the GH secretagogue receptor type 1a (GHSR1a) and stimulates pituitary GH secretion. Inversely, GH inhibits ghrelin secretion (15,16).

At the hypothalamic level, GH secretion is positively regulated through the GH releasing hormone (GHRH) and negatively through somatostatin (SST), also known as somatotropin release-inhibiting factor (SRIF) (12). GHRH is released from neurosecretory axons of the hypothalamic arcuate nucleus, and arrives to the anterior pituitary gland through the portal system. This molecule shows a structural homology with neuroendocrine gut peptides like glucagon, secretin or vasoactive intestinal peptide (VIP) that also stimulates GH secretion but with lower potency (12,17). GHRH binds to the GHRHR, activating a Gs protein that causes a cascade of cAMP via Adenylate cyclase (18). GHRH stimulates GH secretion and acts also at gene transcription level, activating new GH synthesis (19).

Somatostatin is synthesized in the hypothalamic periventricular nuclei, the pancreatic islets, gastrointestinal, neural and epithelial cells. The plasma half-life of somatostatin is about 2 minutes and it inhibits GH, ACTH and TSH release at the pituitary, and insulin and glucagon at the pancreatic islet (20,21). Somatostatin receptors 1 to 5 (SSTR1-5) are specific membrane high-affinity receptors for somatostatin (22). Somatostatin suppresses GH release but not GH biosynthesis (19). GHRH and somatostatin interact to regulate GH secretion to generate pulsatile GH release (23).

The GH also has an autoregulation loop, promoting somatostatin secretion and desensitizing from GHRH effects. Somatostatin and GHRH also regulate its own secretion (Bilezikjian et al., 1986; Peterfreund and Vale, 1984; Rosenthal et al., 1986; Ross et al., 1987; Sheppard et al., 1978) (Figure 2). Moreover, a wide range of physiological factors modify GH secretion like age, gender, sleep, exercise, stress, and nutritional and metabolic factors (12,29).

Figure 2.

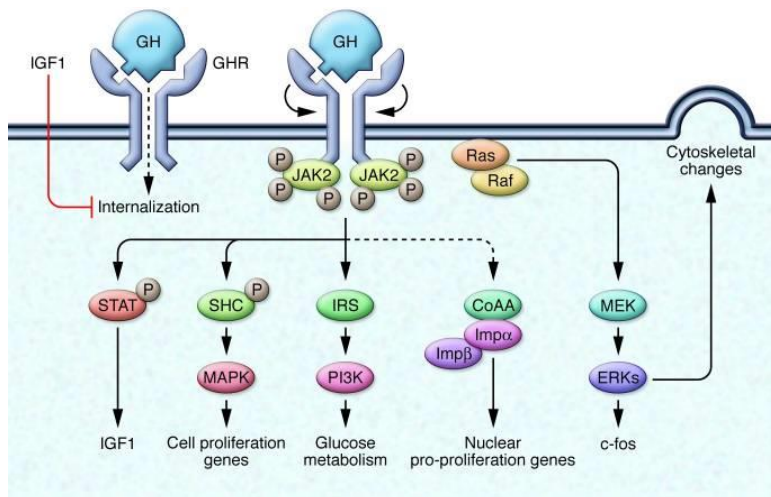


Central and peripheral GH regulation. SST: Somatostatin. GHRH: Growth Hormone Realising Hormone. GH: Growth Hormone. FFA: Free Fatty Acids. *R. Coutant, N. Bouhours-Nouet. Endocrine Control and Regulation of Growth Hormone: An Overview.*

1.1.4 Peripheral GH actions

The GH binds to the GH receptor (GHR) inducing its dimerization and transducing the signal through the JAK/STAT pathway, mainly involving JAK2, STAT1 and STAT5 (30,31). Other GH actions are mediated by MAPK pathway, IRS-1 and c-fos; and promote insulin synthesis, cytoskeleton changes and cell proliferation (12). The GHRs are located mainly in the liver and some peripheral tissues like muscle or fat, which present less amount of the receptor (30). GH also induces differentiation and growth factor IGF-1 secretion that also regulates GH through a negative feedback loop (32). (Figure 3).

Figure 3.



GH binds a dimerized GHR resulting in JAK2 phosphorylation. GH targets include IGF-1, c-fos, cell proliferation genes, glucose metabolism, and cytoskeletal proteins. The dotted lines referred to GHR internalization and translocation that induces pro-proliferation genes in the nucleus via importin α/β . IGF-1 could inhibit this last process. *Melmed S. Acromegaly pathogenesis and treatment. J Clin Invest 2009*

The IGF-1 gene is GH-independently expressed in mesenchymal cells and fetal connective tissue whereas in adult liver, lung, pancreas and heart, the major regulator of IGF-1 is GH (33). IGF-1 ubiquity favors its endocrine function as well as a paracrine/autocrine function (34). Other stimulators of IGF-1 paracrine function are ACTH, TSH and LH in their respective target tissues

(35,36). The nutritional status is also an important regulator of IGF-1 (37). The majority of IGF-1 biological actions are mediated by the IGF-1 receptor, a cell surface tyrosine kinase, very similar to the insulin receptor (Jones and Clemmons, 1995). IGF-1 is secreted associated with high-affinity circulating IGF-binding proteins (IGFBPs), which determine the availability of free IGF-1. These binding proteins are cysteine enriched proteins with a high affinity to IGF-1 and are also hormonally regulated (39).

Due to the GH involvement in the regulation of many physiological processes, such as glucose, lipid and bone metabolism, growth, reproduction, osmoregulation and the immune system regulation, it is considered a pleiotropic hormone (12). It possesses both anabolic and catabolic actions. GH is a catabolic hormone with low IGF-1 levels during fasting but becomes anabolic in the presence of IGF-1 after food intake as IGF-1 mediates GH anabolic functions (40,41). The most important anabolic action is the stimulation of cellular differentiation and growth, while catabolic actions of GH come from its lipolytic effects and the inhibition on lipogenesis which results in elevated free fatty acids (FFAs) (42–44). Interestingly, GH and IGF-1 display opposing roles on insulin homeostasis. Whereas GH counter-regulates the effects on insulin, IGF-1 promotes insulin sensitivity (45).

1.2 Acromegaly

1.2.1 History of acromegaly

Acromegaly is a stunning disease of disordered somatic growth and has intrigued clinician for centuries. Nonetheless, it was in 1886 when the neurosurgeon Pierre Marie published the first clinical description of the disease and his recognition of five other cases previously described (46). The term “acromegaly” is from Greek meaning “large extremities” and was forged by Pierre Marie himself. However, there are clinical reports of this disease from many centuries ago (47,48). In 1900, Carl Benda discovered that pituitary adenomas comprised of mainly adenohypophyseal eosinophilic cells are the cause of acromegaly (49). Harvey Cushing and colleagues introduced the terminologies “hyperpituitarism” and “hypopituitarism” and demonstrated clinical remission of signs of acromegaly after surgical resection of pituitary tumors (Cushing, 1909, 1912; Davidoff, 1926), helping to establish the link between a hyperfunctioning adenoma, in particular the hypersecretion of GH and the disease.

1.2.2 Epidemiology

According to a recent meta-study, the annual incidence rate of acromegaly ranges between 0.2 and 1.1 cases/100,000 people and the total prevalence ranges between 2.8 - 13.7 cases per 100,000 people. Many cases go unreported for years due to the insidious presentation and the

lack of awareness of acromegaly among physicians. The median age at diagnosis is in the fifth decade of life with a median diagnostic delay of 4.5–5 years (53). In Spain, the diagnostic delay is even bigger, 50% of patients refers more than 9 years of delay since the beginning of symptoms (54).

1.2.3 Pathogenesis

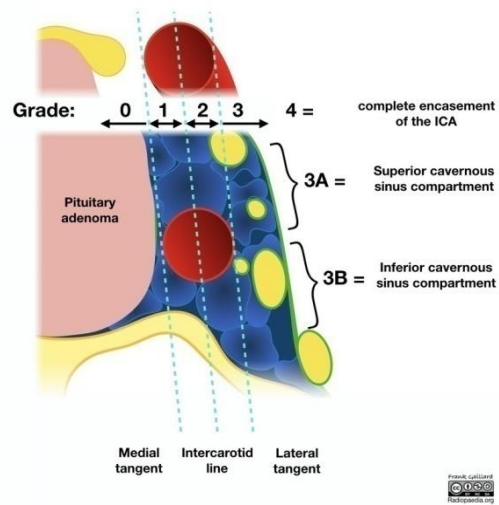
The cause of acromegaly is mainly a pituitary tumor (>95%) (55). But, the disorder is caused by elevated levels of GH and IGF-1 regardless of the etiology (56). Histologically, these tumors contain either densely (slow growing) or sparsely (rapidly growing) staining cytoplasmic GH granules (57). There are also mixed GH-PRL cell adenomas that can be composed by two different cell types or by single mature cell expressing both GH and PRL (58). The tumors composed by the two cells types are usually invasive and rapidly growing, and hyperprolactinemia may be the predominant feature. Little correlation has been proved between blood hormone levels and hormone staining (Akirov et al., 2019).

Although, there are locally invasive somatotropinomas that could be aggressive, without a proof of distant metastases these tumors are considered benign adenomas (60). Nonetheless, the occurrence of such metastases is extremely rare (61). Invasive pituitary macroadenomas represent an intermediate form between well-circumscribed adenomas and carcinomas.

Pituitary adenomas can be classified according to their invasive growth in the sella turcica. The current classification using magnetic resonance imaging is the Knosp classification (62,63). This classification is based in four grades, Grade 0 representing a healthy pituitary, and Grade 4 corresponding to the total encasement of the intracavernous carotid artery (Figure 4). According to this classification, surgically proven invasion of the cavernous sinus space is present in all Grade 4 and Grade 3 cases and in some of the Grade 2 cases; no invasion is present in Grade 0 and Grade 1 cases. Therefore, the critical area where invasion of the cavernous sinus space becomes very likely and can be proven surgically is located between the intercarotid line and the lateral tangent, which is represented by Grade 2.

Figure 4.

Knosp classification



Knosp grading system for showing invasion of cavernous sinus by pituitary macroadenomas. The more laterally an adenoma grows and encircles the internal carotid artery (ICA), the more invasive the tumor is and, therefore a higher grade level is assigned. Source: <https://radiopaedia.org/cases/knosp-classification-diagrams>

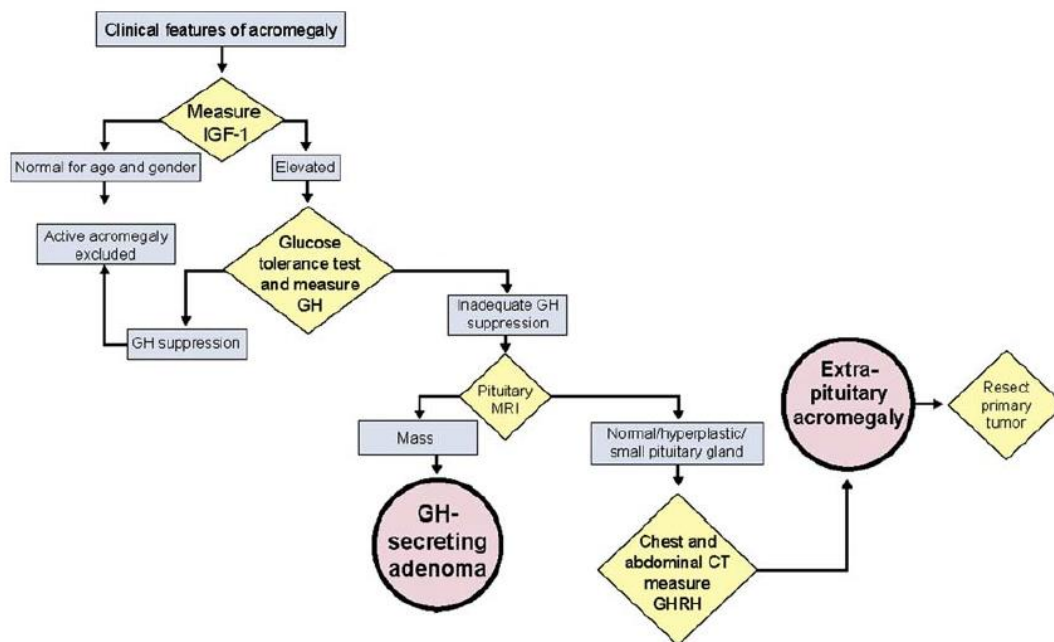
Somatotropinomas, as all neuroendocrine tumors, show an intrinsic heterogeneity (64), ranging from small localized microadenomas with limited biochemical activity to large invasive highly active macroadenomas. Interestingly, applying cluster analysis of clinical, histopathological, and radiological characteristics to 242 acromegaly patients Cuevas-Ramos et al. were able to classify acromegaly patients into three groups associated with different clinical outcomes (65):

- Type 1: the most common, old patients, densely granulated small tumor with abundant somatostatin receptor 2 (*SSTR2*).
- Type 2: the rarest, noninvasive, densely or sparsely granulated macroadenomas.
- Type 3: young patients, sparsely granulated, larger and invasive microadenomas with low *SSTR2*.

1.2.4 Diagnosis

To properly diagnose acromegaly, a demonstration of autonomous hypersecretion of GH and high levels of IGF-1 must be done. Due to the short half-life of GH and its pulsatility, a single random GH measure is not recommended (66). On the other hand, serum IGF-1 levels are stable (15 hours half-life), regardless of food intake or time of the day and, show a logarithmic correlation with GH (67). Normal IGF-1 levels adjusted by age exclude acromegaly diagnosis. In some cases, the lack of suppression of GH ($< 1 \mu\text{g/l}$) following an oral glucose tolerance test (OGTT) is necessary to confirm the diagnosis of acromegaly (68).

Figure 5.



Diagnosis of acromegaly. Modified from: Melmed S. Medical progress: acromegaly. N Engl J Med 2006;355(24):255873.

Advanced acromegaly patients tend to develop diabetes mellitus that can make unreliable the serum IGF-1 measures that should only be assessed when a good glycemic control has been achieved. Other processes such as hepatic or renal failures, malnutrition, systemic illnesses or the use of oral oestrogens could induce to false negative interpretation of IGF-1 levels (69,70). Furthermore, there is a remarkable variability between different IGF-1 immunoassays that has to be considered (71,72).

Finally, a contrast magnetic resonance imaging (MRI) of the pituitary to localize the tumor and asses the size, invasiveness and exact localization is mandatory. Clinicians usually distinguish between microadenomas (≤ 1 cm) and macroadenomas (≥ 1 cm) as a measure of the possible severity of the disease (73).

1.2.5 Clinical manifestations

Acromegaly manifestations are due to the local pressure effects of the pituitary tumor or peripheral actions of chronic excess of GH and IGF-1 (74).The local effects of the expanding tumor are common to all pituitary adenomas and include headache, visual dysfunction due to chiasmal compression cranial nerve palsy due to impingement of cranial nerves III, IV, and VI

causing diplopia, or nerve V leading to trigeminal facial pain. The local signs present an obvious higher preponderance in macroadenomas (> 65%) (75).

The effects of hypersomatotrophism on soft tissue growth and the extremities, as well as metabolic function, occur insidiously over lustrums (76). The more striking manifestations are altered facial appearance large fleshy nose, spade-like hands, frontal bossing or enlargement of the extremities (Nabarro, 1987). The growth of soft tissue cause a generalized visceromegaly with enlargement of bones, heart, thyroid, spleen, liver, tongue and salivary glands (78). IGF-1 causes new bone formation leading to teeth separation, frontal bossing, maxillary widening, mandibular overgrowth with prognathism, jaw malocclusion and overbite, and nasal bone hypertrophy (79). Arthropathy with painful signs of joint symptoms severe enough to impair daily activities are also very common, specially carpal tunnel syndrome (80). Oily skin and hyperhidrosis are common early signs in more than 70% of patients (81). Regarding cardiovascular manifestations, hypertension, arrhythmias, valvular disease, and sodium and fluid retention leading to expanded extracellular fluid volume are common manifestations (Berg et al., 2010; Sharma et al., 2017). These cardiovascular comorbidities are the major cause of morbidity and mortality in acromegaly (84). The tissue growing also impairs the respiratory function that contribute to sleep apnea and even narcolepsy (85,86). All these changes damage the psychological status of the patient and severely affect the quality of life (87).

Prolonged exposure to excess GH leads to the development of gastrointestinal malignancies (88). Moreover, GH and IGF-1 have complex effects on glucose metabolism. Their chronic exposure leads to diabetes mellitus through hyperinsulinaemia, insulin resistance and increased gluconeogenesis (89).

1.3 Treatment of Acromegaly

The general aim of therapy in acromegaly is to suppress hypersecretion of GH and IGF-1, consequently eliminating morbidity and reducing mortality rates (90).

1.3.1 Surgery

Transsphenoidal surgery is the primary treatment for patients with well-circumscribed somatotropinomas or for large tumors causing important local effects (91). Surgical outcome can usually be correlated with the preoperative GH and IGF-1 levels, tumor invasiveness and surgical skills of the neurosurgeon. In the cases of microadenomas or non-invasive macroadenomas, remission rates achieve about 80%. Unfortunately, for invasive tumor this rate drops to 20-30% (92,93). The success of neurosurgery is followed by a normalization of GH and

IGF-1 with a low cost compared to life-long medical therapy. However, surgery has side effects, mainly due to some sort of hypopituitarism (around 30% of cases) (94).

1.3.2 Radiation treatment

During the early 1900s radiotherapy played a central role in the management of acromegaly (95). However, nowadays is considered as the last option for acromegaly treatment in most centers. The recommendation for radiotherapy is for residual tumors if all the other therapeutic options are unsuccessful or unavailable (90). Usually, conventional radiotherapy is administered in 20-30 fractions with a total dose of 40-45 Gray and obtains a 50% remission rate at 10 year follow-up (96). Unfortunately, radiotherapy has main side-effects, such as, hypopituitarism (50 – 80%), increased mortality risk (due to cerebrovascular disease) and joint problems (97–99). Nowadays, modern stereotactic radiotherapy has strongly decreased these latter comorbidities.

1.3.3 Dopamine agonists

In 1974, it was discovered that dopaminergic stimulation, contrary to what happens in physiological condition, reduced GH secretion in acromegaly (100,101). Dopamine receptor D2 (DRD2) is the predominant receptor found on these adenomas (102,103) and until the 80s dopamine agonists (DA) were the only pharmacological agents for acromegaly treatment. The first DA was bromocriptine but it was replaced by cabergoline due to its higher efficacy and better tolerability (104). It presents a very safety profile with mild side-effects, is cheap and can be taken orally (105). However, the efficacy is relatively low on IGF-1 levels (around 30% reduction only) (90).

1.3.4 Somatostatin receptor ligands (SLRs)

Somatostatin, as explained before, is a physiological inhibitor of GH secretion. As remnant of its somatroph origin, somatotropinomas express somatostatin receptors (SSTRs), specially SSTR2 and SSTR5 (106). The first generation short acting SRLs, **octreotide** and **lanreotide**, were the first developed (107,108). Both show a high affinity for SSTR2 receptor. However, the two hour half-life of these compounds made necessary several daily injections (109). Luckily, to date long acting formulations of both octreotide (octreotide Long Acting Release-LAR) and lanreotide (lanreotide autogel-ATG) allow for weekly injections. They are equivalent in terms of safety and efficacy (110). There is also a small tumor reduction effect that makes them interesting for pituitary acromegaly (111,112). Furthermore, lanreotide ATG and octreotide LAR have a IGF-1-independent mild effect in reducing insulin secretion which makes the drugs relevant in patients with insulin resistance and diabetes (113).

SRLs are considered the first line medical acromegaly treatment (114). They present a better performance in normalizing GH and IGF-1 levels than cabergoline reaching about 50% of patients with normalized biochemistry (115,116), although large differences in biochemical response rates of SRLs have been reported (ranging between 25% - 70%), probably due in part to the heterogeneity in the definition of biochemical response (117). The criteria to define a full response to SRLs are generally similar across all studies, although with some variations in GH threshold levels, but some studies consider both parameters, IGF-1 and GH levels, as separate efficacy endpoints while others report a composite efficacy endpoint. On the other hand, some authors combine the biochemical effects with the antitumoral effects in the definition of response to SRLs, but the majority of articles lack a clear cut-off when using this criteria (116,118).

Importantly, some authors define a partial response to SRLs. This definition tries to reflect a clinical reality in which the majority of clinicians use SRLs in combination with other drugs if they consider that SRLs' effect is significant but not enough to normalize GH and IGF-1 levels.

One of the most used classifications is the one proposed by Colao et al. which defines full response to SRLs as control of GH and IGF-1 levels and 20% tumor shrinkage in patients treated first-line, or control of GH and IGF-1 levels and 20% tumor shrinkage or stabilization of tumor remnant in patients treated second-line, or no tumor on magnetic resonance imaging at baseline. They consider as partial responders those patients showing a significant decrease (50%) of GH and/or IGF-1 levels with no achievement of control levels and/or 20% tumor shrinkage in patients treated first-line or second-line. And finally, poor response or resistance to SRLs is defined as non-significant decrease of GH and IGF-1 levels with no achievement of control and no tumor shrinkage in patients treated first-line or increase in tumor size in any patient (119).

To avoid the variability over time of IGF-1 measurement, other authors use IGF-1 SD score (SDS). In this case, controlled disease or full response is considered when IGF-1 values are below 2 SDS, partial response if between 2 and 3 SDS, and non-response when greater than 3 SDS (120). SRLs have been recommended as first-line therapy in non-resectable GH-producing tumors, even if they provide biochemical control in less than 50% of cases. Therefore, enhancing SRLs response could be very useful. Several studies have proven that surgical debulking of these tumors improves SRLs response (121–125). Consequently, the current general consensus is to perform surgical debulking even if surgical cure is unlikely, both to alleviate mass effect and to improve SRLs treatment response (126–128). Improvement of SRLs response after surgical

debulking seems to be mostly related to the reduction in tumor size, but not all tumors show the same response to SRLs after this procedure, even with a similar residual tumor mass. No biological studies have been performed so far in this matter.

SRLs are also used as preoperative treatment for ameliorating comorbidities and reducing tumor volume to improve surgical outcome (56). However, a recent metaanalysis demonstrates better short-term cure rates in acromegaly patients after presurgical SRLs treatment, but its impact on the long-term results is unclear (129). This is another factor to take into account when comparing response rates to SRLs after surgery.

Pasireotide-LAR was developed as a multireceptor-targeted SRL with a superior clinical efficacy over octreotide-LAR and it is considered a second-generation SRLs (130,131). However, after several studies an expert group recently recommended a more reluctant use of pasireotide LAR. They recommended its use as a second-line therapy in young patients who show tumor growth while receiving medical therapy, monotherapy in patients with headache not responsive or intolerant to the other medical treatment, and as third-line treatment or even in combination if the other combination therapies do not control biochemical parameters or disease symptoms (132).

Pasireotide-LAR shows a great tolerability profile of intramuscular injections similar to first SRLs. However, hyperglycaemia-related adverse event is a common effect and should be carefully monitored. It is of some concern for the use of the drug, especially in patients categorized as diabetic or prediabetic at baseline (133,134).

1.3.5 Pegvisomant

Pegvisomant was discovered by John Kopchick and Wen Chen at Ohio University in 1987 and approved for the treatment of acromegaly in 2003 (135). The substitution of glycine at position 120 of the third alpha helix in binding site 2 of GH glycine by lysine blocks intracellular signaling, converting the modified GH molecule into a GHR antagonist (136). The GHR antagonist was PEGylated with polyethylene glycol (PEG) molecules, extending the half-life to about 70 hours. Currently, it is used as second line treatment for patients not controlled with first generation SRLs (90).

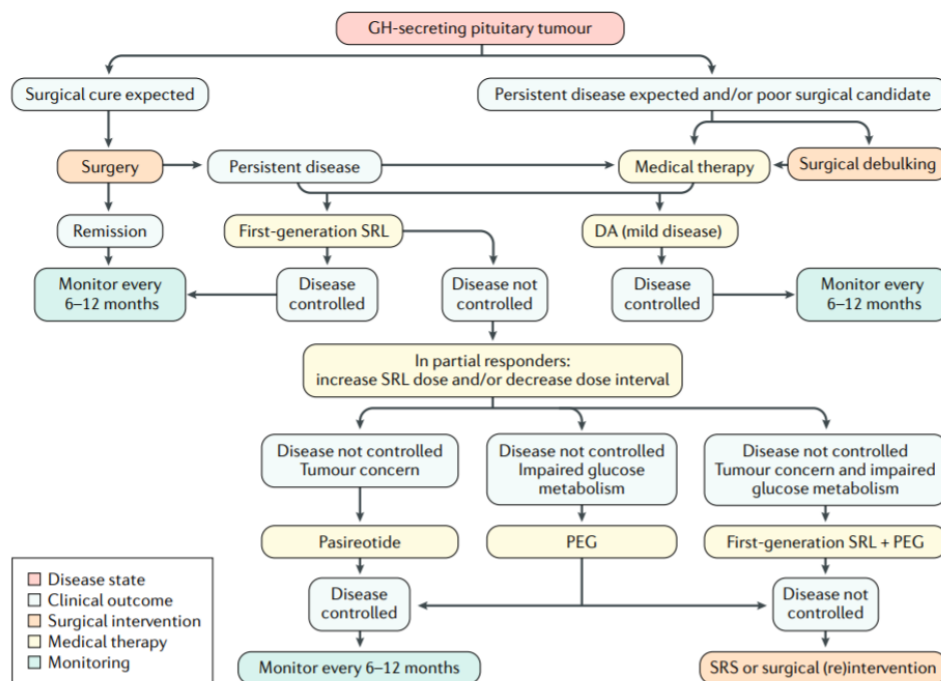
The first initial trials demonstrated over a 90% of IGF-1 normalization in patients resistant to first generation SRLs (137,138). Virtually all patients with acromegaly can be controlled with pegvisomant but, recent registries of clinical routine practice showed lower IGF-1 remission rates (60-70%) (138–141). Pegvisomant rapidly decrease IGF-1 levels in serum and rise GH levels

due to the hypothalamic feedback loop (142). Therefore, the only biochemical marker of pegvisomant performance is IGF-1.

1.3.6 Choice of therapy

With all these available therapeutic options, choosing the best of them for each patient can be difficult. The current guidelines recommend medical therapy in those cases with persistent disease after surgical resection or for patients in whom surgery is not appropriate. They recommend first generation SRLs or cabergoline as monotherapy as first line medical therapy. After that, the second line therapy would be to increase SRLs dosage or frequency of injections or add cabergoline to SRLs. In case of minimal or no response, the clinician could choose between pasireotide and pegvisomant in monotherapy; or pegvisomant in combination with SRLs. That decision depends mostly on the tumor concern and the impaired glucose metabolism (Figure 6). Finally, the last considered option is radiotherapy, surgical reintervention or, in rare aggressive tumors, temozolomide (an alkylating agent used as a treatment of some brain cancers) (90,143).

Figure 6.



Current proposed algorithm of acromegaly treatment by experts (2019). Colao, A., Grasso, L.F.S., Giustina, A. et al. *Acromegaly. Nat Rev Dis Primers* 2019

This "trial and error" approach together with additional treatment options plus the high rate failure of first generation SRLs and the primary surgery make the treatment of acromegaly patients really challenging. The delay in controlling the disease in patients that do not respond to first line treatment could be measured in years since every change in the medical treatment needs some months to be fully evaluated. Taking all this into account, it is easily understandable why many authors propose that acromegaly patients should benefit enormously of personalized medicine by using molecular analysis (144–147). In many other pathologies, there has been a shift towards individualized treatments that best match a specific patient. However, personalized medicine has not yet been established in the management of patients with acromegaly.

1.4 Clinical and molecular predictors to medical therapy response

During the last years, many studies have tried to explain why some patients do not respond to first generation SRLs. Epidemiological studies have proven that men are more resistant to first generation SRLs (65,148), especially young men (149). Clinicians also have looked for characteristics that could define non-responsive patients to SRLs. **Tumor size** is a determinant of response to SRLs, with a higher adjusted IGF-1 normalization Colao et al., 2006b). **Knosp classification** also inversely correlates with SRLs response (151)

From a pathological point of view, the evaluation of somatotropinomas by electron microscopy defines two main subtypes: **densely granulated** and **sparsely granulated**, the former being associated with a good response to SRLs. On the contrary, sparsely granulated tumors are related to no response to SRLs (59,152,153). Nowadays, the immunostaining for Cam 5.2 keratin is the most used method to identify the two subtypes. It identifies perinuclear keratin in all of the densely granulated adenomas (57).

The **T2 MRI signal** also helps to identify those somatotropinomas harboring histological densely granulated pattern (120,154). Most, if not all, densely granulated tumors show a hypointense T2 signal while the majority of sparsely granulated tumors are either isointense or hyperintense in relation to the cerebral cortex signal. The MRI signal as a predictor of response to SRLs is also useful after surgical failure and should always be considered, as surgery does not modify MRI tumor signal. A hypointense T2-weighted MRI signal was associated with a better response to SRLs specifically.

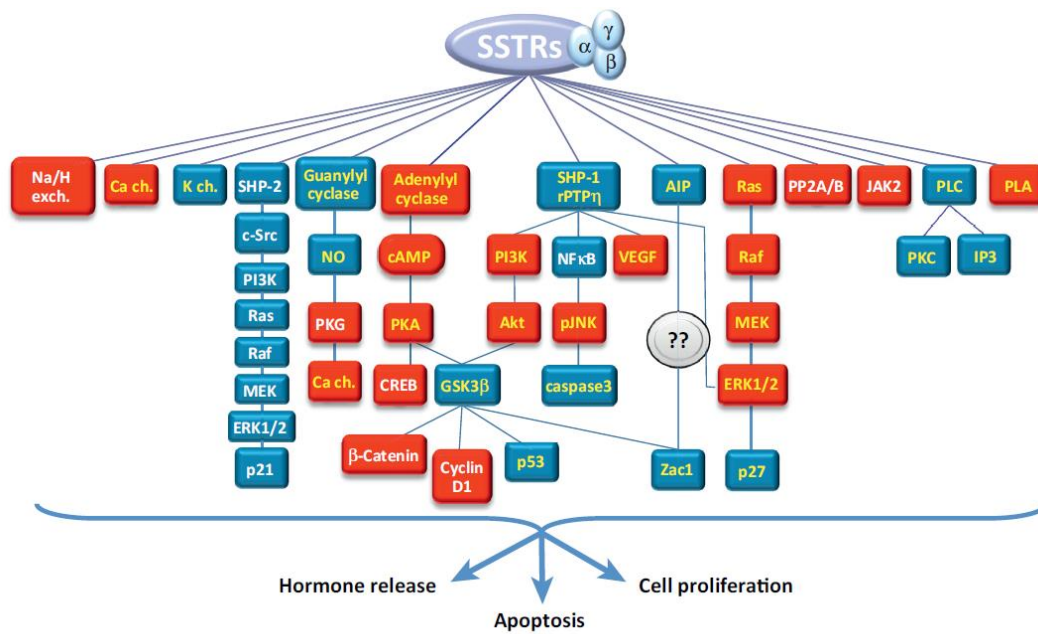
Another feature that was associated with no response to SRLs is a high **Ki-67** index, a marker of proliferation (155). However, it is unknown whether tumors with higher intrinsic proliferative activity are more resistant depicting Ki-67 (156). From a biochemical point of view, high **levels of GH and IGF-1 at diagnosis** have also been associated with lack of response to SRLs (157).

It has also been demonstrated that the different SSTRs as well as the downstream signaling molecules can explain the different degrees of response to SRLs (158). The expression of **SSTR2** has been extensively associated with good sensitivity to SRLs (159–161). However, some authors argue that what is important is the **ratio between SSTR2 and SSTR5** (162). In addition to the five main somatostatin receptors, two truncated variants of SSTR5 have been recently described, with four and five transmembrane domains, **sst5TMD4** and **sst5TMD5**, respectively (163), being the expression of sst5TMD4 the one with the highest correlation with a poor response to SRLs (164).

Dopamine receptors can influence SRLs response in acromegaly due to an heterodimerization of SSTRs and dopamine receptors (165–167). A property that it is really interesting taking into account that dopamine agonists can be used in combination with SRLs (56). In a study including 39 patients treated with octeotride LAR, *DRD1* was inversely correlated with GH reduction, and *DRD5*, positively with IGF-1 decrease in a short 3 months treatment (168).

Different molecules downstream the signaling cascade of somatostatin receptor, such as Arrestin-beta 1 (*ARRB1*) and Arrestin-beta 2 (*ARRB2*) (169,170), Raf kinase inhibitory protein (*RKIP* or *PEBP1*) (171), PLAG like zinc finger 1 (*PLAGL1*, also known as *ZAC1*) (172), Aryl hydrocarbon receptor interacting protein (*AIP*) (172–174) or Alpha stimulating activity polypeptide 1 (*GNAS*) (175), have also been associated with response to SRLs (Figure 7).

Figure 7.



TRENDS in Endocrinology & Metabolism

Pathways involved in SRLs the mechanism of action of SRLs. The mechanism of action includes several transmembrane ion channels, very classical pathways such as MAPK pathway, PI3K-Akt axis, NF-κB and cAMP-PKA. Another important pathway that is not well-understood involves the connection of AIP and PLAGL1 (Zac1). All converge in the main roles of SRLs, inhibiting hormone release and proliferation; and enhancing apoptosis. Red boxes represent inhibition by SSAs and blue boxes stimulation. Source: Gadelha MR, Kasuki L, Korbonits M. Novel pathway for somatostatin analogs in patients with acromegaly. Trends Endocrinol Metab. 2013

In one particular study, **ARRB1** and **ARRB2** were significantly lower in adenoma tissues from complete responders to SRLs (170). They are members of beta-arrestin family, being their main role the desensitization of G protein coupled receptors causing the dampening of cellular responses to diverse stimuli such as hormones or neurotransmitters (176).

The Ras-Raf-MEK-ERK1/2-p27 pathway is activated downstream from SSTRs and regulates hormone release, cell proliferation and cell death. Raf kinase inhibitory protein **PEBP1** or **RKIP** inhibits RAF1 kinase phosphorylation attenuating mitogen-activated protein kinase **MAPK** signaling. **PEBP1** protein levels correlate with octreotide responses, specifically low levels of **PEBP1** and the consequent lack of RAF kinase inhibition are associated with lack of response to SRLs (171).

GNAS is a very well-known tumor growth promoter. Tumors usually harbor mutations that induced its constitutive activation. Almost half of somatotropinomas harvest a mutation on the **GNAS** gene, an upstream regulator of cyclic AMP responsive genes. Furthermore, this mutation has been linked to SRLs resistance (175).

Acromegaly patients harbouring **AIP** mutations in the context of familial isolated pituitary adenoma (FIPA) tend to be diagnosed at a younger age with larger, more aggressive, and SRLs resistance tumors (172). As its name indicate, it is a receptor for aryl hydrocarbons and a ligand-activated transcription factor. The protein can be found bound to a protein complex in the cytoplasm, but it is translocated to the nucleus as it is bind by its ligand (177). These mutations are also rarely detected in young patients with sporadic adenoma (178). Some studies have shown that *AIP* is an important mediator of SRLs response (174), and *AIP* expression has been found to be a SRLs response predictor (172). In this regard, *AIP* seems to play its role in SRLs response through the activation of **PLAGL1**, a zinc-finger protein that functions as a suppressor of cell growth (179).

The expression of the **hormone ghrelin** at the pituitary adenoma has been also linked to SRLs resistance (180). Furthermore, errors in splicing have been associated with somatotropinomas with no sensitivity to SRLs such as **In1-GHRL** (a *GHRL* transcript that contains the first intron) (180) and SSTR5MD4-5 (truncated variants of *SSTR5*) (164).

Other authors propose that the Epithelial-Mesenchymal transition (EMT) phenomena is involved in the loss of sensitivity to SLRs and propose **E-cadherin** as a marker (181–183). E-cadherin is the most well-known member of the cadherin family and a calcium-dependent cell-cell adhesion molecule with fundamental roles in epithelial cell behavior and cytoskeleton organization (184). E-cadherin loss is known to be associated with poor prognosis and high grade tumors in almost all solid neoplasias derived from epithelial cells (185). The loss of E-cadherin is a key characteristic of EMT, the transdifferentiation of epithelial cells into mesenchymal cells (186). During EMT, well polarized epithelial cells lose their junctions and apical–basal polarity, reorganize their cytoskeleton, and reprogram gene expression. All these changes allow epithelial cells to acquire invasion and motility properties. EMT is a developmental cell program; however, it is often activated in cancer cells and associated with tumor progression and metastasis. Pituitary tumors, although typically benign, can be locally invasive. Different studies have shown the association of EMT (182,187) and the loss of E-cadherin (183,188) with increased tumor size and invasion as well as a poor response to SRLs treatment in GH-producing adenomas. It has been proposed that **Epithelial Splicing Regulator 1 (ESRP1)** may be a master regulator of EMT in these tumors by altering splicing programs (182,187). Interestingly, the alteration by SRLs treatment of the expression of some genes, such as **RAR-related orphan receptor C (RORC)** also involved in EMT, may be influenced by E-cadherin levels, and thus by the progression of EMT (181). The relation between SRLs resistance and EMT can also be found in AIP-mutated tumors.

The transcriptome of these tumors, which are more aggressive and often present SRLs resistance (174), shows an enrichment for EMT pathway genes (173).

A better understanding of the mechanisms involved in the resistance to SRLs would help to predict which patients will respond to different medical therapies based on biomarkers.

1.5 Personalized medicine in acromegaly

Personalized or precision medicine is the medical model that try to overcome the different individual responses of patients customizing the medical decisions and therapies to subgroups of patients (189). New technologies allow the definition of subgroups of patients based on molecular and functional assays. The information provided by this assays and systems biology characterize an individual patient's disease at molecular level and, finally, this characterization is used to address a targeted treatment. The possibility to use precision medicine as routine in clinical practice depends on the availability of molecular profiling tests (190).

Personalized health care uses predictive tools to design personalized health algorithms. On this behalf, data mining has been proposed as the best combination of methodology to develop these predictive tools based on systems biology. Very briefly, data mining use an intersection of statistics, machine learning and database management systems to discover patterns in huge datasets. This allows the definition of the different subgroups based in the clinical parameter of interest by some measurements provided in the datasets, usually gene expression (191). The success of personalized medicine depends on having accurate biomarkers and tools that identify patients who can benefit from targeted therapies.

So, the appliance of personalized medicine in acromegaly would fit perfectly since there are many treatment valid and available options, furthermore some biomarkers of response to these options have been already published. Theoretically, it will reduce the time that the clinicians need to adequate the treatment to the patient. Thus, there is an urgent need of identifying accurate predictive markers of response to SRLs in acromegaly patients to improve the current treatment algorithms addressing the biochemical control of the disease and its associated comorbidities.

The main limitation is that this strategy feeds from really huge and standardized datasets. The actual published data is compartmented in studies with a relatively small number of patients, especially in molecular studies, and measuring RNA or protein with different methodologies. Despite of that, some authors venture to propose treatment algorithms based on the already

published studies using published biomarkers (Kasuki et al., 2018; Picó, 2019; Puig Domingo, 2015; Puig-Domingo and Marazuela, 2019). However, another obstacle quickly appears, which is the cut-off values for decision-making. For example, there is a general consensus that high levels of *SSTR2* are considered to define good responders to SRLs; but, how can be scientifically defined what is high from what is not without a cut-off? For that reason a non-subjective homogenous quantification should be used. Summarizing, with a standardized huge dataset and data mining technique, personalized medicine would not be difficult to achieve.

2. Hypotheses

Pharmacologic treatment of acromegaly is currently based upon assay-error strategy, changing or adding another drug in case of insufficient response, which can lead to an important delay in finding the correct treatment for a given acromegaly patient. This is especially worrying for those non-responder cases to SRLs as the delay can be at least of more than a year. This delay can cause important comorbidities in the patient that has an active disease with a hormonal imbalance. Here, we try to propose a modification of the current acromegaly therapeutic guidelines and treatment algorithms using information that can help to personalize the treatment for minimizing the time that the patients remains with active disease. The goal is shifting from the “treat-fail-change treatment” philosophy to “identifying the right treatment for a given patient”. The **main hypothesis** of this thesis is that *SRLs response of acromegaly patients can be predicted by the addition of molecular data to clinical information; therefore, the inclusion of this information in the current therapeutic algorithm will prevent unsuccessful treatment with SRLs in non-responsive patients.*

For decades, biomarkers have been discovered to explain the lack of response in some patients to SRLs, thus in results parts 1, 2 and 3 we specifically hypothesize that *the addition of these markers to the pharmacological treatment algorithm of acromegaly will benefit finding the correct treatment.* In addition, *further understanding of molecular bases of SRLs resistance will provide more markers to predict SRLs response.*

Virtually all published studies, including ours, that focus on the discovery and quantification of biomarkers in acromegaly use classical statistics. However, it is difficult to account for many biological, clinical and molecular variables with small but added effects in the response to SRLs. Data mining is a modality of mathematical analysis that allows efficient subclassification of heterogeneous populations. Thus, in Study 4 we hypothesize that *advanced model techniques will allow better fitting of the pharmacological treatment algorithm of acromegaly to the reality of clinical practice.*

3. Objectives

Based on these hypotheses, this project has as **main objective** to develop an algorithm with relevant molecular and clinical data to help clinicians to provide the best available medical treatment to each acromegaly patient. To achieve this objective, we proposed the following **specific objectives**:

- To validate previously reported biomarkers of SRLs response to ponder its inclusion in the pharmacological treatment algorithm of acromegaly (Study 1).
- To evaluate the EMT process in acromegaly as a source of SRLs resistance (Study 2).
- To identify molecular markers of response to SRLs after surgical debulking in GH-secreting adenomas (Study 3).
- To apply data mining to further evaluate valuable data and find the best mathematical strategies to develop therapeutically statistical models (Study 4).

4. Material and Methods

4.1 Patients

A transnational cohort consisting of 100 acromegaly patients from 26 tertiary centers from all over Spain who had undergone pituitary surgery and had tissue availability (RNA later preserved tumor sample) were included in the present thesis. In those patients in which more than one surgery was performed, only one sample tumor per patient was analyzed. This cohort of patient tumors was collected under the REMAH initiative (192) and it is the effort of 4 REMAH nodes: Santiago de Compostela, Alacant, Madrid and Catalonia. The description of the phenotypic characteristics of the cohort is presented in Table 1. The heterogeneity of the included patients reflects the daily practice of acromegaly management.

Table 1.

PATIENTS CHARACTERISTICS	
Cohort (N)	100
Male / Female	44 / 56
Age	45.5 ± 13.28
Medical Treatment	
DA treated	12
SRLs presurgery	67
Comorbidities (%)	
Diabetes	27
HBP	29
Dyslipidemia	27
Cancer	6
Cerebrovascular Accident	3
Cardiovascular Incident	13
Visual Alterations	18
Tumor Characteristics (%)	
Macroadenoma	79
Extrasellar Growth	77
Sinus invasion	61

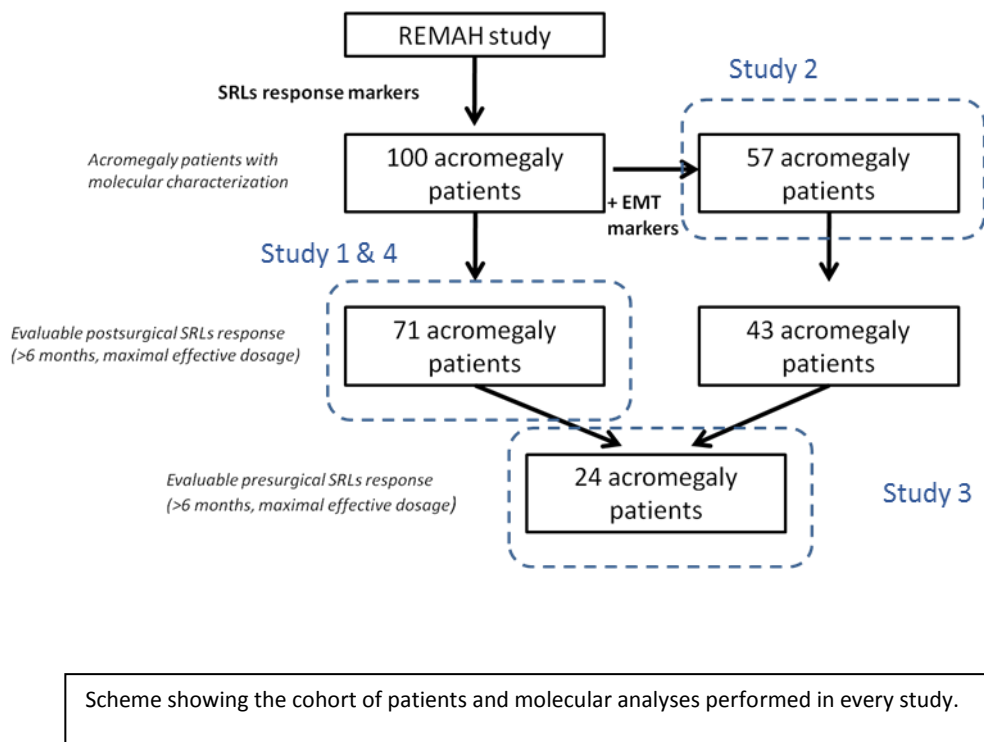
Cohort description. HBP: high blood pressure.

The 100 patients were not included in all studies of the present thesis but we used different subsets of patients in each study as indicated in Figure 8. Additionally, every Study of the Results section is headed by a summary and a description of the characteristics of the patients used.

Briefly, the whole cohort of 100 patients was used in Studies 1 and 4. Of these 100 patients, 67 had received SRLs treatment (octreotide or lanreotide) before surgery and 33 had not received treatment before surgery. All patients in which clinical information was available at follow-up and were treated after surgery for at least 6 months under maximal effective therapeutic (octreotide or lanreotide) doses according to IGF-1 values were included in the analysis; this was possible in 71, including 51 out of 67 cases (51% females, mean age 45.3 +/- 13y) who had

received SRLs treatment before surgery and 20 out of 33 patients who had not (51% females, mean age 44.6 +/- 13 y). In the 29 remaining patients, 22 were cured after surgery and 7 were lost to follow-up. Based on sample availability, 57 out of the 100 patients were used in Study 2 to analyze EMT markers (Figure 8).

Figure 8.



4.2 Biochemical and hormonal assays

After an overnight fast, blood samples were collected from patients at baseline and at different follow-up times. Serum IGF-1 was measured by two different methods and normalized for comparisons by expressing SDS values. Method 1, a two-site immunoradiometric assay (Immunotech IGF-1 kit; Immunotech-Beckman, Marseille, France). Expected values depending on age were: 20–30 yr, 220–550 ng/ml; 30–40 yr, 140–380 ng/ml; 40–50 yr, 54–330 ng/ml; and 50–60 yr, 94–285 ng/ml. Intra-assay CV was less than 6.3%; inter-assay CV, 6.8%; and sensitivity, 30 ng/ml. Method 2 was a non-extraction immunoradiometric assay (Diagnostic Systems Laboratories, Webster, Texas, USA). The theoretical sensitivity, or minimum detection limit, calculated by interpolation of the mean plus two SD values of 20 replicates of the 0 ng/ml IGF-1 standard was 2 ng/ml. The inter-assay CV was 7.4 and 4.2, respectively, for the concentration 32.5 and 383.8 ng/ml. The inter-assay CV was 7 and 3.9, respectively, for the mean concentration values 34.03 and 373.86 ng/ml.

SRLs IGF-1 Results regarding IGF-1 levels are expressed as SDS according to sex and age (Studies 1 and 4) and percentage of decrease over basal value (Studies 2 and 3). Therefore, IGF-1 greater than 3 SDS was considered not responsive to SRLs treatment, between 2 and 3 SDS was considered a partial response to SRLs, and less than 2 SDS was considered a complete response to SRLs treatment (120). In Study 3-4, on the other hand, patients were categorized according to the therapeutic response to SRLs before and after surgical treatment as complete responders (CR) if IGF-I was normal, partial responders (PR) if IGF-I was reduced by more than 30% from diagnosis levels but without achieving hormonal control, or non-responders (NR) when IGF-I reduction observed during SRLs treatment was less than 30% at 6 months follow-up and at full SRLs dose.

4.3 Bioethical statement

All the studies were conducted in accordance with the ethical principles of the Declaration of Helsinki and implemented and reported in accordance with the International Conference on Harmonised Tripartite Guideline for Good Clinical Practice. The studies were approved by the Germans Trias i Pujol Hospital Ethical Committee for Clinical Research. The protocol and informed consent forms were approved by the institutional review board of the participating centers, independent ethics committee, and/or research ethics board of each study site. All patients provided written informed consent to participate in the trial.

4.4 DNA and RNA isolation

Total RNA was isolated from pituitary adenomas using AllPrep DNA/RNA/miRNA Universal Kit (Qiagen). The quantity and purity of extracted DNA and RNA was quantified by measuring optical density at 260 and 280 nm using NanoDrop™ 1000 Spectrophotometer (RRID:SCR_016517, Thermo Fisher Scientific, Waltham, Massachusetts, USA). Integrity of the RNA was checked by agarose gel electrophoresis.

4.5 Retrotranscription

Five hundred nanograms of total RNA were reverse transcribed using SuperScript IV reverse transcriptase (Invitrogen, Carlsbad, California, USA,) and random hexamers in a final volume of 20 μ L according to the manufacturer's protocol.

4.6 Quantitative polymerase chain reaction

Gene expression was quantified using Taqman assays (Applied Biosystems, Fosters City, California, USA) (Table 2). We selected *TBP*, *MRPL19* and *PGK1* reference genes based on their

stability in our samples according to Chainy software (available on: <http://maplab.imppc.org/chainy/>) (193).

Table 2.

Target genes		
Name	Symbol	Taqman probe
Somatostatin Receptor 2	<i>SSTR2</i>	Hs00990356_m1
Somatostatin Receptor 3	<i>SSTR3</i>	Hs00265633_s1
Somatostatin Receptor 5	<i>SSTR5</i>	Hs00990408_s1
short dopamine receptor 2 isoform	<i>sh DRD2</i>	Hs01014210_m1
long dopamine receptor 2 isoform	<i>lo DRD2</i>	Hs01024460_m1
Arrestin Beta 1	<i>ARRB1</i>	Hs00930516_m1
Pleiomorphic Adenoma Gene-Like 1	<i>PLAGL1</i>	Hs00414677_m1
Phosphatidylethanolamine Binding Protein 1 / Raf Kinase Inhibitory Protein	<i>PEBP1 / RKIP</i>	Hs01110783_g1
E-cadherin	<i>CDH1</i>	Hs01023894_m1
Ki-67	<i>MKI67</i>	Hs01032443_m1
Ghrelin And Obestatin Prepropeptide	<i>GHRL</i>	Hs01074053_m1
Aryl Hydrocarbon Receptor Interacting Protein	<i>AIP</i>	Hs00610222_m1
Snail Family Transcriptional Repressor 1	<i>SNAI1</i>	Hs00195591_m1
Snail Family Transcriptional Repressor 2	<i>SNAI2</i>	Hs00950344_m1
Epithelial splicing regulatory protein 1	<i>ESRP1</i>	Hs00214472_m1
RAR related orphan receptor C	<i>RORC</i>	Hs01076112_m1
N-cadherin	<i>CDH2</i>	Hs00983056_m1
Twist family bHLH transcription factor 1	<i>TWIST1</i>	Hs00361186_m1
Vimentin	<i>VIM</i>	Hs00958111_m1
Intron 1 Ghrelin	In1-GHRL	AJ89KWC
Reference genes		
Name	Symbol	Taqman probe
Hypoxanthine Phosphoribosyl transferase 1	<i>HPRT1</i>	Hs99999909_m1
Proteasome 26S Subunit ATPase 4	<i>PSMCA4</i>	Hs00197826_m1
Glucuronidase Beta	<i>GUSB</i>	Hs00939627_m1
TATA-Box Binding Protein	<i>TBP</i>	Hs00427621_m1

Mitochondrial Ribosomal Protein L19	<i>MRPL19</i>	Hs01040217_m1
Phosphoglycerate Kinase 1	<i>PGK1</i>	Hs00943178_g1

Quantitative polymerase chain reactions (qPCR) were carried out in a 7900HT Fast Real-Time PCR System (Applied Biosystems, Fosters City, California, USA). We used TaqMan Gene

Taqman assays used in qPCRs experiments

Expression Master Mix (Applied Biosystems, Fosters City, California, USA), and the amplification reactions were performed in triplicate for each sample in a final volume of 10 μ L in 384-well plates. To minimize the inter-assay variation, all genes, including the reference genes, for each sample were analyzed in the same plate. To quantify relative gene expression we calculated a normalization factor for each sample based on the geometric mean of the selected reference genes, according to geNorm (RRID:SCR_006763, <https://genorm.cmgg.be/>) algorithms (Vandesompele et al., 2002).

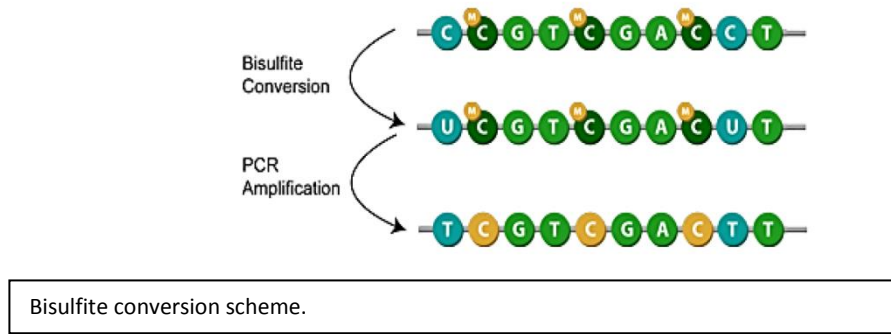
4.6 *GNAS* sequencing

Mutations in Guanine nucleotide binding protein (G protein), alpha stimulating activity polypeptide 1 (*GNAS*, also known as *GSP* oncogene) were screened by Sanger sequencing (Eurofins, Luxembourg). Samples were analyzed for mutations at codons 201 and 227 in exons 8 and 9, respectively, using cDNA and the primers 5'-CAAGCAGGCTGACTATGTGCCGA-3' (forward) and 5'-CCACCACGAAGATGATGGCAGTC-3' (reverse).

4.7 E-cadherin promoter methylation assessment

There are different methods to analyze DNA methylation at specific genomic *loci* (195), sodium bisulfite modification followed by sequencing being the gold standard. Sodium bisulfite treatment deaminates unmethylated cytosines (C) to uracils which will be recognized as thymines (T) in subsequent PCR and sequencing; instead, methylated cytosines (mC) will remain unaltered allowing them to be distinguished from unmenthylated C (Figure 9).

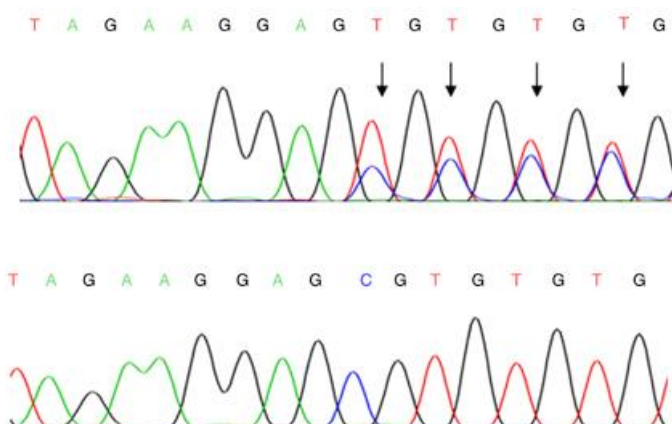
Figure 9.



Bisulfite treatment was performed on 300 ng DNA using the EZ DNA Methylation-Gold Kit (Zymo Research, Irvine, California, USA) according to the manufacturer's instructions. Bisulfite converted DNA was used as a template for a nested-PCR to analyze the promoter of E-cadherin. The sequence of primers was: 5'-GATTTTAGGTTTGTAGT-3' (sense) and 5'-CCTACAACAACAACAACA-3' (antisense) for the external PCR (annealing temperature: 50°C, 447 bp product); and 5'-GTAATTTTAGGTTAGAGGG-3' (sense) and 5'-CTCCAAAACCCATAACT-3' (antisense) for the internal PCR (annealing temperature: 50°C, 321 bp product). For the PCR amplification, we used the IMMOLASE DNA Polymerase (Bioline USA Inc., Tennessee, USA) following the manufacturer's protocol and processed samples in duplicate to ensure a representative methylation profile. The PCR program was as follows: 10 min at 95°C (initial polymerase activation); 30s at 94°C, 30s at 50°C and 30s at 72°C for 25 cycles in the external PCR and for 35 cycles in the internal PCR; and 8 min at 72°C (final elongation). The duplicates were pooled, purified (Exonuclease I [Exo I] and FastAP Thermosensitive Alkaline Phosphatase, Thermo Fisher Scientific, Waltham, Massachusetts, USA) and analyzed by Sanger sequencing (GATC Biotech, Cologne, Germany).

By comparing the sequence of the bisulfited DNA with the original sequence, the methylation state of the original DNA can be inferred (figure 10). The degree of methylation was calculated by comparing the peak height of the cytosine residues with the peak of the thymine residues $[C/(C+T)*100]$ in the sequencing chromatogram. We considered ranges of DNA methylation, specifically 0-10%, 11-25%, 27-50%, 51-75%, 76-100%, for each CpG. Results were represented using the Methylation Plotter, a web tool for dynamic visualization of DNA methylation data (available on: http://maplab.cat/methylation_plotter) (196).

Figure 10.



Bisulphite Sanger sequencing example. In the upper figure the four consecutively CpGs are partially methylated (indicated by arrows), the lower figure shows one fully methylated and three unmethylated CpGs.

Those markers that performed better in the gene expression analysis were subsequently evaluated at protein level by immunohistochemistry. Thus, forty-six somatotropinoma tissues samples were available for immunostaining of E-cadherin, *SSTR2 α* , *Ki-67* and cytokeratin CAM 5.2. CAM 5.2 has previously demonstrated to identify accurately densely granulated and sparsely granulated somatotropinomas with good identification power of responsiveness and non-responsiveness to SRLs, respectively (57,197).

Formalin-fixed paraffin-embedded tumor samples were cut into sequential 4- μ m-thick sections and stained using a fully automated Ventana BenchMark ULTRA stainer (Ventana, Tucson, Ariz., USA) according to the manufacturer's instructions. Binding of peroxidase-coupled antibodies was detected using diaminobenzidine as a substrate, and the sections were counterstained with hematoxylin.

The mouse monoclonal anti-cytokeratin antibody and the mouse monoclonal anti-E-cadherin antibody (Ventana, Tucson, Ariz., USA) were purchased as prediluted antibodies, with a concentration of 11 μ g/dL and 0.314 μ g/dL, respectively. The rabbit monoclonal anti-SSTR2 α antibody (clone UMB-1, Abcam, Cambridge, UK) was used at a dilution of 1:100. To analyze Ki-67 we used the rabbit monoclonal anti-Ki67 antibody 30-9 (ready-to-use formulation; Ventana, Tucson, Ariz., USA). Normal appendix tissue served as the positive control for CAM 5.2 staining and mammary invasive ductal carcinoma for E-cadherin staining.

Immunostaining for E-cadherin was scored in three intensities (0: negative, 1+: weak positivity, 2+: strong positivity) and for each intensity, the percentage of cells was determined. For the classification of the intensities, we considered 0 (negative) when there was no positivity; 1+ (weak positivity) when the adenoma cells seemed negative at low magnification (x40) but were truly positive at high magnification (x200); and we considered 2+ when the adenoma cells were clearly positive at low magnification (x40). We calculated an IHC score multiplying the percentage of cells of each intensity by the score intensity (0-200). Loss of E-cadherin was considered for IHC scores equal to 0. Partial loss of E-cadherin was considered for IHC scores below 100.

Immunostaining for *SSTR2* was scored using a H-score as performed in Franck et al. 2017 (198). First, membrane and cytoplasmic staining intensity (0: no staining, 1+: weak positivity, 2+: moderate positivity, 3+: strong positivity) was determined for each field and then, the percentage of cells at each staining intensity level was calculated. An H-score was assigned using the following formula: $[1 \times (\% \text{ cells } 1+) + 2 \times (\% \text{ cells } 2+) + 3 \times (\% \text{ cells } 3+)]$.

Ki-67 score was expressed as the percentage of the number of immunostained nuclei among the total number of nuclei of tumor cells regardless of the immunostaining intensity. The counting was performed in three randomly selected fields of the adenoma tissue section at x400 magnification.

For the CAM 5.2 staining, the adenomas were classified in two groups: dot-type (when the pattern was exclusively dot-type which identifies accurately sparsely granulated somatotropinomas) and not-only-dot-type (when there were other patterns in addition or not to the dot-type pattern which identifies accurately densely granulated somatotropinomas).

4.8 Standard Statistical Analysis

Descriptive results were expressed as mean \pm standard deviation or median and 25th to 75th percentiles, as appropriate. Samples from all groups within an experiment were processed at the same time.

Spearman or Pearson bivariate correlations were performed for all quantitative variables (age, BMI, basal GH levels, GH after oral glucose overload, IGF-1 diagnostic values, tumor maximum diameter (mm), and time under SRLs therapy). Furthermore, for quantitative variables a Kolmogorov-Smirnov test was applied to assess the normality of the samples. The differential behaviour of the variables studied according to SRLs response groups was analysed applying a t-student test, or a Wilcoxon-rank test. Multi-test correction was performed according to

Benjamini-Hochberg method under the false discovery rate parameter (FDR). Also, a Pearson's Chi-squared test independence analysis was performed between categorical variables (verification of lack of biases between clinical centres, *GNAS* mutation status, sex, extrasellar growth, sinus invasion, T1 and T2 categorical intensity, presurgical visual alterations, presurgical hypopituitarism, history of diabetes, high blood pressure, dyslipidaemia, cancer, cerebrovascular disease and cardiovascular disease) and SRLs response.

A multinomial logistic regression model was used to determine the differences in each normalized gene expression between complete response and resistant patients. The model was adjusted by age, gender and SRLs presurgical treatment. Receiver operating characteristic (ROC) curve analyses were performed to assess the classification power of each logistic regression model. The ROC curves were plotted using pROC package (Display and Analyze ROC Curves, <https://CRAN.R-project.org/package=pROC>).

The P values were two-sided, and statistical significance was considered when $P < 0.05$. All statistical analyses were performed using STATA (StataCorp LLC, College Station, Texas, USA, RRID:SCR_012763) and R version 3.3.2 (R Project for Statistical Computing, RRID:SCR_001905). The graphical representation was done using package ggplot 2 (RRID:SCR_014601, Wickham <https://CRAN.R-project.org/package=ggplot2>) and the P values were added using ggpubr package ('ggplot2' Based Publication Ready Plots, <https://CRAN.R-project.org/package=ggpubr>). Alluvial plots were plotted using the ggalluvial package (ggalluvial: Alluvial Plots in 'ggplot2', <https://cran.r-project.org/package=ggalluvial>).

Unsupervised hierarchical clustering was used to investigate the potential identification of patient's response subgroups based on their molecular expression profile. Unsupervised hierarchical clustering was performed using the R package pheatmap (Pretty Heatmaps, <https://CRAN.R-project.org/package=pheatmap>).

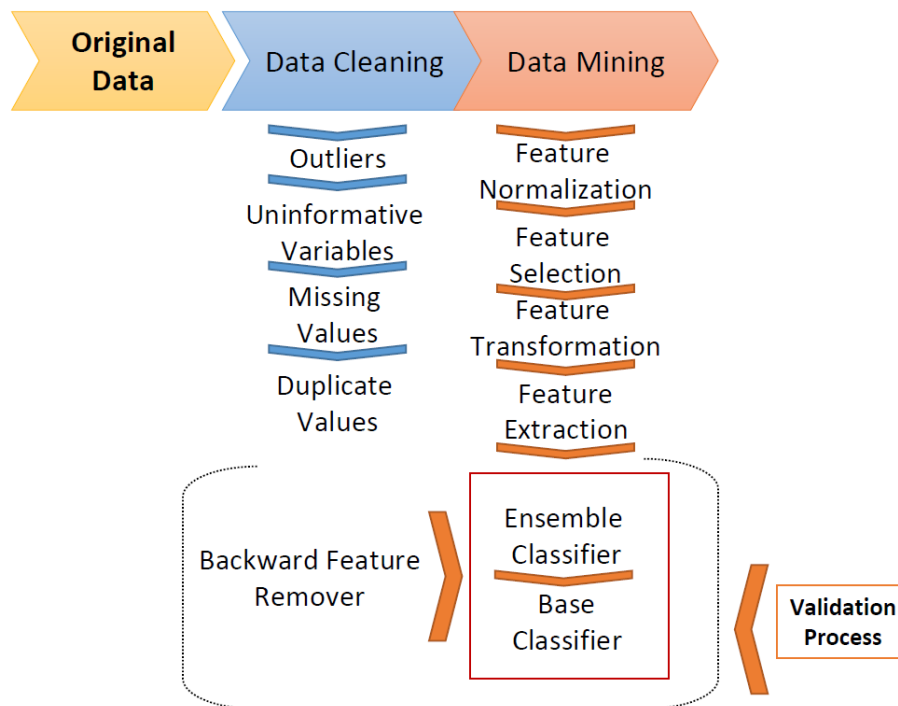
4.9 Data mining analyses

Data mining is an interdisciplinary subfield of computer science and statistics and was used in Study 4. It allows discovering hidden patterns in large data sets (databases) and involves methods at the intersection of machine learning, statistics and database systems. Among other applications, the identification of patterns in the data set can be used to define classifiers, which are mathematical functions, implemented by a classification algorithm that maps input data to a category (e.g. a mathematical function that assigns a patient to the responders or non-

responders group based on the numerical values obtained for a set of biochemical variables). Since no single form of classification is appropriate for all data sets, a large toolkit of classification algorithms have been developed through the years (linear regression, logistic regression and naïve Bayes, among others) (12,13).

Data Mining strategy was applied by Anaxomics S.L. (<http://www.anaxomics.com>) to identify the best classifiers (Figure 11) (199).

Figure 11.



Biomarker data mining analyses procedure. First, a Data Cleaning process was performed to eliminate outliers, uninformative variables, missing values, and duplicate variables. Next, this new cleaned data set was used to train the model of the Data Mining process which is subdivided in different mathematical sub-processes: Feature Normalization to guarantee that the values of all variables are in the same range; Feature Selection to select the input variables that show the strongest relationship with the outcome; Feature Transformation consisting in mathematical transformations of the input data required for the Base Classifiers; Feature Extraction to reduce the number of random variables (it was not necessary); Base Classifier (different algorithms generated different Base Classifiers with a good performance); Ensemble Classifiers were able to improve the performance of the Base Classifiers. Finally, the Validation process to estimate the accuracy of the predictive model was performed using the original database by several methods: 10-K fold and Leave-one-out.

First, a Data Cleaning process was performed to eliminate outliers (values >3 times the standard deviation of the rest of values), uninformative variables (not considered because the values for all the samples are the same or variables with 100% coincidence with the outcome of the analysis), missing values, and duplicate variables (variables containing the same information). Next, this new cleaned data set was used to train the model of the Data Mining process. All the variables of the data set were individually evaluated for their capability as classifiers. When the classifier contains only one variable, the discriminant function is a constant that is determined as the threshold value that separates samples from different groups with the best accuracy (Supplementary Fig. S1A). The threshold value is determined iteratively and a cross-validation protocol is performed. In contrast, when the classifier contains two or more independent variables, the discriminant function is generated by applying Data Science approaches that identify the best classifiers (Supplementary Fig. S1B-C). This process was subdivided in different mathematical sub-processes: Feature Normalization, Feature Selection, Feature Transformation, Feature Extraction, Ensemble Classifier, Base Classifier, Backward Feature Removal and Validation (Figure 11). By means of artificial intelligence, different mathematical algorithm approaches previously published were explored for each sub-process, allowing an exhaustive exploitation of the data (Table 2). The Feature Normalization determined that the values of all the variables were in the adequate range for the analysis, thus no further method of normalization was required. It was not necessary to apply a Feature Extraction to reduce the number of random variables. Finally, a Validation process to estimate the accuracy of the predictive model was performed using the original database.

Table 3.

Sub-Process	Algorithm	Reference
Backward removal features	Backward elimination	(200)
Base classifier	Elastic net	(201)
	K-nearest neighbors (K-NN)	(202)
	Boosted Generalized Additive Models (B-GAM)	(203)
	Tree	(204)
	Support vector machine (SVM)	(205)
	Multilayer perceptron (MLP)	(206)
	MLP ensemble	(206)
	Linear search	(207)
	Linear regression	(207)
	Quadratic	(207)
	Random linear	(207)
	Generalized linear model binomial	(208)
	Ridge regression	(209)
	Naïve bayes	(210)
	Lasso regression	(211)

	Radial basis function (RBF)	(212)	
Cost function	Accuracy	(213)	
	Balanced accuracy	(213)	
	Balanced cost matrix	(213)	
	Cost matrix	(213)	
	F1 score	(213)	
	Matthews correlation coefficient (MCC)	(214)	
	Area Under Curve (AUC)	(215)	
Dimensionality reduction	Principal component analysis (PCA)	(216)	
	T-distributed Stochastic Neighbor Embedding (t-SNE)	(217)	
	Multidimensional scaling (MDS)	(218)	
	Hessian locally linear embedding (HLLE)	(219)	
	Isomap	(220)	
	Latent Dirichlet allocation (LDA)	(221)	
	Locally linear embedding (LLE)	(222)	
	Sammon projection	(223)	
	LandMark ISOMAP (L-ISOMAP)	(224)	
	Laplacian	(225)	
	Gaussian process latent variable model (GPLVM)	(226)	
	Kernel PCA	(227)	
	Independent component analysis (ICA)	(228)	
	Non-negative matrix factorization (NMF)	(229)	
	Factor analysis	(230)	
	Probabilistic principal component analysis (PPCA)	(231)	
	Local tangent space alignment (LTSA)	(232)	
	Ensemble classifier	Bootstrap	(233)
		Bootstrap respecting prevalence	(233)
		Balanced bootstrap	(233)
Ensemble method	Bootstrap	(234)	
	Bootstrap respecting prevalence	(234)	
	Balanced bootstrap	(234)	
Feature selection	K-nearest neighbors (K-NN)	(202)	
	Receiver operating characteristic (ROC)	(235)	
	Bhattacharyya	(236)	
	Ridge regression	(236)	
	Wilcoxon	(237)	
	Wilcoxon + correlation	(237)	
	minimum Redundancy Maximum Relevance (mRMR) Mean discretized	(238)	
	Boolean balanced three-valued logic rules	(239)	
	Sequential floating forward selection (SFFS)	(240)	
	Support vector machines recursive feature elimination (SVM-RFE)	(241)	

	Random forest	(242)
	Chow-Liu	(243)
	Simple regression	(207)
	Relieff	(244)
	Random generalized linear model	(208)
	One variable brute force	(245)
	Bhattacharyya + Correlation	(246)
	Entropy	(246)
	Entropy + Correlation	(246)
	Matteest	(246)
	T-test	(246)
	T-test + Correlation	(246)
	minimum Redundancy Maximum Relevance (mRMR)	(247)
	Lasso	(211)
	Elastic net	(248)
	Double Cross-Validation regression	(249)
Feature transformation	Sigmoid	(246)
	Gaussian; the value used is the value obtained after being submitted to a Gaussian function	
	No value transformation	
	The value used is the original value multiplied by itself	
	The value used is the square root of the original value	
Multiclass classifier	Generalized coding	(246)
	One versus all (OVA) binary classified applied	
	One versus one (OVO) binary classifiers applied	
Normalization	Sigmoidal mean variance	(246)
	Trimmed mean variance	(246)
	Mean variance	
	Median dispersion	
	Min Max: each value is divided by the difference between the maximum and the minimum value	
	Winsorizing mean variance	
Validation	Bootstrap	(250)
	K-Fold	(251)
	LeaveOneOut (LOO)	(246)

Mathematical methods explored during the different processes included in the Data Mining strategy.

Since our goal is the prediction of SRLs response for an individual case, we want to estimate how accurately a predictive model will perform in clinical practice. In order to flag selection bias or overfitting in our models, we used cross-validation techniques for assessing how the model will generalize to an independent data set. We confronted the model obtained with a subset of training data with the test data using two iterative strategies: 10-K fold (where the original

sample is randomly partitioned into 10 equal sized subsamples, a single subsample is retained as the validation data for testing the model while the remaining 9 subsamples are used as training data; this cross-validation process is repeated 10 times with each of the 10 subsamples used once as the validation data), and Leave-one-out (where we use a single sample as the validation data and the remaining samples as the training data, and this is applied once for each sample). Therefore, we obtain a more exact estimation of the accuracy of the model taking the average of all the accuracy estimations obtained after each iteration. We used the accuracy (ACC) as the simplest parameter for evaluating the model, being the proportion of correct predictions (both true positives and true negatives) among the total number of samples. Accuracy levels are referred in these terms: accuracy 100-95%, excellent; 95%-80%, very good; 80%-70%, good; below 70%, to be improved.

In order to add the information of the categorical data to the models, we divided the samples according to a categorical variable in what it is called “fragmented population”, for example, biological sex, and applied all the data mining strategies to the obtained subsets. This procedure was applied to different categorical variables. The fragmentation of population deconstructs the heterogeneity to overcome molecular differences and reduce statistical noise that is not due to SRLs response.

5. Results

Results are divided in four studies:

Study 1: Molecular profiling for acromegaly treatment: a validation study

This study was conceived as a validation study of previously reported biomarkers of response to SRLs. We aimed to evaluate all these markers in a large series of Spanish acromegaly patients treated with SRLs to identify those markers with the highest predictive capacity.

Study 2: Association of Epithelial-mesenchymal transition (EMT) markers with response to somatostatin receptor ligands in GH secreting tumors

In this work, our aim was to study the relationship between EMT and SRLs response. By evaluating the expression of EMT-related genes in a well-characterized acromegaly cohort, we wanted to identify new predictors of SRLs response that may provide a more personalized approach in acromegaly treatment.

Study 3: Molecular determinants of enhanced response to somatostatin receptor ligands after debulking in large GH producing adenomas

The main objective of this study was to analyze the relationship between the biomarkers reported in the two first studies and debulking in large and invasive GH producing tumors regarding SRLs response. This may allow to clearly determine if SRLs response biomarkers could be useful in the worst clinical scenario.

Study 4: Data mining analysis in acromegaly

In this study we applied data mining techniques to molecular and clinical data to enhance the predictive power obtained in the previous study described in Study 1. Data mining is an interdisciplinary subfield of computer science and statistics. It allows discovering hidden patterns in large data sets (databases) and involves methods at the intersection of machine learning, statistics and database systems. Here we provide a proof-of-concept study by applying data mining strategies to identify high accuracy classifiers of SRLs response categories.

5.1 Study 1: Molecular profiling for acromegaly treatment: a validation study

Pharmacologic treatment of acromegaly is currently based upon assay-error strategy, the first-generation somatostatin receptor ligands (SRLs) being the first-line treatment. However, about 50% of patients do not respond adequately to SRLs. Our objective was to evaluate the potential usefulness of different molecular markers as predictors of response to SRLs. We used somatotropinoma tissue obtained after surgery from a national cohort of 100 acromegalic patients. Seventy-one patients were treated with SRLs during at least 6 months under maximal therapeutic doses according to IGF-1 values. We analyzed the expression of *SSTR2*, *SSTR5*, *AIP*, *CDH1* (E-cadherin), *MKI67* (Ki-67), *KLK10*, *DRD2*, *ARRB1*, *GHRL*, In1-Ghrelin, *PLAGL1* and *RKIP* (*PEBP1*) by RT-qPCR and mutations in *GNAS* gene by Sanger sequencing. SRLs IGF-1. From the 71 patients treated, there were 27 CR (38%), 18 PR (25%) and 26 NR (37%). *SSTR2*, Ki-67 and E-cadherin were associated with SRLs response ($P < 0.03$, $P < 0.01$ and $P < 0.003$, respectively). E-cadherin was the best discriminator for response prediction (AUC = 0.74, $P < 0.02$, PPV of 83.7%, NPV of 72.6%), which was validated at protein level. *SSTR5* expression was higher in patients pre-treated with SRLs before surgery. We conclude that somatotropinomas showed heterogeneity in the expression of genes associated with SRLs response. E-cadherin was the best molecular predictor of response to SRLs. Thus, the inclusion of E-cadherin in subsequent treatment-decision after surgical failure may be useful in acromegaly.

This study has been published:

Manel Puig-Domingo, Joan Gil*, Miguel Sampedro-Nuñez, Mireia Jordà, Susan M Webb, Guillermo Serra, Laura Pons, Isabel Salinas, Alberto Blanco, Montserrat Marques-Pamies, Elena Valassi, Antonio Picó, Araceli García-Martínez, Cristina Carrato, Raquel Buj, Carlos Del Pozo, Gabriel Obiols, Carles Villabona, Rosa Cámara, Carmen Fajardo-Montañana, Clara V Alvarez, Ignacio Bernabéu, Mónica Marazuela. Molecular profiling for acromegaly treatment: a validation study. *Endocr Relat Cancer*. 2020 Jun;27(6):375-389. doi: 10.1530/ERC-18-0565. PMID: 32302973.*

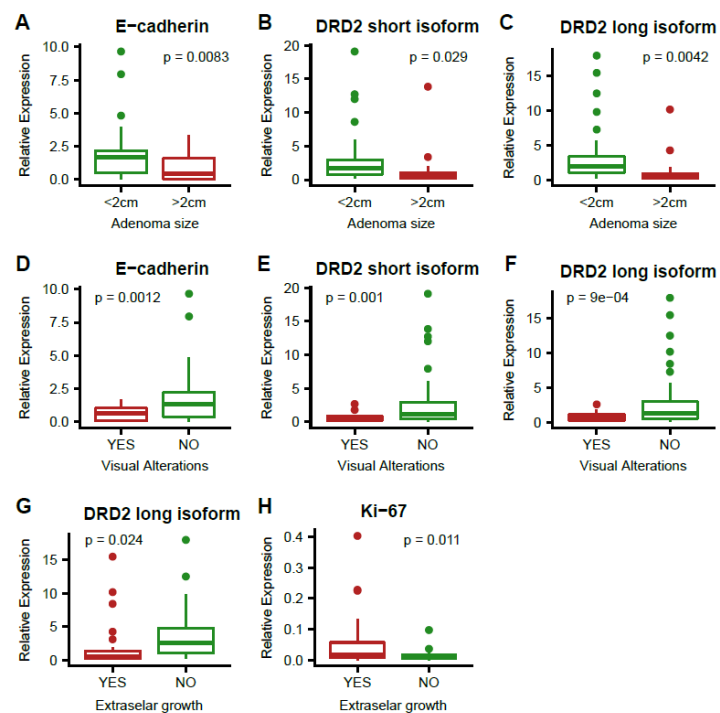
Patients

In this study, we used the whole cohort of 100 patients described in Material and Methods section. The 71 patients with evaluable SRLs response were categorized according to therapeutic response to SRLs as complete response (CR = 27), partial (PR = 18) or non-responders (NR = 26) if IGF-1 was normal, between $>2 < 3$ SDS or >3 SDS IGF-1 at 6 months follow-up, respectively.

Clinical variables according to biomarkers expression

In the whole cohort (n=100) we analyzed the expression of 12 genes previously reported to be involved in SRLs response, including *SSTR2*, *SSTR5*, *AIP*, E-cadherin, Ki-67, *KLK10*, *DRD2*, *ARRB1*, *GHRL*, In1-Ghrelin, *PLAGL1* and *RKIP*. Tumor size was related to *SSTR2* (Pearson's $r=0.25$, $p=0.01$) and showed a negative association with *DRD2* (short *DR2D* isoform Pearson's $r=-0.29$, $p<0.01$, and long *DRD2* isoform Pearson's $r=-0.37$, $p<0.001$) and E-cadherin (Pearson's $r=-0.28$, $p<0.01$). Extrasellar extension was also related to long *DRD2* isoform ($p=0.01$) and Ki-67 ($p=0.04$). Moreover, visual alteration was negatively related to *DRD2* ($p=0.01$ for both isoforms) and E-cadherin ($p=0.02$) (Figure 12).

Figure 12.



Boxplot showing gene expression according to tumor characteristics. Relative expression in tumors smaller and larger than 2 cm (an arbitrary threshold that separates our cohort in two equivalent subsets) (A, B and C), in tumors causing visual alterations before the surgery (D, E and F) and in tumors with or without extrasellar extension (G and H).

We also found a negative correlation between IGF-1 levels at diagnosis and expression of *ARRB1* (Pearson's $r = -0.31$, $p = 0.002$), *KLK10* (Pearson's $r = -0.23$, $p = 0.02$) and E-cadherin (Pearson's $r = -0.29$, $p = 0.003$). Furthermore, we analyzed the correlation of the expression of each marker with IGF-1 index at diagnosis and IGF-1 % decrease after SRLs treatment, E-cadherin was the only marker that showed significant correlations with the three IGF-1 -related measurements (Table 4), while Ki-67 has the strongest correlation with IGF-1 % decrease (Pearson's $r = -0.357$, $p = 0.002$).

Table 4.

Gene list	IGF1 at diagnosis		IGF1 index at diagnosis		IGF1 % decrease after treatment		Kruskal-Wallis test for CR, PR and NR	Wilcoxon test for CR vs NR	Wilcoxon test for CR vs PR + NR
	Pearson's r	p-value	Pearson's r	p-value	Pearson's r	p-value	p-value	p-value	p-value
<i>SSTR2</i>	-0.104	n.s.	-0.277	0.005	0.120	n.s.	0.064	0.025	0.016
<i>SSTR5</i>	-0.054	n.s.	-0.018	n.s.	-0.113	n.s.	0.338	0.134	0.207
<i>DRD2</i> short isoform	-0.128	n.s.	-0.006	n.s.	0.211	n.s.	0.434	0.249	0.171
<i>DRD2</i> long isoform	-0.173	n.s.	-0.066	n.s.	0.290	0.014	0.353	0.178	0.174
<i>ARRB1</i>	-0.308	0.001	-0.179	n.s.	0.143	n.s.	0.958	0.794	0.976
<i>PLAGL1</i>	0.174	n.s.	0.159	n.s.	0.051	n.s.	0.701	0.912	0.441
<i>RKIP</i>	0.115	n.s.	0.121	n.s.	0.005	n.s.	0.282	0.162	0.303
E-cadherin	-0.286	0.003	-0.225	0.024	0.256	0.031	0.006	0.002	0.001
Ki-67	0.163	n.s.	0.231	0.020	-0.357	0.002	0.029	0.010	0.105
<i>GHRL</i>	-0.002	n.s.	0.044	n.s.	-0.238	0.045	0.723	0.52	0.432
In1-Ghrelin	-0.002	n.s.	-0.018	n.s.	-0.081	n.s.	0.736	0.68	0.406
<i>AIP</i>	-0.026	n.s.	-0.130	n.s.	0.027	n.s.	0.175	0.054	0.046
<i>KLK10</i>	-0.233	0.019	-0.097	n.s.	-0.062	n.s.	0.69	0.587	0.502
<i>SSTR2/SSTR5</i>	-0.132	n.s.	-0.171	n.s.	0.076	n.s.	0.826	0.873	0.548

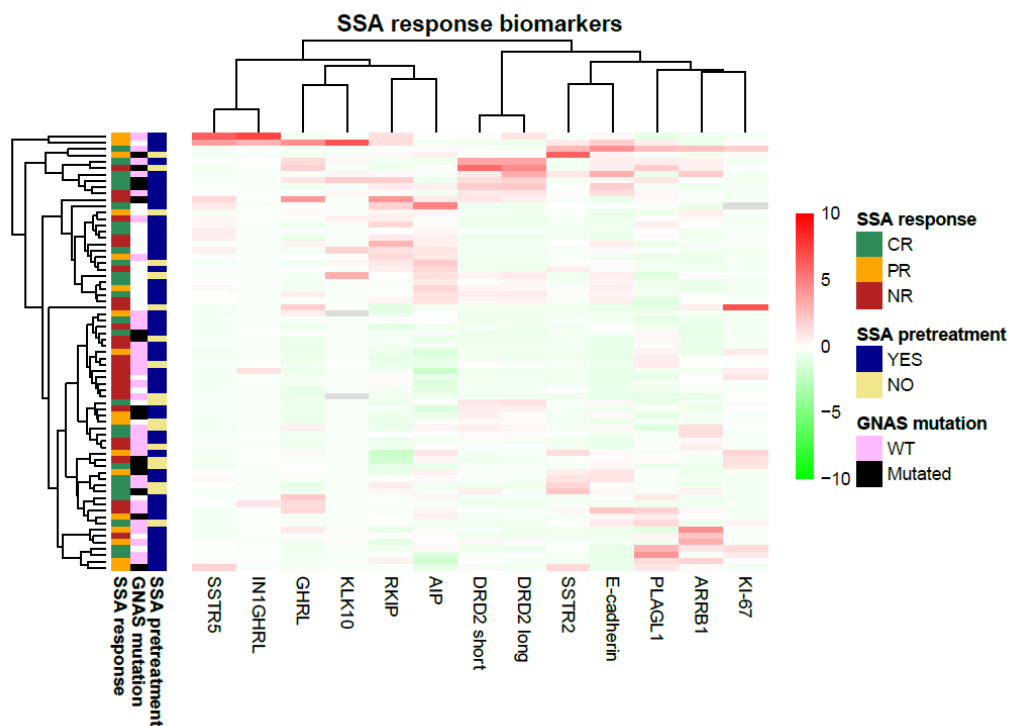
Statistical measures of correlations between each molecular marker and SRLs response. Data is presented as Pearson's correlation's and p-values for continuous variables, and Kruskal-Wallis or Wilcoxon test p-values for categorical variables. Significant p-values are shown in bold. CR: complete responder, PR: partial responder, NR: non-responder, n.s.: non-significant

According to SRLs biochemical categorized response analyzed in 71 patients, 27 patients (38%) were CR, 18 (25%) PR and 26 (37%) were considered NR. In 20 of these 71 cases, treatment with SRLs was only given after surgical procedure, while the rest received SRLs therapy before and after surgery. When an unsupervised hierarchical clustering analysis of the expression of the studied genes was performed in all 71 cases, we found that clustering was not related to or influenced by either the overall SRLs response or the SRLs treatment given before or after surgery (Figure 13). This indicates that as a group, acromegaly patients treated with SRLs do not present a specific pattern of expression in relation to a given response to SRLs, and thus, confirming the heterogeneous nature of somatotropinomas.

GNAS mutation analysis

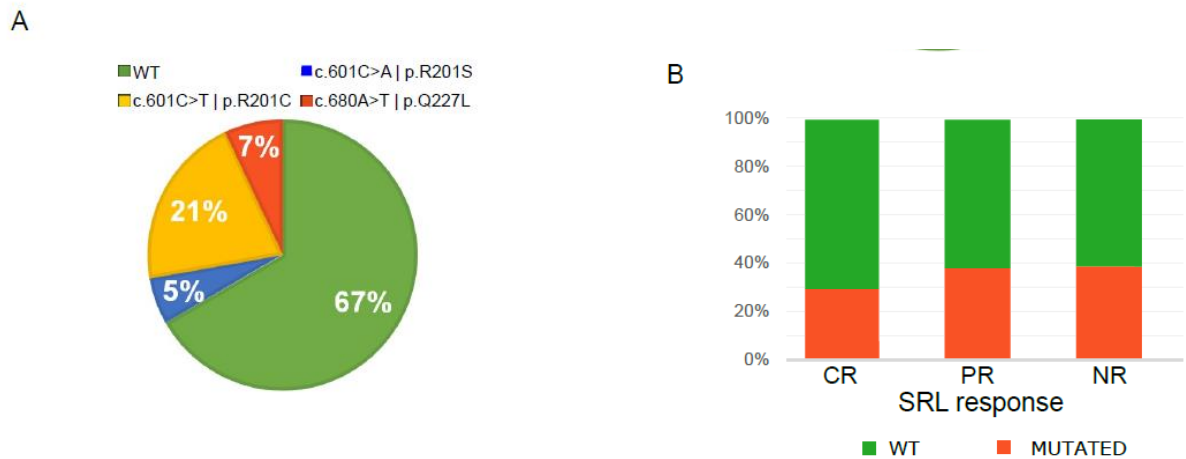
GNAS mutations were studied in a subset of 50 patients and we found mutations in 33%, c.601C>T being the most frequent (Figure 14). SRLs response was not significantly different in those patients presenting GNAS mutations; mutated cases were found in 29% of CR group, 38% of PR and 36% of NR. No clinical variables were related to mutational status regarding comorbidities, tumor size and age among the patients in which the analysis was performed. Neither do we found any association with the expression of the different analyzed markers with GNAS mutations (Figure 13).

Figure 13.



Dendrogram and unsupervised hierarchical clustering heat map of the expression of analyzed SRLs response biomarkers using Ward's minimum variance method and Minkowski distance. For every patient, GNAS mutation, SRLs treatment before surgery and SRLs response category are shown if available (n = 71).

Figure 14.

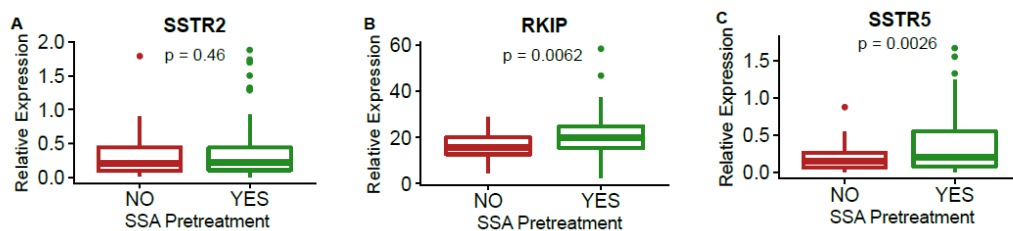


Results from mutational analysis of *GNAS* gene (n = 50). (A) Percentage of the different mutations found in our cohort. (B) Proportion of patients carrying *GNAS* mutations grouped according to therapeutic response to SRLs in complete responders (CR), partial responders (PR) and non-responders (NR).

Influence of SRLs treatment given before or after surgery in the expression of molecular markers

Molecular markers expression was compared between patients who had received SRLs treatment before surgery (n= 67) and not receiving treatment before surgery (n= 33). We found that those in which presurgical treatment was performed showed higher expression levels of *RKIP* and *SSTR5* (p=0.006 and 0.017, respectively) than those not pre-treated (Figure 10). Interestingly, the expression of the *SSTR5* in the pre-treated patients was not different according to the SRLs response (0.46 +/- 0.61, 1.41 +/- 2.39 and 0.51 +/- 0.39, *SSTR5* expression for CR, PR and NR, respectively, p = 0.087), suggesting that the mechanism regulating *SSTR5* expression upon SRLs treatment is different from that reducing GH secretion. By contrast, *SSTR2* expression was not affected by presurgical treatment (p=0.46) at mRNA level. We validated this result by *SSTR2a* immunohistochemistry (IHC) (p=0.28).

Figure 15.



Relative expression of *SSTR2* (A), *RKIP* (B) and *SSTR5* (C) in tumors receiving SRLs or not receiving SRLs before surgery (n = 100).

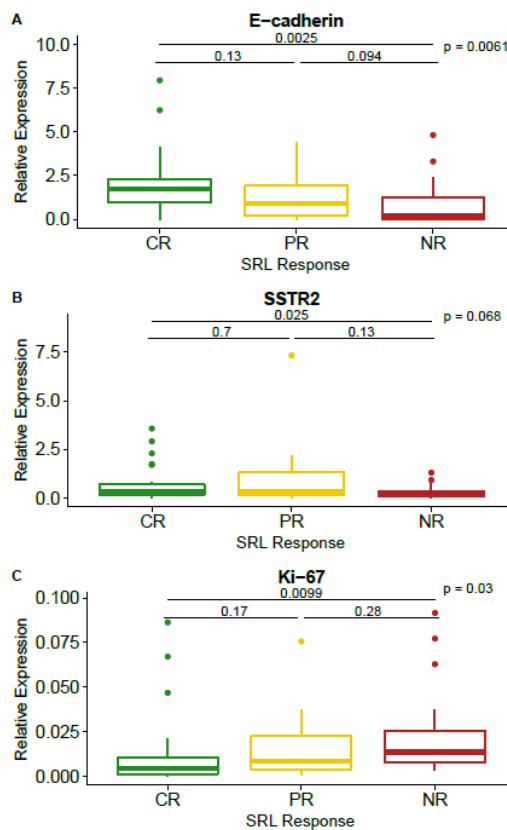
Predictive response to SRLs according to molecular markers expression

Neither *SSTR5*, nor *SSTR5/SSTR2* ratio, *ARRB1*, *PLAGL1*, *GHRL*, In-1-Ghrelin, nor *RKIP* showed any statistical different expression among the three therapeutic response categories when the 71 cases were analyzed as a whole. *AIP* showed a trend towards significance when extreme phenotypes were compared (CR vs NR) with a $p=0.054$ (Table 3).

However, E-cadherin, *SSTR2* and Ki-67 expression were associated with response to SRLs ($p=0.006$, $p=0.068$ –near significance- and $p=0.03$, respectively) (Figure 11). Higher expression of E-cadherin and *SSTR2* was observed in CR group when compared to NR ($p<0.003$ and $p<0.03$, respectively). The opposite pattern was observed for Ki-67, as NR showed higher levels ($p<0.001$). Interestingly, E-cadherin and Ki-67 showed expression differences in a stepwise manner. E-cadherin was the marker that presented more differences between the three different categories of therapeutic response, showing a tendency between PR and NR ($p<0.1$). E-cadherin presented 2.41-fold change between CR and NR, and 1.52 when PR were compared to NR.

In addition, categorical analyses for each normalized gene expression in quintiles were performed to evaluate any nonlinearity in estimated effects. Interestingly, *SSTR2* did not show any further risk increase over the second quintile. Similarly, E-cadherin expression levels did not increase the risk above the third quintile. This finding indicates the non-linearity of gene expression for these two variables, suggesting that SRLs response is related to a specific expression level conferring a permissive effect regarding therapeutic response closer to a categorical behaviour of these biomarkers rather to a dose-response effect.

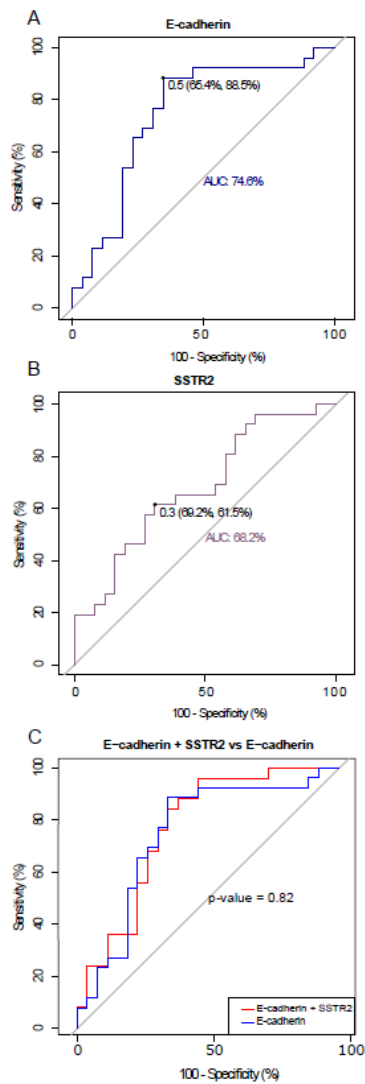
Figure 16.



Relative expression of SSTR2 (A), Ki-67 (B) and E-cadherin (C) in complete responders (CR), partial responders (PR) and non-responders (NR) (n = 71).

When multinomial logistic regression was constructed for extreme phenotypes (NR and CR), *SSTR2* showed an AUC-ROC curve of 0.68, for a cut-off of 0.3, with a sensitivity of 61.5%, specificity of 69.2%, positive predictive value of 66.0% and negative predictive value of 62.6%; the OR for sensitivity towards response to SRLs treatment was 3.729 (IC 97.5:1.242 – 21.619; $p=0.06$, non-significant). In contrast, ROC curve for E-cadherin showed an AUC of 0.74 and a sensitivity of 65.4%, specificity of 88%, positive predictive value of 83.7% and a negative predictive value of 72.6%. The effect sensitivity to SRLs expressed as OR was 1.9319 (IC 97.25: 1.207 – 3.52; $p<0.02$). When Ki-67 was analyzed by the multinomial logistic model no significant results were obtained ($p=0.14$). When ROCs were constructed combining both the expression of *SSTR2* and E-cadherin together no additional predictive power was obtained from the one observed for E-cadherin alone ($p=0.824$) (Figure 17).

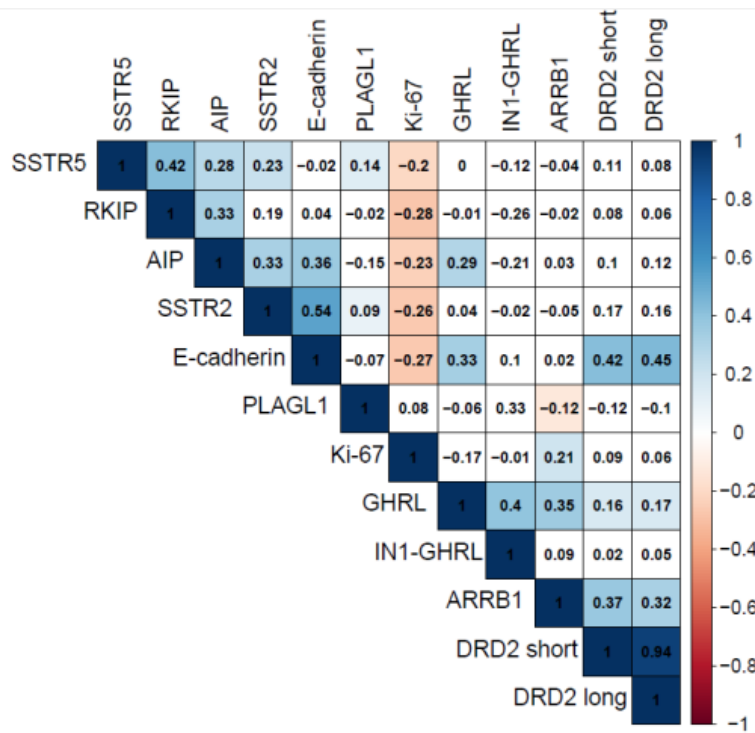
Figure 17.



ROC curves calculated with extreme phenotypes, complete responders (CR) (n = 27) and non-responders (NR) (n = 26) to SRLs for E-cadherin (A) and SSTR2 (B). Comparison of the ROC curve obtained with E-cadherin expression alone or in combination with SSTR2 expression (C).

In addition, gene expression correlations were explored to assess their possible relationships (Figure 18). Interestingly, E-Cadherin and *SSTR2* had a moderate-strong positive correlation $r = 0.539$ ($p < 0.00001$). Other correlations -either positive or negative- were also found between different biomarkers indicating a multiplicity of functional relationship between them.

Figure 18.

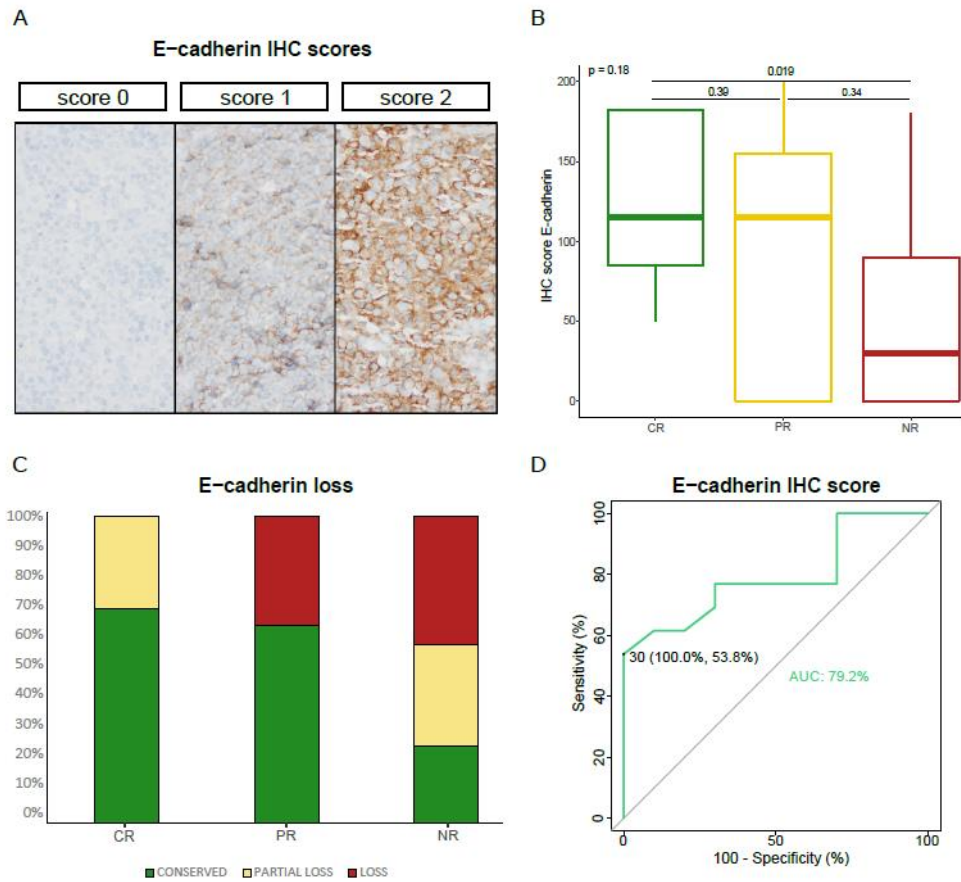


Spearman's correlation matrix among the genes studied (n = 100). Genes are ordered according to hierarchical clustering using complete linkage method. Spearman's correlation coefficients are shown in the matrix; the intensity of color reflects the correlation magnitude.

Validation of E-cadherin expression by immunohistochemistry

We analyzed the protein amount of E-cadherin, SSTR2a and Ki-67 in 47 samples by IHC. E-cadherin H-score correlated with E-cadherin mRNA expression (Pearson's $r = 0.4$, $p < 0.003$), and likewise E-cadherin H-score showed significant differences in SRLs response stratification between CR and NR ($p = 0.019$) (Figure 19 A). Interestingly, E-cadherin loss by IHC defined as non-staining was found in PR and NR but not in CR (Figure 19 B). This behaviour did not occur with partial loss which was found in both CR and NR. When multinomial logistic regression was constructed for extreme phenotypes (NR and CR), E-cadherin H-score showed an AUC-ROC curve of 0.79, for a cut-off of 30, with a sensitivity of 53.8%, specificity of 100%, positive predictive value of 100% and negative predictive value of 81.3% (Figure 19 C). These findings suggest that a completely negative IHC for E-cadherin may discard a complete biochemical control of IGF-1 levels using only first generation SRL.

Figure 19.

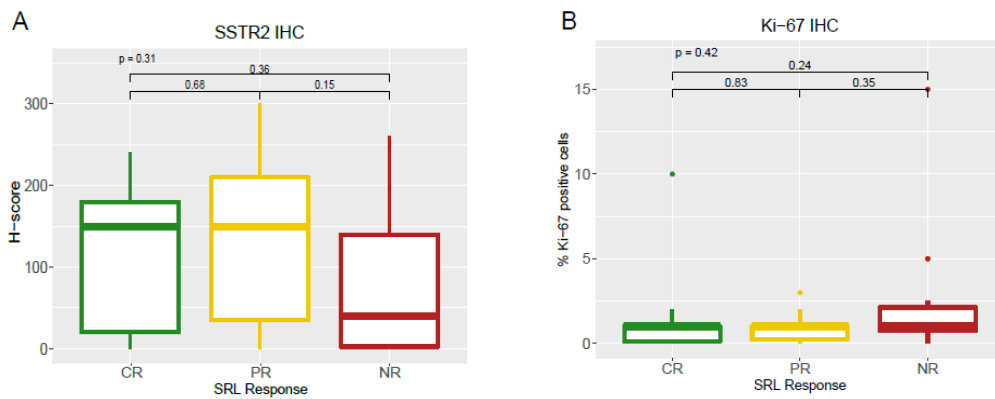


Representative images of E-cadherin immunohistochemical scores in somatotropinomas (200×) (A). E-cadherin IHC score in complete responders (CR), partial responders (PR) and non-responders (NR) (n = 47) (B). E-cadherin IHC categorized in loss, partial loss and conserved in CR, PR and NR (C). ROC curve calculated with extreme phenotypes, complete responders (CR) (n = 13) and non-responders (NR) (n = 14), to SRLs for E-cadherin IHC (D).

SSTR2 H-score also showed a correlation with *SSTR2* mRNA (Pearson's $r=0.46$, $p<0.01$). However the highest *SSTR2* H-scores were found in the PR instead of the CR patients (Figure 20 A). Furthermore, when multinomial logistic regression was constructed for CR vs NR and PR vs NR comparisons, *SSTR2* showed an AUC-ROC curve of 0.62 (sensitivity of 50% and specificity of 77.8%) and an AUC-ROC curve of 0.70 (sensitivity of 60.2% and specificity of 76.2%) respectively, but neither of them were significant ($p=0.41$ and $p=0.19$, respectively).

Ki-67 IHC did not show any significant difference between the groups (Figure 20 B). Moreover, the correlation between mRNA and protein was not significant (Pearson's $r=0.21$, $p=0.144$). We think that the superior performing of the qPCR in comparison to IHC could be explained by the low levels of Ki-67 on these adenomas that make the levels difficult to quantify.

Figure 20.

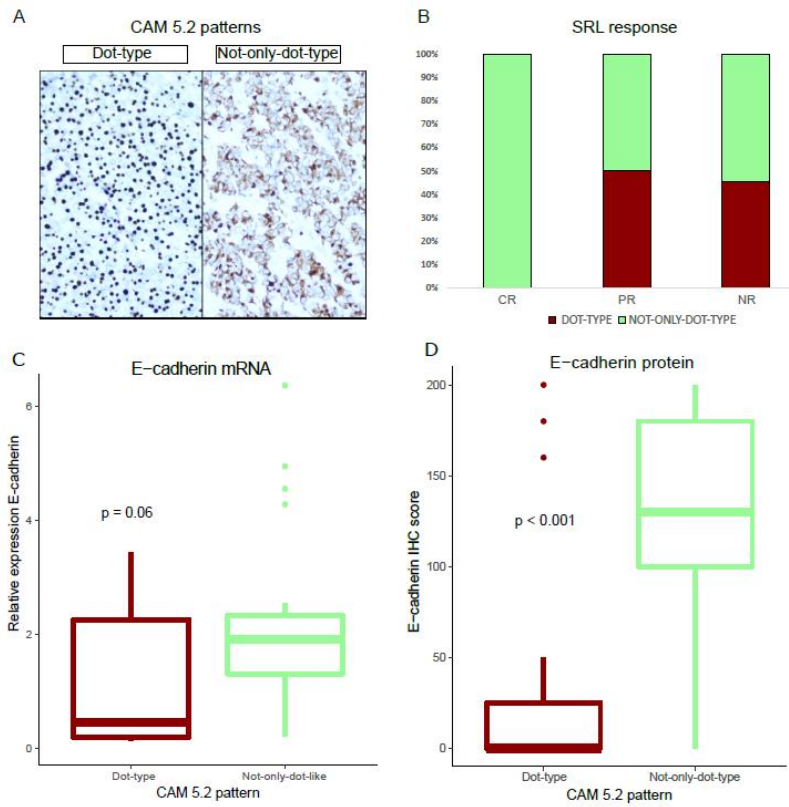


H-score of SSTR2 (a) and % positive Ki-67 cells (b) in complete responders (CR), partial responders (PR) and non-responders (NR) (N = 47).

Influence of histological pattern on SRLs response and E-cadherin expression

Finally, we analyzed the cytokeratin CAM 5.2 by IHC as SRLs response has been linked to histological subtypes (152) and, particularly CAM 5.2 immunostaining (197). Only 15 (32%) out of 47 samples presented a dot-type pattern. However, we observed that CR patients did not present dot-type tumors. Moreover, dot-type immunostaining for CAM 5.2 was negatively related to E-cadherin expression (Figure 21). Altogether, these results suggest a link between the histological pattern, E-cadherin expression and SRLs response in somatotropinomas.

Figure 21.



Representative images of cytokeratin CAM 5.2 immunohistochemical patterns in somatotropinomas (200×) (A). Proportion of tumors with dot-type pattern and not-only-dot-type pattern according to therapeutic response to SRLs (B). Relative expression of E-cadherin (C) and E-cadherin IHC score (D) in dot-type CAM 5.2 pattern and not-only-dot-type.

5.2 Study 2: Association of Epithelial-mesenchymal transition (EMT) markers with response to somatostatin receptor ligands in GH secreting tumors

First generation somatostatin receptor ligands (SRLs) are the first-line treatment in acromegaly. Several studies have linked E-cadherin loss and Epithelial-mesenchymal transition (EMT) with resistance to SRLs in this disease. Our aim was to study the relationship between EMT and SRLs to further understand resistance to treatment in acromegaly. We analyzed the expression of E-cadherin, *SNAI1*, *SNAI2*, *ESRP1*, *RORC*, N-cadherin (*CDH2*), *TWIST1*, *VIM*, *SSTR2*, and Ki-67 in 57 patients bearing GH-producing macroadenomas. E-cadherin loss was not explained by promoter hypermethylation but could be related to an underlying EMT process occurring in GH-secreting tumors, although we did not find a clear mesenchymal phenotype. Instead, we found that the majority of tumors showed a hybrid epithelial/mesenchymal expression phenotype. Interestingly, high *SNAI1* expression levels were related to invasive and SRLs non-responsive tumors. Furthermore, we observed that *RORC* was overexpressed in tumors that had been treated with SRLs before the surgery and this increase was higher in tumors that normalized IGF-1 levels upon SRLs treatment. Thus, *RORC* expression may be used to predict which tumors will normalize postsurgical IGF-1 levels (AUC=81%, p=0.02) in patients presurgically treated with SRL. In conclusion, the analysis of EMT process in acromegaly may be helpful to personalize the treatment of the disease but this factor alone cannot account for the heterogeneous response to SRLs. We propose the inclusion of *RORC* analysis to predict SRLs response and avoid ineffective treatment for months in non-responders.

Manuscript in preparation

Patients

Fifty-seven acromegaly patients from the cohort of 100 patients described in the Materials and Methods section were used in this study. The description of the phenotypic characteristics of the cohort is presented in Table 8. All tumors were macroadenomas. The cohort was formed by 44% of males with a mean age of 46. Of the 57 patients, 45 received SRLs treatment (octreotide or lanreotide) before surgery while 12 did not. SRLs response categorization was done during postsurgical follow-up. Thus, patients were categorized as complete responders (CR = 18) if IGF-1 was normalized, partial responders if IGF-1 decreased >30% from basal status without normalization (PR = 14), or non-responders (NR = 13) if IGF-1 decreased <30%. Evaluation of SRLs response was possible in 45 patients, 40 of which received pre-surgically SRLs treatment. All patients categorized for SRLs response were treated for at least 6 months under maximal effective therapeutic (octreotide or lanreotide) doses according to IGF-1 decrease after the surgical procedure.

Table 5.

PATIENTS CHARACTERISTICS	
Cohort (N)	57
Male / Female	25 / 32
Age, mean \pm SD	45.74 \pm 12.35
Medical Treatment	
SRLs presurgery	45
SRLs response	
Non-Responders	13
Partial Responders	14
Complete Responders	18
NA	12
Tumor Characteristics (%)	
Macroadenoma	47 (82%)
Extrasellar Growth	39 (68%)
Sinus invasion	27 (48%)
Hypopituitarism	19 (33%)
Maximum tumor diameter (mm), mean \pm SD	19.49 \pm 10.03

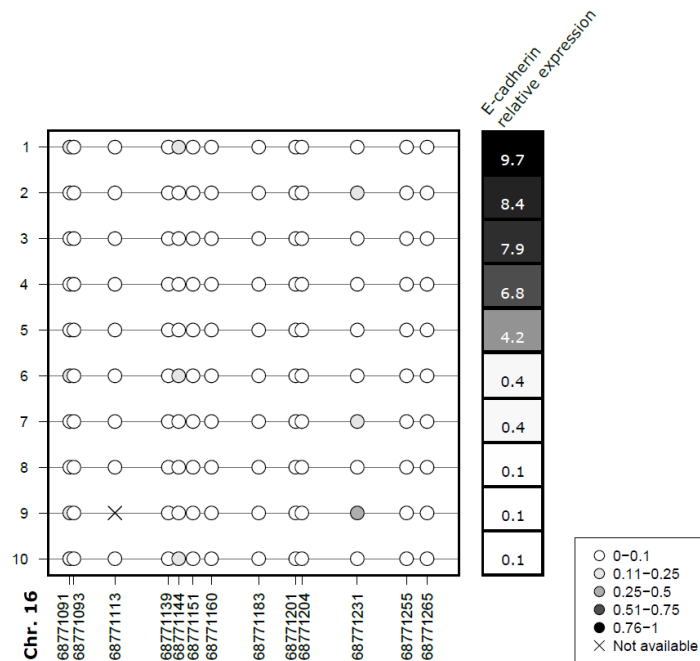
General and clinical characteristics of the patients and tumors included in the study.

E-cadherin expression does not correlate with promoter methylation in acromegaly

In the previous study we validated the potential of E-cadherin as predictor of response to SRLs, so that low levels of E-cadherin were associated with a worse response; however, we did not study the mechanisms underlying E-cadherin repression. The epigenetic silencing of E-cadherin by the hypermethylation of its promoter has been reported in a wide variety of tumor types

(252); thus, to investigate if the loss of E-cadherin expression in GH-producing adenomas is epigenetically regulated, we analyzed the DNA methylation of the promoter. Specifically, we used 10 tumors with extreme levels of E-cadherin expression, 5 with low expression and 5 with high expression, from our previous work (253). Results showed that the promoter of E-cadherin was unmethylated in all the samples with no correlation with expression (Figure 22).

Figure 22.



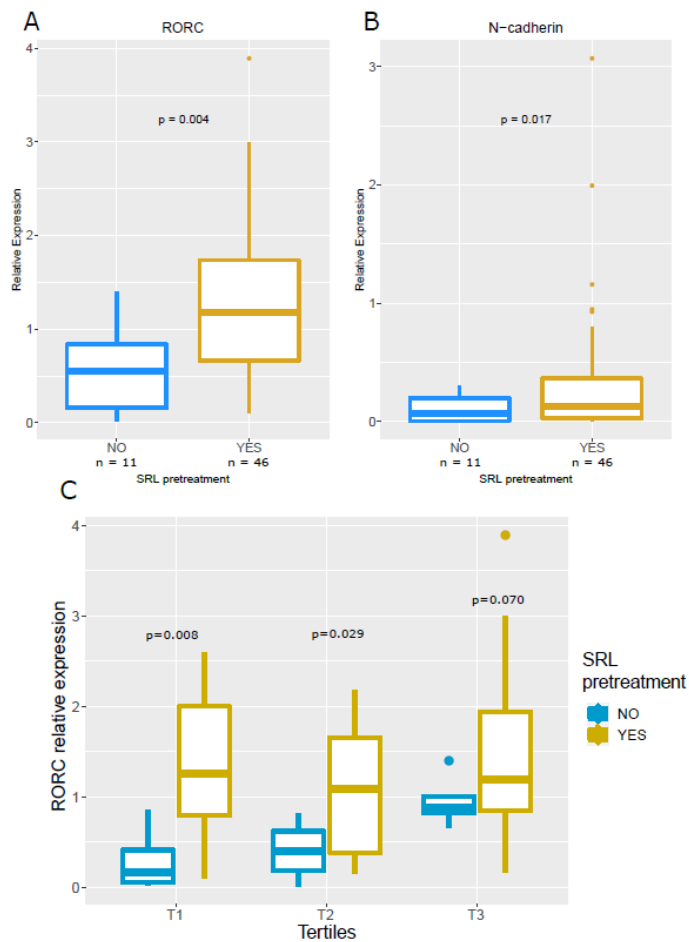
DNA methylation of E-cadherin promoter. Lollipop plot displaying the methylation levels of the CpG sites (circles) within the E-cadherin promoter assessed by bisulfite sequencing in 10 pituitary tumors from acromegalic patients. Levels of DNA methylation are plotted using a grayscale (methylation ranges are indicated) and levels of mRNA E-cadherin expression are shown on the right using a grayscale. The methylation plot was generated using Methylation Plotter (http://maplab.cat/methylation_plotter).

SRLs treatment before surgery affects the expression of *RORC* and N-cadherin

To study the relationship between EMT and response to SRLs we analysed the expression of 8 genes involved in EMT, including the epithelial markers E-cadherin (data obtained in the previous study) and *ESRP1*, the mesenchymal markers vimentin, N-cadherin, *SNAI1*, *SNAI2* and *TWIST1* (the last three being transcription factors), and *RORC*, which has been recently related to EMT in acromegaly (181). Additionally, we included the expression of *SSTR2*, involved in the response to SRL, and Ki-67, a marker of proliferation, in the analysis (data obtained in the previous study). As 80% patients were pre-surgically treated with SRLs, we compared the expression of the different genes between patients who did or did not receive SRLs treatment

before surgery (n=46 and n=11, respectively). We found that *RORC* and N-cadherin showed higher expression levels in tumors pre-surgically treated with SRLs (p=0.004 and p=0.017, respectively) (Figure 23 A-B). The other genes did not show any alteration by pre-surgical SRLs treatment. As the effect of the pre-surgical SRLs treatment on *RORC* expression had been reported to be dependent on E-cadherin levels (181), we divided the E-cadherin mRNA levels of the non-pre-treated and the pre-treated patients into tertiles. *RORC* expression was high and similar in the three tertiles, and differences between non-pre-treated and pre-treated patients were found in the first and second tertiles (FC=4.49, p=0.008, and FC=2.53, p=0.029, respectively), but not in the third tertile (FC=1.83, p=0.070) due to increased *RORC* levels in non-pre-treated patients (Figure 23C).

Figure 23.

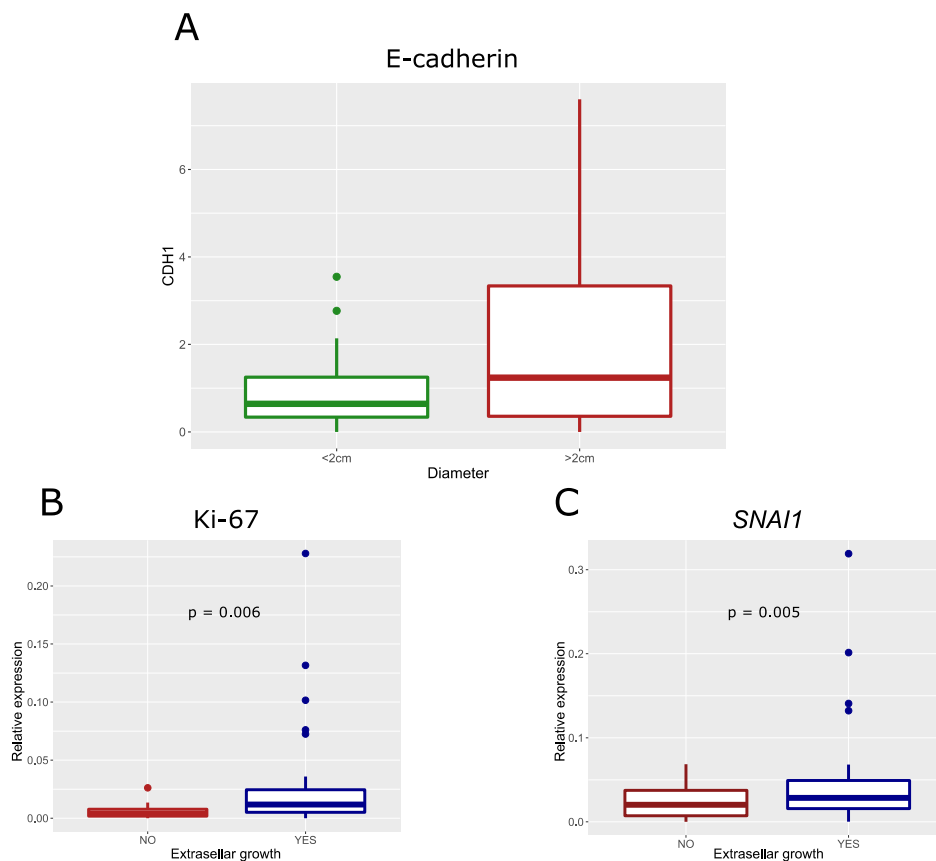


Effect of SRLs pre-surgical treatment in *RORC* and N-cadherin expression. Boxplots showing relative expression of *RORC* (A) and N-cadherin (*CDH2*) (B) in patients treated or not pre-surgically with SRL. (C) *RORC* relative expression of patients that were treated or not with SRLs before according to tertiles of E-cadherin relative expression.

Association of EMT markers with clinical variables

We analyzed the correlation of EMT molecular markers with the different clinical variables. We confirmed our previous results (253) regarding the higher levels of E-cadherin in smaller tumors ($p=0.0041$) (Figure 24 A) and the higher levels of Ki-67 in tumors with extrasellar growth ($p = 0.006$) (Figure 24 B). Interestingly, tumors with extrasellar extension also showed higher levels of *SNAI1* ($p=0.005$) (Figure 24 C). In addition, we found a significant correlation between *RORC* and the percentage decrease of IGF-1 in patients pre-surgically treated with SRLs treatment (Pearson's $r=0.40$, $p=0.007$). In patients without pre-treatment the correlation was very good (Pearson's $r=0.81$) but IGF-1 reduction data was only available for 5 cases. We did not find any association between the other genes and clinical variables.

Figure 24.

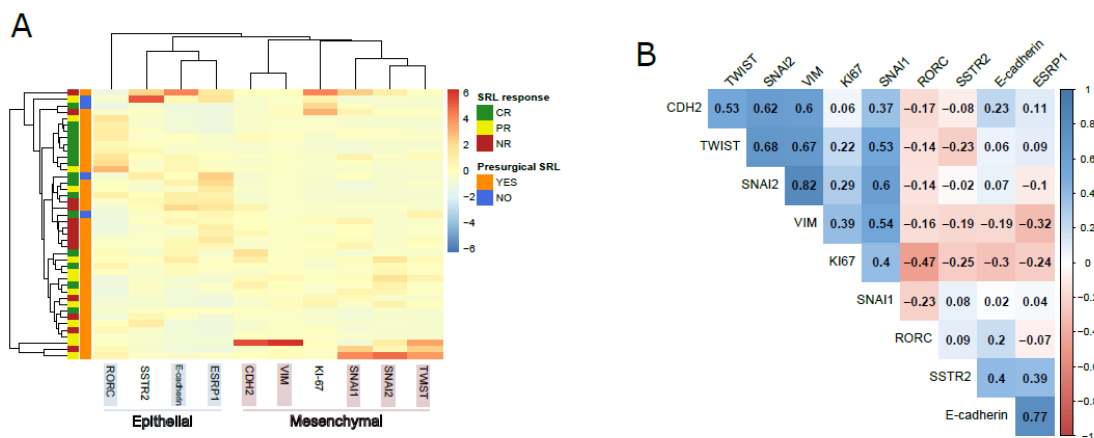


Boxplots showing relative expression of E-cadherin according to tumor size (A); Ki-67 (B) and *SNAI1* (C) according to tumor extrasellar growth.

Somatotropinomas show different EMT states with no association with SRLs response

Unsupervised hierarchical clustering based on the expression of the analyzed genes separated patients in several clusters with different expression patterns (Figure 25 A) that may correspond to different EMT transition states (186,254). Only 3 out of 57 tumors (5.3%) presented a distinctive mesenchymal phenotype indicating a full EMT, while most of the tumors showed a hybrid epithelial/mesenchymal phenotype. This indicates that as a group, acromegaly tumors present different EMT states, adding more heterogeneity to somatotropinomas. Interestingly, mesenchymal genes and Ki-67 clustered together while epithelial genes and *SSTR2* formed another independent cluster, which suggests a coordinated gene program behind the EMT process in acromegaly, as occurs in many other tumors (255). In this line, the analysis of gene expression correlations showed a cluster of positive correlations between epithelial markers and *SSTR2*, and, another cluster between mesenchymal markers and Ki-67 (Figure 25 B). As expected, these two clusters presented negative correlation between them.

Figure 25.



(A) Dendrogram and unsupervised hierarchical clustering heatmap of the expression of the analyzed markers using Minkowski distance and Ward's minimum variance method. For every patient SRLs treatment before surgery and SRLs response category are shown if available. (B) Spearman's correlation matrix among the genes studied (n = 57). Genes are ordered according to hierarchical clustering using complete linkage method. Spearman's correlation coefficients are shown in the matrix; the intensity of color reflects the correlation magnitude.

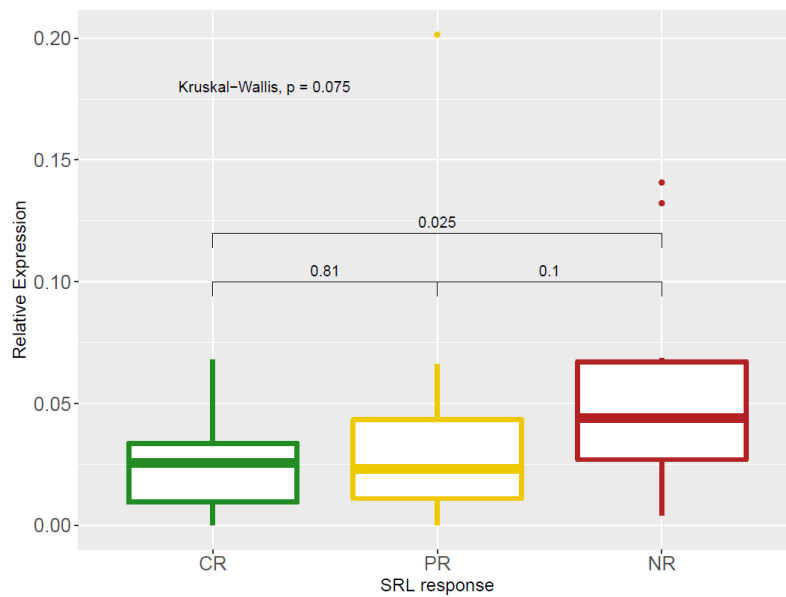
According to SRLs biochemical response available for 45 patients, 18 patients (40%) were complete responders (CR), 14 (31%) partial responders (PR) and 13 (29%) were considered non-responders (NR). In 5 of these 45 cases, treatment with SRLs was only given after surgical procedure, while the rest received SRLs therapy pre- and post-surgically. Unsupervised hierarchical clustering showed a subcluster of CR with remarkably high levels of *RORC*. However,

EMT signature was not able to clearly distinguish the different SRLs response categories. Clustering was not related to pre-surgical SRLs treatment either (Figure 25 A).

Association of *SNAI1* and *RORC* expression with SRLs response

From all EMT markers, *SNAI1* and *RORC* expression were associated with SRLs response categories. *SNAI1* expression presented an increasing trend from CR patients through PR to NR ($p=0.075$) (Figure 26), NR patients having significant higher levels of *SNAI1* than CR ($p=0.025$). The opposite pattern was found for *RORC* in the SRLs pre-treated group ($p=0.003$) (Figure 27 A). Specifically, *RORC* expression was higher in CR compared to PR and NR ($p=0.051$, and $p<0.001$, respectively), while PR and NR, showed differences in *RORC* levels between them but they were not significant ($p=0.082$). The analysis was not performed in the non-pre-treated group because of the low number of cases and the lack of NR. However, we observed higher levels of *RORC* in CR and PR ($p<0.001$ and $p=0.03$, respectively) but not in the NR group ($p=0.42$).

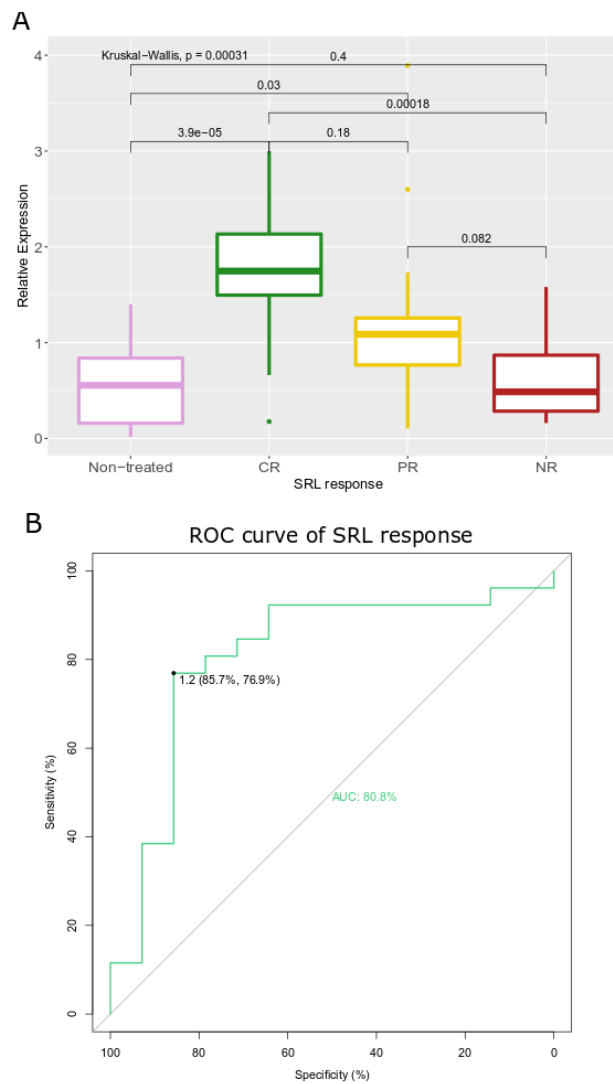
Figure 26.



Boxplots showing relative expression of *SNAI1* according to SRLs response categories.

In addition, categorical analyses for each normalized gene expression in quartiles were performed to evaluate any nonlinearity in estimated effects. Interestingly, *RORC* did not show any further risk increase over the third quartile. This finding indicates the non-linearity of gene expression for *RORC*, suggesting that SRLs response is related to a specific expression level conferring an effect regarding therapeutic response closer to a categorical behaviour of *RORC* rather than to a dose-response effect. When binomial logistic regression was constructed for phenotypes that normalize and do not normalize IGF-1 (CR vs. PR and NR), *RORC* showed an AUC-ROC curve of 0.81, for a cut-off of 1.2, with a sensitivity of 85.7%, specificity of 76.9%, positive predictive value of 75.3% and negative predictive value of 89.5%; the OR for sensitivity towards resistance to SRLs treatment was 0.889 (CI 95: 0.812 - 0.957; $p=0.016$) (Figure 27 B).

Figure 27.



(A) Boxplots showing relative expression of *RORC* according to SRLs response categories. (B) ROC curve for *RORC* calculated with patients that normalized IGF-1 levels (CR) and patients that did not (PR and NR).

Study 3: Molecular determinants of enhanced response to somatostatin receptor ligands after debulking in large GH producing adenomas

Large somatotrophic adenomas depict poor response to somatostatin receptor ligands (SRLs). Debulking has shown to enhance SRLs effect in some but not all cases and tumor volume reduction has been proposed as the main predictor of response. No biological studies have been performed so far in this matter. We aimed to identify molecular markers of response to SRLs after surgical debulking in GH-secreting adenomas.

We performed a multicenter retrospective study for 24 patients bearing large GH producing tumors. Clinical data and SRLs response both before and after surgical debulking were collected and 21 molecular biomarkers of SRLs response were studied in tumor samples by gene expression. From the 21 molecular markers studied, only two of them predicted enhanced SRLs response after surgery. Tumors with improved response to SRLs after surgical debulking showed lower levels of Ki-67 (*MKI67*, FC=0.17 and p=0.008) and higher levels of RAR related orphan receptor C (*RORC*) (FC=3.1 and p<0.001). When a cut-off of no detectable expression was used for Ki-67, the model provided a sensitivity of 100% and a specificity of 52.6% with an area under the curve of 65.8%. Using a cut-off of 2 units of relative expression of *RORC*, the prediction model showed 100% of sensitivity and specificity. Thus, high levels of *RORC* and low levels of Ki-67 identify improved SRLs response after surgical debulking in large somatotrophic adenomas. To determine their expression would facilitate medical treatment decision making after surgery.

This study has been published:

Joan Gil, Montserrat Marqués-Pamies, Mireia Jordà, Carmen Fajardo-Montañana, Araceli García-Martínez, Miguel Sampedro, Guillermo Serra, Isabel Salinas, Alberto Blanco, Elena Valassi, Gemma Sesmilo, Cristina Carrato, Rosa Cámara, Cristina Lamas, Paula Casano-Sancho, Clara V Alvarez, Ignacio Bernabéu, Susan M Webb, Antonio Picó, Mónica Marazuela, Manel Puig-Domingo. Molecular determinants of enhanced response to somatostatin receptor ligands after debulking in large GH producing adenomas. Clin Endocrinol (Oxf). 2020 Sep 26. doi: 10.1111/cen.14339.. PMID: 32978826.

Patients

In this study we included 24 patients from the cohort of 100 patients described in the Materials and Methods section who had GH-secreting tumors that received multiple surgical treatments as well as SRLs before and after surgery. The main inclusion criterion was that all patients had received SRLs treatment (octreotide or lanreotide long acting formulations) before the first surgery for at least 6 months under maximal effective therapeutic doses according to IGF-1 values but none of them were cured after surgery, thus SRLs treatment was restarted 3 months after surgery and maintained thereafter for at least 6 months under maximal effective therapeutic doses. None of these patients had received radiotherapy at the time of the study. As it might be expected, this subsample was enriched in tumors more invasive (Knosp grade >2) and larger than the overall REMAH cohort, all tumors being macroadenomas with a mean largest diameter of 30.7 ± 11.1 mm at diagnosis. Surgical debulking achieved > 50% reduction of the original tumor mass in 70% the cases. The mean largest diameter after surgery was 19.07 ± 9.05 mm; 58.3% of the patients were males with an average age of 42.7 ± 15.2 years. In those cases in which multiple surgeries were performed, the tumor sample obtained from the first surgery was the sample analyzed.

Patients were categorized according to the therapeutic response to SRLs before and after surgical treatment as complete responders (CR) if IGF-1 was normal, partial responders (PR) if IGF-1 was reduced by more than 30% from diagnosis levels but without achieving hormonal control, or non-responders (NR) when IGF-1 reduction observed during SRLs treatment was less than 30% at 6 months follow-up and at full SRLs dose. We used these different response categories to define subsequent medical treatment modalities, in which CR was kept on SRLs as monotherapy, PR in combination therapy either with dopamine agonists or pegvisomant, and NR were assigned to monotherapy with pegvisomant.

Effects of surgical debulking on SRLs response

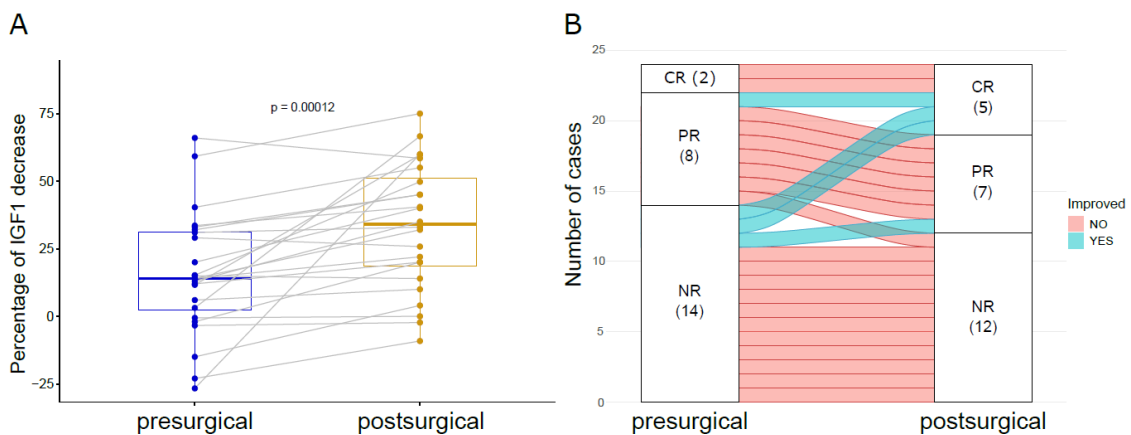
During the preoperative period SRLs treatment accounted for a normalization of IGF-1 in 2 patients (complete responder category -CR-); in 8 patients, the therapeutic response was partial (PR), and in 14 patients it was insufficient (NR). An enhanced IGF-1 reduction in comparison to a preoperative diminution was observed in the majority of patients when SRLs treatment was reinstated after surgical treatment. Thus, the decrease of IGF-1 levels from baseline was lower in the presurgical than in the postsurgical treatment phase ($15.6\% \pm 23.7\%$ versus $33.51\% \pm 24.4\%$). Baseline was considered IGF-1 at diagnosis for the presurgical stage and IGF-1 value at

3 months after surgery and not receiving any medical therapy for the postsurgical phase (Fig. 28 A). Moreover, in 18 out of 24 patients the percentage value of IGF-1 reduction after surgery increased, while in 5 of them the final IGF-1 levels after the second SRLs course did not change. One patient showed a decrease of IGF-1 reduction after surgery, although this patient presented a normalized IGF-1 before and after the surgery with SRLs treatment.

SRLs response category changes after debulking

Patients were classified as complete responders (CR), partial responders (PR) or non-responders (NR) if IGF-1 was normal, showed a reduction of more than 30% from diagnosis levels but without achieving hormonal control, or was reduced by less than 30% at 6 months of follow-up, respectively (119,120). After surgical debulking, 4 out of 24 patients (16.6%) changed from one category to another, all improving. Two patients changed from NR to CR, one from PR to CR and another patient from NR to PR (Fig. 28 B).

Figure 28.



Evaluation of SRLs response before and after debulking. Percentage of IGF-1 decrease upon SRLs treatment before and after the surgery (A). Alluvial plot that represent the change between SRLs response categories before and after partial tumor removal (B).

Molecular determinants associated to SRLs enhanced response after surgical debulking

When comparing the characteristics of the 4 patients that improved, most after SRLs by changing their response category against those that did not (Table 6), no differences were found regarding clinical phenotype, radiological parameters and tumor behavior, nor residual tumor left.

Table 6.

	Improved (n=4)	Not improved (n=20)	p.value
Sex (Men %)	75%	55%	0.61
Age	46.32±6.42	41.97±16.47	0.39
BMI	27.44±4.22	27.97±2.02	0.75
Biochemical characteristics at diagnosis			
Basal GH	97.6±124.96	30.93±27.72	0.44
IGF-1 levels	1131.25±315.14	929.69±472.61	0.34
Tumor characteristics			
GNAS mutation	50%	15%	0.18
Max diameter at diagnosis	30.25±5.25	31.05±11.89	0.83
Extrasellar growth	75%	90%	0.44
Sinus invasion	75%	85%	0.54
Hypointense T2 signal	25%	40%	1
Visual alterations	0%	50%	0.11
Hypopituitarism	25%	55%	0.59
Dot-like CAM 5.2 IHC	50%	55%	1
Postsurgical characteristics			
Max diameter of surgical remnant	19.67 ± 9.24	16.11 ± 7.44	0.59
IGF-1 levels after surgery	696.75 ± 393.25	711.69 ± 318.96	0.95

General and clinical characteristics of the patients that improve or not the SRLs category upon postsurgical SRLs treatment. Statistical test revealed no significant differences between clinical characteristics before and after surgery. The numerical variables were presented using the mean ± Standard Deviation. BMI: body mass index. IHC: Immunohistochemistry.

Furthermore, we searched for molecular differences in 20 previously described SRLs response biomarkers and epithelial–mesenchymal transition (EMT) markers (Table 7).

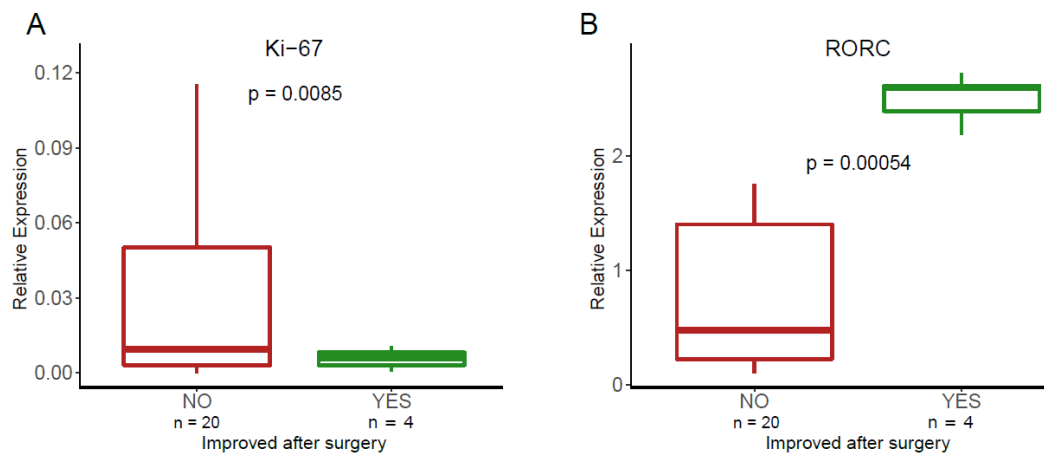
Table 7.

	Improved (n=4)	Not improved (n=20)	p.value
<i>SSTR2</i>	0.450±0.126	0.498±0.149	0.811
<i>SSTR3</i>	0.099±0.077	0.466±0.316	0.275
<i>SSTR5</i>	0.870±0.512	1.127±0.743	0.779
<i>DRD2</i> short isoform	2.364±1.136	0.680±0.182	0.235
<i>DRD2</i> long isoform	2.238±1.011	0.760±0.185	0.241
<i>ARRB1</i>	0.214±0.039	0.198±0.028	0.743
<i>PLAGL1</i>	2.817±0.732	4.261±0.745	0.195
<i>PEBP1</i>	32.068±9.625	19.082±1.568	0.271
E-cadherin (<i>CDH1</i>)	0.893±0.268	0.711±0.487	0.756
Ki-67	0.005±0.002	0.031±0.008	0.008*
<i>GHRL</i>	0.038±0.021	0.020±0.005	0.449
<i>AIP</i>	2.138±0.442	1.689±0.172	0.398
<i>In1-GHRL</i>	0.038±0.026	0.095±0.068	0.437
<i>KLK10</i>	0.001±0.000	0.003±0.002	0.343
<i>SNAI1</i>	0.040±0.014	0.027 ±0.009	0.483
<i>SNAI2</i>	0.036±0.017	0.039±0.023	0.917
<i>ESRP1</i>	0.375±0.349	0.854 ± 0.360	0.301
<i>RORC</i>	2.472±0.143	0.854 ±0.280	0.000*
<i>CDH2</i>	0.079±0.032	0.142 ±0.047	0.488
<i>VIM</i>	1.142±0.337	1.157 ±0.352	0.987
<i>TWIST</i>	0.008±0.004	0.005±0.001	0.542

surgery debulking and patients that did not receive surgery. Values are expressed as mean ± standard error.

We found that the tumors that improved SRLs response category after surgical debulking showed lower levels of Ki-67 mRNA expression (FC=0.17 and p=0.008) and higher levels of RORC (FC=3.1 and p<0.001) (Fig. 29).

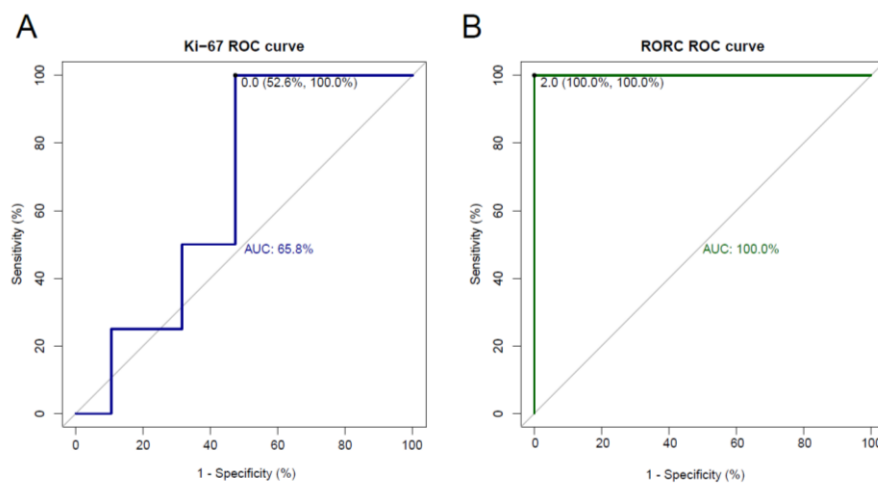
Figure 29.



Boxplots showing relative expression of Ki-67 (A) and RORC (B) in patients that improved after debulking (n=4) and patients that did not (n=20).

We also did find the same difference in Ki-67 levels by IHC, the mean value of Ki-67 positive cells being 1% for patients that improved SRLs category response and 3.1% for patients that did not; however, the difference was not significant ($p = 0.074$). Furthermore, when a cut-off of no detectable expression was used for Ki-67, the model provided a sensitivity of 100% and a specificity of 52.6% with an area under the curve (AUC) of 65.8% (Fig 27A). But, notably, using a cut-off of 2 units of relative expression of RORC, a model with 100% of specificity, sensitivity and AUC was obtained (Fig 27B).

Figure 30.



ROC curve calculated with patients that did not improved after debulking (n=20) and patients that did it (n=20) for Ki-67 (A) and RORC (B).

5.4 Study 4: Data mining analyses for precision medicine in acromegaly

Predicting which acromegaly patients could benefit from somatostatin receptor ligands (SRLs) is crucial to avoid months of ineffective treatment for non-responding cases. Although many biomarkers linked to SRLs response have been identified, there is no consensus criterion on how to assign pharmacologic treatment according to biomarker levels. We used advanced mathematical modelling and artificial intelligence to provide better predictive tools for a more accurate acromegaly patient stratification regarding the ability to respond to SRL. Different models of patient stratification were obtained regarding SRLs response, with a much higher accuracy when the studied cohort is fragmented according to relevant clinical characteristics. Considering all the models, a patient stratification based on the extrasellar growth of the tumor, sex, age and the expression of E-cadherin, *GHRL*, *IN1-GHRL*, *DRD2*, *SSTR5* and *PEBP1* is proposed, with accuracies that stand between 71 to 95%. Furthermore, we show an association between extrasellar growth and high BMI for SRLs non-responding patients. The use of data mining is necessary for implementation of personalized medicine in acromegaly and requires an interdisciplinary effort between computer science, mathematics, biology and medicine. This new methodology opens a door to more precise personalized medicine for acromegaly patients.

Manuscript in preparation

Patients

In this study, we used the whole cohort of 100 patients described in Material and Methods section. The 71 patients with evaluable SRLs response were categorized according to therapeutic response to SRLs as complete response (CR = 27), partial (PR = 18) or non-responders (NR =26) if IGF-1 was normal, between >2<3 SDS or >3 SDS IGF-1 at 6 months of follow-up, respectively.

Phenotypical characterization according to SRLs response

For the data mining analysis we used the data generated in Study 1. However, before data mining analysis, a phenotypical characterization was performed according to SRLs response to verify that no dependent association was not reported and taken into account for the final data mining analysis. The analysis showed that SRLs resistance was strongly associated with tumor extrasellar extension (Pearson χ^2 p-value: 0.004) as shown in Table 8. Furthermore, NR patients presented more hypopituitarism and sinus invasion before surgery in contrast to CR or PR (Pearson χ^2 p-value: 0.01 and 0.05, respectively).

Table 8.

	Group	SRLs response ^a			Pearson χ^2 p-value ^b
		CR	PR	NR	
Presurgical hypopituitarism	Yes	42%	15%	55%	0.01
	No	68%	85%	45%	
Presurgical visual alterations	Yes	13%	27%	19%	0.62
	No	87%	73%	81%	
T2 signal intensity	Hypointense	31%	22%	36%	0.90
	Isointense	38%	56%	36%	
	Hyperintense	31%	22%	28%	
T1 signal intensity	Hypointense	61%	40%	53%	0.75
	Isointense	39%	50%	38%	
	Hyperintense	0%	10%	8%	
Gender	Male	46%	35%	62%	0.07
	Female	54%	65%	38%	
GNAS mutation	Mutated	29%	38%	36%	0.83
	WT	71%	62%	64%	
Sinus Invasion	Yes	22%	35%	59%	0.05
	No	78%	65%	41%	
Extrasellar growth	Yes	48%	60%	95%	0.004
	No	52%	40%	5%	

Clinical categorical variables related to SRLs response. ^a SRLs response columns indicate the percentage of patients with CR, PR, or NR dictated by the presence or absence of the clinical condition. ^b Pearson χ^2 p-values are shown. Statistically significant values (p-value <0.05) are reported in bold.

Additionally, differences in the value of quantitative clinical variables according to SRLs response categories were evaluated for the studied comparisons and the results are displayed in Table 9. High BMI and IGF-1 levels at diagnosis were associated with NR patients.

Table 9.

Variable	CR + PR vs NR		CR vs NR		PR vs NR		CR vs PR	
	p-value	Log2FC	p-value	Log2FC	p-value	Log2FC	p-value	Log2FC
IGF-1 diagnosis	0.035	-0.33	0.007	-0.47	0.722	-0.16	0.081	-0.31
IGF-1 index diagnosis	0.051	-0.41	0.086	-0.39	0.063	-0.43	0.838	0.04
Basal GH	0.590	1.04	0.134	0.94	0.429	1.17	0.134	-0.22
GH after OGTT	0.622	1.27	0.728	1.29	0.633	1.25	0.941	0.03
BMI	0.094	-0.13	0.044	-0.17	0.452	-0.07	0.316	-0.10
Maximum diameter	0.178	-0.27	0.092	-0.35	0.532	-0.16	0.708	-0.19
Age	0.197	0.14	0.272	0.13	0.802	-0.03	0.276	0.16

Clinical numerical variables showing differences between the evaluated comparisons. T-test or Wilcoxon-test p-values are shown. Statistically significant values (p-value <0.05) are reported in bold. Log2FC: Log2 Fold Change

Algorithms classifying SRLs response in acromegaly patients

Several algorithms were identified for the discrimination of patients regarding SRLs response (cross-validated p-value < 0.05); those displaying the highest accuracy are shown in Table 10. All the significant predictive models are presented at Supplementary Table S1. The strongest and most accurate single predictive biomarker for SRLs response was E-cadherin, as it was the only marker discriminating between 3 of the 4 comparisons categories evaluated: 1) CR vs PR accuracy 65.8% at cut-off values of 0.513 and 0.007; 2) CR vs NR accuracy 73.1% at cut-off value 0.535; 3) CR+PR vs NR accuracy 62.6% at cut-off values of 0.348 and 0.013. Moreover, E-cadherin was also found in many of the dual and triad panels obtained by the analysis. After E-cadherin, the most frequent contributor to enhance classification power was *SSTR2*. The combination of E-cadherin and *SSTR2* increased the accuracy by 6-7% more than E-cadherin alone. The addition of *AIP* (172) or *In1-GHRL* (180) showed a moderate enhancement of the classification power, reaching 75% of accuracy. Finally, adding *PEBP1* (171) displayed nearly a 70% accuracy at cut-off 15.56, specifically in the discrimination between CR and PR.

Table 10.

Evaluated comparison	Panel of classifiers	ACC	p-value
CR+PR vs NR	E-cadherin	62.61%	0.027
	<i>GHRL</i>	67.26%	0.002
	<i>SSTR2</i> + E-cadherin	69.95%	0.001
CR vs NR	<i>DRD2</i> long isoform	69.23%	0.006
	E-cadherin	73.08%	0.001
	<i>SSTR2</i> + E-cadherin + <i>AIP</i>	75.00%	1.95E-04
	<i>SSTR2</i> + E-cadherin + <i>IN1GHRL</i>	75.00%	2.66E-04
PR vs NR	<i>SSTR2</i> + Ki-67	67.87%	0.02
	<i>SSTR2</i> + <i>SSTR5</i> + <i>ARRB1</i>	69.68%	0.004
CR vs PR	E-cadherin	65.84%	0.028
	<i>PEBP1</i>	69.68%	0.004

Best classifiers in the whole cohort. All individual classifiers and those panels with 2 or 3 classifiers that display an improvement in accuracy are presented in this table. ACC: Accuracy.

For those panels including more than one marker, in pairs or triads, cut-off values showed dynamic values (the values change with respect the variables of the model as a function because the variables are interdependent) as shown in Supplementary Figure S2 B-C.

Fragmented population analysis achieves higher predictive accuracy

For analysis purposes, the cohort was subsequently segregated according to different clinical and biological variables, such as sex, extrasellar growth of the tumor, radiological sinus invasion, the mutational status of *GNAS*, and pre-surgical SRLs treatment. The fragmented population studied is detailed in Supplementary Table 2.

The first analysis fragmented the cohort according to SRLs pre-treatment or not before surgery. In those patients not receiving pre-surgical SRLs therapy, *SSTR2* and E-cadherin expression together with age achieved 100% accuracy in discriminating the 3 response categories. However, the number of patients with no pre-surgical treatment was very low in our cohort; thus, this result requires further confirmation with higher number of cases. In pre-surgically treated patients, *PEBP1* expression was added in some models, with 77% accuracy of discrimination between CR vs PR (shown in Table 11 A).

When fragmenting according to extrasellar growth, *GHRL* (180) discriminated between CR and PR vs NR with extrasellar growth (accuracy 72%). Furthermore, 2 panels of classifiers also discriminated between CR and PR, both containing *SSTR5* expression in combination with *PEBP1* or In1-GHRL and E-cadherin with an overall accuracy ranging from 80-88% (shown in Table 11 B).

Fragmenting the population by tumor sinus invasion identified *AIP* at a cut-off value of 1.404 as an individual marker, for discrimination between CR and PR vs NR patients with an accuracy of 77% (shown in Table 11 C).

Analyzing the population according to sex increased the accuracy of SRLs response classification. Among females, *PEBP1* in different combinations with E-cadherin, *GHRL*, *AIP* and *SSTR2*, at different dynamic cut-off values, showed an accuracy of 73-80%. In males, age and E-cadherin levels displayed 81-85% discriminating accuracy between CR and PR vs NR patients (shown in Table 11 D).

Finally, when fragmenting according to the *GNAS* mutational status, the same molecules appeared as predictors (E-cadherin, Ki-67 and *PEBP1*) at accuracy levels ranging 72-90% (shown in Table 11 E).

Table 11.

Fragmenting condition	Evaluated comparison	Fragmented population N ^a	Best panel of classifiers	ACC	p-value	
A. SRLs presurgical treatment	CR + PR vs NR	No (9 vs 7)	<i>PLAGL1</i> + <i>PEBP1</i> + E-cadherin	88.89%	0.003	
		Yes (33 vs 19)	<i>SSTR5</i> + <i>DRD2</i> long isoform + E-cadherin	70.65%	0.001	
	CR vs NR	No (6 vs 7)	Age + <i>SSTR2</i> + E-cadherin	100.00%	5.83E-04	
		Yes (20 vs 19)	<i>PLAGL1</i> + <i>IN1GHRL</i> + E-cadherin	76.97%	9.43E-04	
	PR vs NR	No (3 vs 7)	Not found	-	-	
		Yes (13 vs 19)	<i>SSTR5</i> + <i>PEBP1</i>	74.29%	0.003	
	CR vs PR	No (6 vs 3)	<i>SSTR2</i> + E-cadherin	100%	0.012	
		Yes (20 vs 13)	<i>PEBP1</i> + <i>IN1GHRL</i>	76.82%	4.02E-04	
	B. Extrasellar growth	CR + PR vs NR	No (18 vs 1)	Not found	-	-
			Yes (20 vs 19)	<i>GHRL</i>	71.32%	0.005
CR vs NR		No (12 vs 1)	Not found	-	-	
		Yes (11 vs 19)	Not found	-	-	
PR vs NR		No (6 vs 1)	Not found	-	-	
		Yes (9 vs 19)	Not found	-	-	
CR vs PR		No (12 vs 6)	<i>SSTR5</i> + <i>PEBP1</i>	87.50%	0.004	
		Yes (11 vs 9)	<i>SSTR5</i> + <i>IN1GHRL</i> + E-cadherin	79.80%	0.012	
C. Sinus Invasion	CR + PR vs NR	No (26 vs 7)	Not found	-	-	
		Yes (12 vs 10)	<i>AIP</i>	77.50%	0.015	

	CR vs NR	No (18 vs 7)	<i>SSTR2 + ARRB1 + KLK10</i>	81.75%	0.007
		Yes (5 vs 10)	<i>PEBP1 + AIP + IN1GHRL</i>	85.00%	0.017
	PR vs NR	No (8 vs 7)	Ki-67 + <i>IN1GHRL</i>	85.71%	0.007
		Yes (7 vs 10)	Not found	-	-
	CR vs PR	No (18 vs 8)	<i>SSTR2 + IN1GHRL + KLK10</i>	86.61%	0.009
		Yes (5 vs 7)	Not found	-	-
D. Gender	CR + PR vs NR	Female (25 vs 10)	<i>PEBP1 + GHRL</i>	73.78%	0.007
		Male (18 vs 16)	Age + E-cadherin	80.83%	0.001
	CR vs NR	Female (14 vs 10)	<i>PEBP1 + E-cadherin + AIP</i>	79.76%	0.005
		Male (12 vs 16)	Age + <i>PLAGL1 + E-cadherin</i>	85.45%	4.91E-04
	PR vs NR	Female (11 vs 10)	Not found	-	-
		Male (6 vs 16)	<i>SSTR2 + PLAGL1 + GHRL/ARRB1</i>	85.35%	0.003
	CR vs PR	Female (14 vs 11)	<i>SSTR2 + PEBP1</i>	74.68%	0.016
		Male (12 vs 6)	<i>DRD2</i> short and long isoform + E-cadherin	80.00%	0.018
E. GNAS mutational status	CR + PR vs NR	WT (19 vs 14)	<i>SSTR2 + DRD2</i> long isoform + <i>ARRB1</i>	77.07%	0.003
		Mutated (10 vs 5)	Not found	-	-
	CR vs NR	WT (10 vs 14)	Not found	-	-
		Mutated (5 vs 5)	<i>PLAGL1 + E-cadherin + Ki-67</i>	90.00%	0.024
	PR vs NR	WT (9 vs 14)	<i>SSTR5 + ARRB1</i>	72.22%	0.014
		Mutated (5 vs 5)	Not found	-	-
	CR vs PR	WT (10 vs 9)	<i>PEBP1 + E-cadherin</i>	84.44%	0.004
		Mutated (5 vs 5)	Not found	-	-

Best classifiers in patients with or without SRLs pre-surgical treatment, extrasellar growth, sinus invasion, biological sex and GNAS mutational status. For each subgroup, the best panel/s of classifiers (with accuracy higher than the maximal one achieved by the classifiers using the whole cohort without fragmentation) in each comparison are shown. ^aThe third column refers to the condition in the first column. ACC: Accuracy.

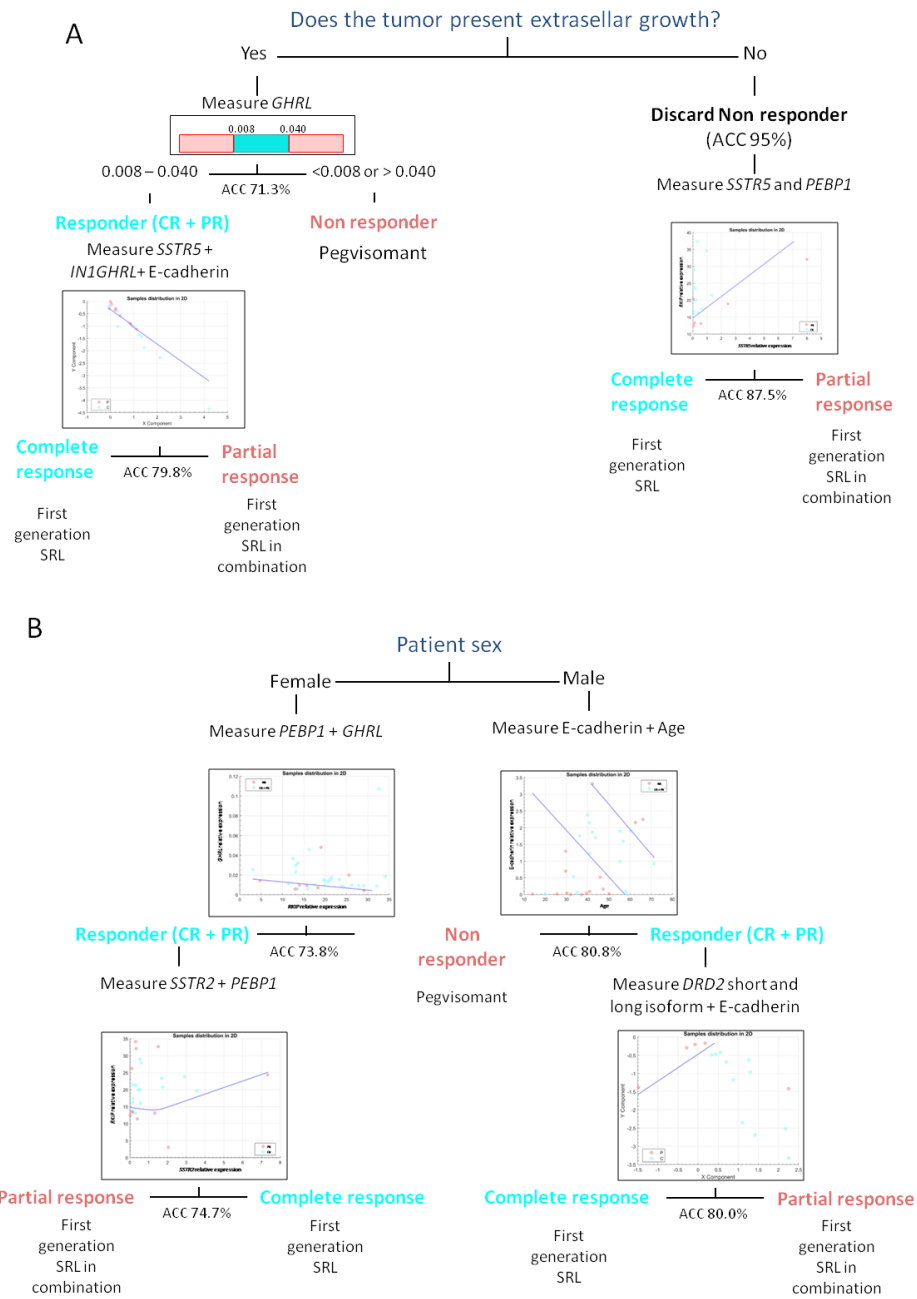
Overall, the algorithms generated achieved a much higher cross-validated accuracy in the fragmented rather than in the whole cohort for prediction of SRLs response (shown in Supplementary Table S3).

Decision tree therapeutic algorithms based on mathematical modelling

The present analyses allow the development of decision trees that can be used in clinical practice for individual patients. Two trees were formulated. The first one is based on the extrasellar tumor growth and different molecular biomarkers (Figure 32 A). A patient without extrasellar growth is discarded as NR with an accuracy of 95%, and for distinction between CR and PR, the measurement of *PEBP1* and *SSTR5* is required achieving an accuracy of 87.5%. When tumor extrasellar growth is present the decision tree segregates NR patients from responders (CR and PR) using levels of *GHRL* expression with an accuracy of 71.3%. To differentiate between CR and PR, *SSTR5*, In1-GHRL and E-cadherin should be measured, (accuracy of 79.8%). A second tree based on the patient's sex showed an accuracy of 73.8-80.8% to distinguish between NR, CR and PR patients, being higher for men than for women (Figure 32 B). Detailed mathematical information regarding these decision trees such as cut-off values can be found in Supplementary Figures S2-8.

Both algorithms show a high accuracy to identify NR patients (accuracy ranging from 71.3% to 95%) which is particularly important since NR are the patients that suffer the largest delay using the current therapeutic decision chart. In all cases, measuring the expression of one or two molecules would be enough to define the response markers for this type of patient. The accuracy to distinguish between CR and PR patients is lower except for patients without extrasellar growth, thus we recommend the use of these algorithms specially to identify NR patients.

Figure 32.



Best therapeutic tree decision algorithms based on mathematical modelling. (A) Decision tree to determine the first line drug for a given acromegaly patient based on the extrasellar tumor growth and molecular information. A patient without extrasellar growth is automatically classified as CR/PR without performing any molecular analysis (NR category is discarded with an accuracy of 95%). Then, by measuring the gene expression of *SSTR5* and *PEBP1* a clinician would be able to assign the right treatment with an accuracy of 87.5%. If the tumor has extrasellar growth, the gene expression of *GHRL* should be measured. If levels are <0.008 or >0.04 , the patient is classified as NR with an accuracy of 71.3%, while if levels are between 0.008 and 0.04, the patient is classified as CR/PR. Then, by measuring the gene expression of *SSTR5*, *IN1GHRL* and E-cadherin a clinician would be able to assign the right treatment with an accuracy of 79.8%. When classifiers are composed of more than one variable (e.g. *SSTR5* and *PEBP1* or *SSTR5*, *IN1GHRL* and E-cadherin), the distribution of CR and PR patients is defined by a mathematical function (the blue line in the scatterplots) that separates CR from PR patients (blue and pink dots in the scatter plots, respectively). The details of the scatter plots and the mathematical models can be found in the Supplementary Figures S3-S4. (B) Decision tree exploiting molecular differences according to sex to accurately treat an acromegaly patient. If the patient is a male, the expression of E-cadherin should be measured and together with age it would be able to classify the patient as NR with an accuracy of 80.8%. If it is classified as CR/PR, the expression of the short and long DRD2 isoforms should be analyzed and together with E-cadherin it would be able to assign the right treatment with an accuracy of 80.0%. If the patient is a female, the expression of *PEBP1* and *GHRL* should be measured and this will allow to classify the patient as NR with an accuracy of 73.8%. If it is classified as CR/PR, the expression of the short and long DRD2 isoform should be analyzed and together with E-cadherin it would allow to assign the right treatment with an accuracy of 74.7%. The details of the scatter plots and the mathematical models can be found in the Supplementary Figures S5-S8. ACC: Accuracy; CR: complete responder; PR: partial responder; NR: non-responder.

6. Discussion

The need of consistent biomarkers of response to SRLs treatment in acromegaly

Acromegaly is a rare disease caused mostly by somatotropic tumors located in the pituitary gland that requires a prompt diagnosis in order to amend what often happens currently, where patients are diagnosed after suspicions are aroused by the visual identification of long-running phenotypic anatomical changes. If this was not already an important unresolved challenge, a second and equally necessary one is the need for an effective treatment for each patient to be delivered in a timely way.

Nowadays, treatment decision in acromegaly is still made on a trial and error basis, either before or after surgery (144), even though about 50% of patients fail to respond adequately to SRLs, still being the first line recommended treatment. Different factors, such as age and sex (65,149), radiologic such as T2 MRIs signal intensity (120), and histopathologic such as granularity pattern (153) are related to therapeutic outcomes. Tumor expression of *SSTR2* and other molecules have offered additional insights in relation to treatment response (253,256). However, these markers have limitations. Thus, the discovery and quantification of biomarkers that identify pharmacologic treatment response may be helpful for the clinician and is the basis of personalized and predictive medicine also in acromegaly. This is precisely the main objective of this thesis, the identification of biomarkers to improve the current therapeutic algorithm of acromegaly and individualize the treatment of patients. The experimental design to get this objective has been based on two strategies: classical statistics (Study 1, 2 and 3) and data mining methods (Study 4), both used to analyze clinical variables and molecular markers measured by candidate-gene approaches.

E-cadherin, SSTR2 and Ki-67, but not other SSTRs nor downstream effectors, are consistent predictive biomarkers of response to SRLs in somatotropinomas (Study 1)

In the first study we aimed to evaluate the mRNA expression of a combined panel composed of almost all SRLs response biomarkers published in the last decades including SSTRs and downstream effectors, for verification of previous results and definition of their predictive power; those showing the best predictive performance were validated at protein level. We found that among all the biomarkers studied E-cadherin, *SSTR2* and Ki-67 showed potential usefulness for incorporation into clinical practice and therapeutic personalized guidelines. E-cadherin expression was the best predictor between the SRLs response categories. None of the

other evaluated biomarkers showed statistical differences among the different response categories, although some of them showed a trend toward statistical significance, in particular *AIP* ($p=0.06$). The *SSTR2/SSTR5* ratio was not different among response categories and nor was *PLAGL1 (ZAC1)*, a molecule which participates in the downstream pathway of *SSTR2*, in close relation to *AIP* (172). Discrepancies with previous reports could be partially explained because of the methodology used and the population studied. We analyzed the gene expression of the panels of markers while other studies measured the markers by IHC as in the case of *AIP* (172) and *KLK10* (257); or by western blot as in the case of *RKIP* (171). In the case of *SSTR2*, the concordance between RNA levels and IHC staining has been previously confirmed (161), as we also found. Regarding the discordance of *SSTR2/SSTR5* ratio in our study with the work by Taboada (162), it could be due to the fact that we used probe-base qPCR (Taqman technology) to measure gene expression, while the later designed the primers and used intercalating dye-based qPCR which is less specific.

Of particular interest is the fact the ROC curve analyses of E-cadherin and *SSTR2* or their combination showed similar results, although E-cadherin presented better predictive power (either positive (84%) and negative (73%) for gene expression and even better for protein expression, positive predictive value of 100% and negative predictive value of 81.3%), and moreover, the combination of E-cadherin and *SSTR2* was not superior than the one showed by E-cadherin alone. This indicates that if one single marker is to be chosen for incorporation into a decision-making therapeutic algorithm, E-cadherin might be the first one to be included to clinical guidelines.

Our study clearly exemplifies the biological heterogeneity of somatotropinomas (64), which by extension is also reflected in the response to SRL, the first-line pharmacological treatment acromegaly recognized nowadays by clinical guidelines. Despite being a benign tumor, we were surprised by the huge heterogeneity showed by these tumors. At beginning of this project, we expected that the aggregation of the markers previously reported would be enough to clearly separate acromegaly patients according to the SRLs response. Unfortunately, the expression of all the biomarkers identified so far is so wide and the variability among groups of responders and non-responders is so high that it leads to an important degree of overlapping among SRLs response categories, which does not allow the definition of specific cut-off values that could be currently applied to clinical practice. In this regard, E-cadherin expression is able to partially resist this overlapping effect among groups, although in some particular patients it may also fail because the overall predictive power -either positive or negative- is around 75% when gene expression is considered. The predictive value of E-cadherin levels was validated at protein levels

which is of paramount importance from a clinical point of view as IHC is easily implementable in the clinical routine.

Why is E-cadherin a better predictive biomarker than the rest when it would be more expected to find better results for the somatostatin receptor family? This issue requires further studies, although some remarkable information has already been generated by some studies, mostly coming from Bollerslev's group (181–183). E-cadherin is, among others, a biomarker of EMT, a biological process that seems also to be operative for somatotropinomas at least in part, and may have implications for SRLs response, as we found in the study of Study 2 and discuss below. As a matter of fact, the more advanced is EMT, the less responsive the tumor may be to SRL. This may explain in some way the biological heterogeneity shown in our cohort in which no specific expression pattern of the different markers evaluated present a strong concordance. The progressive loss of response to SRLs seems to involve a concerted loss of E-cadherin and *SSTR2* expression together with a gain in Ki-67, and thus the tumor losses its classic GH-secreting phenotype with a higher sparsely granulated pathologic pattern, according to cytokeratin CAM 5.2 staining (153). Our results also validated that dot-type CAM 5.2 immunostaining correlate with poor response to SRLs and E-cadherin loss in somatotropinomas (197).

Another interesting finding of our study is that *SSTR5* expression was higher in those cases in which presurgical treatment with SRLs was performed when compared to non-pre-treated patients. These patients were not different in terms of size of the tumor or other clinical variables, thus it is intriguing to understand this finding and it may be even postulated if SRLs may have induced changes in the expression of *SSTR5*, a question that has previously been invoked for *SSTR2* (198,258). We did not find changes for *SSTR2* in our series in cases in which pre-surgical treatment with SRLs was performed. The in deep explanation of our finding requires additional *in vitro* and *in vivo* experiments for its confirmation, but if it would be so, it would open new potential therapeutic options, as the combined and sequential treatment with first-generation SRLs followed by pasireotide may be a new possibility which has never been previously tested.

Finally, what concerns us the most is the lack of reproducibility of previously published results. The majority of measured biomarkers, with the exception of E-cadherin, *SSTR2*, and Ki-67 had been described only by a single publication. This lack of reproducibility makes validation by independent laboratories a mandatory issue. Absence of reproducible results is a worrying matter in actual science and sadly, it is very extended in biomedical research (259), and neuroendocrinology field is not an exception. This is especially true in the field of RNA

biomarkers where the inappropriate use of molecular techniques, such as RT-qPCR, can lead to incorrect results. On this behalf, there are two strategies in relative quantification studies by RT-qPCR: the gene maximization and the sample maximization. The sample maximization method dictates that all samples for a given gene should be analyzed in the same run, which would be the easiest way to reduce potential bias. But as we wanted our method to be able to be used in prospective studies where not all samples are available at the start of the study or to analyze a single sample as a routine technique; thus, we used the gene maximization method. Furthermore, the number of samples with the replicates exceeds the number of available wells in a run, giving difficulty to the use of sample maximization strategy. Those two strategies are well explained in the geNorm manual (<https://genorm.cmgg.be/>).

We performed the corrections and normalizations recommended by the geNorm manual and we calculated also the efficiency of the amplification in every well using the Chainy software (<http://maplab.imppc.org/chainy/>), as recommended in M Pfaff, 2001 (260). Taking all this into account, we are pretty confident that our measures are as accurate as they can be.

The role of EMT in the resistance to SRLs (Study 2)

Results derived from the Study 1 revealed E-cadherin as the best predictor, among the biomarkers we analyzed, of response to SRLs in acromegaly patients; in particular, we found an association of E-cadherin loss with a worse response to SRLs (253). Since the loss of E-cadherin is a hallmark of EMT, we further investigated the relationship between EMT and response to SRL. The Epithelial-Mesenchymal transition (EMT) plays a fundamental role in the development of multiple tissues, including the pituitary gland (261,262). This physiological process is aberrantly used by tumor cells for invasion and dissemination to distant organs, but the underlying molecular mechanisms are not fully understood (263). EMT is associated with advanced solid tumors and seems to occur also in pituitary adenomas (264,265), especially in GH-producing tumors (181,187) where EMT has been related to the response to SRLs (183,253), the primary medical treatment for acromegaly.

To gain insight into the molecular mechanism regulating the loss of E-cadherin in GH-producing tumors, we analyzed the DNA methylation of E-cadherin promoter and found that the promoter region was unmethylated in all cases regardless of gene expression levels, which indicates that E-cadherin silencing is not caused by hypermethylation. This is in disagreement with other previously published results (266–268), which could be explained by the use of a different

technique to assess DNA methylation, Methylation-Specific PCR (MSP), which is a non-quantitative technique prone to false positives (269).

Loss of E-cadherin is not the only important change in gene expression during EMT since this process requires the cooperation of multiple molecular factors including transcription factors and constitutive markers of the epithelial and mesenchymal phenotypes, thus we analyzed the expression of a panel of EMT-related genes. Interestingly, we found that some of them were affected by pre-surgical SRLs treatment. Specifically, *N-cadherin* and *RORC* were overexpressed upon SRLs treatment. The finding regarding *RORC* is partly in agreement with previously published results (181) that showed *RORC* to be upregulated by SRLs treatment although only in tumors with high E-cadherin expression. In contrast, we did not find differences in *RORC* expression depending on E-cadherin levels in pretreated patients but we found an increased *RORC* expression in tumors with high levels of E-cadherin in non-pretreated patients. Given that in the daily clinical practice a high proportion of patients are pre-surgically treated with SRL, this finding is especially important. Taken all together, these data seem to indicate that SRLs treatment induces changes that tend to reestablish a more differentiated phenotype of GH adenoma; in other words, SRLs are anti-EMT drugs.

The clustering analysis based on the signature of the EMT markers studied in this work (Figure 25 A) showed a low number of somatotropinomas displaying expression profiles reflecting a complete EMT process, which is consistent with the benign nature of these tumors. In contrast, most somatotropinomas showed hybrid epithelial/mesenchymal expression profiles which could be explained by the activation of alternative EMT programs and the progression of individual cells to different states along the EMT spectrum. This knowledge adds another layer of information to explain the heterogeneity within GH-producing adenomas (64). However, these results should be taken with caution according to the guidelines from the EMT International Association (270) which considers that EMT status cannot be assessed only on the basis of a small number of molecular markers due to the high complexity of the process, but changes in cellular properties should also be analyzed.

Although the analyzed EMT signature was not able to clearly identify the tumors that respond or not to SRLs when analyzing genes individually, we found that some of them correlated with clinical variables. This is the case for *SNAI1* which was found associated with tumor invasion and SRLs response. The association of high levels of *SNAI1* and invasiveness was also reported in other pituitary tumors (264); however, as far as we know, the relationship between *SNAI1* and SRLs response is reported here for the first time. *SNAI1* is a direct repressor of E-cadherin and a

transcription factor with a key role in EMT modulation (271), so it could be directly related to the E-cadherin loss reported in acromegaly.

Another interesting result involves *RORC*, whose overexpression apparently linked to SRLs administration before surgery was found to correlate with a reduction of IGF-1 levels, in agreement with previous reports (181). Most importantly, we found that high *RORC* levels in GH-producing tumors from pre-surgically treated patients may predict a complete response to SRLs with an AUC of 81%, slightly better than E-cadherin expression (253). In conclusion, *RORC* may be considered a relevant marker useful in personalized medicine for acromegaly patients (144). This finding is in agreement with previously published results reporting the association of attenuated levels of *RORC* with a blunted response to SRLs (181). However, the role of *RORC* is not well understood. It is a RAR-related orphan receptor protein with roles in immunological processes (272,273), circadian regulation (274) and hormone signaling modulation in the thymus (275). *RORC* has also been found to be a master regulator of the cholesterol-biosynthesis program and an attractive target for triple-negative breast cancer (276). Furthermore, *RORC* has been linked to TGF- β -induced EMT in hepatocytes during liver fibrosis (277).

In summary, our data further support the EMT occurrence in acromegaly and its relationship with SRLs response; in particular, *RORC* overexpression in pre-surgically SRLs treated patients and *SNAI1* expression regardless of SRLs pretreatment may be used to predict first-generation SRLs response of patients not cured by surgery. This information may be of value for medical treatment decision-making in acromegaly patients and save unresponsive patients of an ineffective treatment for months or even years.

Molecular predictors of response to SRLs after debulking in large GH-secreting adenomas (Study 3)

As far as we know, our work is the first study that evaluates molecular predictors of response to SRLs after debulking surgery of invasive GH-secreting pituitary tumors. Our data is in the line of other studies showing that surgical debulking improve biochemical response to first generation SRLs in patients with large GH producing adenomas(121–125). In addition, we have identified two molecular markers: Ki-67 and *RORC* linked to the odds of response to SRLs after debulking surgery that could be useful in clinical prediction algorithms.

In accordance to other studies, we observed a statistical and clinically significant additional IGF-1 reduction when SRLs were reinstated after surgical debulking (121–125). In our cohort we

noticed that 1 in every 6 patients (17%) bearing large somatotropinomas had a better response to SRLs after surgical debulking, according to the IGF-1 SDS (253).

From a clinical standpoint, tumors with a better response to SRLs after debulking were not different from those with no additional improvement, either in terms of presurgical tumor volume, postsurgical remnant, age, sex or acromegaly comorbidities. It has been stated that in cases in which evaluation of pre versus postsurgical SRLs treatment has been assessed, the magnitude of GH and IGF-1 decrease is similar in both situations (124). Although the reduction of the tumor volume after debulking seems to be the major factor accounting for the enhanced effect upon SRLs after surgery, our data does not support totally this concept. In fact, the extent of tumor debulking has been related to the subsequent response to SRLs in most of the studies (121–123), although not in all (125). However, somatotropinomas are heterogeneous tumors and may not depict a constant biological behavior over time, thus we hypothesize that tumor debulking may potentially change the ethological cellular relationship within the tumor in the residual lower volume with less intratumoral pressure, as one of the potential playing factors among others. This could induce a different biological expression following surgery in some cases.

It is feasible that less tumor mass could facilitate SRLs effectiveness, but such a simple explanation does not completely account for what we observed in our series. The molecular analysis of our cases indicated that Ki-67 and *RORC* identify those tumors in which the improvement in SRLs response was maximal after debulking. Ki-67 has been linked to SRLs resistance and also linked to cellular proliferation (155). Tumors with a low proliferative activity may be much closer to a well-differentiated somatotroph phenotype and therefore probably more sensitive to the effect of a surgical partial resection in terms of subsequent SRLs response. High levels of *RORC* were observed in those patients that presented an enhancement in the postsurgical response to medical therapy. *RORC* principal function, as well as its relation to SRLs action, is not so well known. *RORC* is a RAR-related orphan receptor protein with roles in immunological processes (272,273), circadian regulation (274) and hormone-signaling modulation in the thymus (275). Moreover, it has been related to SRLs response in acromegaly in an EMT context (181). We showed that high *RORC* levels in tumor could predict an enhanced response to SRLs after tumor debulking with an AUC of 100% and thus, *RORC* could be considered as a clinically relevant biomarker useful in personalized medicine for acromegaly patients (144).

A drawback of our study is its retrospective nature and the relatively low sample size, although the number of cases studied is similar to those previously published regarding this topic, with the exception of the one by Colao et al. in 2006. Thus, in the comparisons between the 4 patients that improved and the remaining 20 that did not, we cannot exclude the possibility of an error type I and, especially, an error type II due to the low number of patients. For example, the difference in the proportion of *GNAS* mutations between groups could not be significant because of the small sample size, although in previous evaluation of our whole cohort of 100 acromegaly tumors, no relationship was found between *GNAS* mutations and SRLs response.

On the other hand, we performed an extensive molecular analysis which has not been previously performed. However, some of the analyzed markers, as we previously reported (253), may change their expression upon SRLs treatment, so these results cannot be extrapolated to SRLs naïve patients.

In summary, our data further supports that surgical debulking should be considered in macroadenomas not just for ameliorating potential mass effect but also because it may help to enhance SRLs response after surgery. However, as shown from the molecular data presented in this work, it cannot be ruled out that the surgical-mediated volume decrease may also be a sensitizing factor for some tumors in which *RORC* as well as Ki-67, for yet unknown biological reasons, are the biomarkers or play an active role in the sensitizing effect to SRLs in these tumors after surgery. High levels of *RORC* in combination of low Ki-67 could identify tumors that would present an enhanced SRLs sensitivity after debulking surgery; this information could be of value for medical treatment decision-making in acromegaly patients bearing invasive tumors not cured by surgery.

The potential of data mining to develop individualized treatment algorithms for acromegaly (Study 4)

The discovery and quantification of biomarkers that identify pharmacologic treatment response may be helpful for the clinician and it is the basis of personalized and predictive medicine also in acromegaly. Currently, the major drawback to transferring this approach to clinical practice is the overlapping of values of these markers between response categories which does not allow the definition of clear cut-offs. Moreover, it is difficult to account for many biological, clinical and molecular variables with small but added effects in the response to SRLs. Applying data mining, a modality of mathematical analysis allowing efficient subclassification of heterogeneous populations, such as those of GH-secreting tumors (64), to the clinical and molecular data generated in the study of Study 1 we have been able to elicit different

combinations of molecular markers expressed in somatotropinomas. When certain clinical characteristics are added to the model, it is possible to segregate patients in whom complete, partial or no valuable response to SRLs can be predicted with reasonable accuracy.

General findings in our cohort included a robust association between SRLs response and extrasellar growth. BMI and IGF-1 basal levels were also slightly associated with SRLs response. Although high BMI use to be associated with acromegaly condition (278), it is the first time that this association has been also identified regarding SRLs response. Additionally, sex was also associated with different molecular characteristics of the tumor related to pharmacologic response. These molecular differences match with the sexual dimorphism of SRLs response (148). In particular, *PEBP1* was associated with the prediction of SRLs response in women more than in men (171). Moreover, age, which has also been considered as a SRLs response factor (157) seems to be more important in men than in women. Most of the molecules that emerged from classical candidate gene approach are fairly represented in the algorithms and decision trees obtained in our analyses using data mining. Thus, from the more than about dozen different molecules previously reported as single markers, E-cadherin, *SSTR2*, *PEBP1*, *GHRL* and In-1-GHRL, and *AIP* are those that contribute -with different combinations at individual level- more robustly to the generation of high accuracy decision trees and models in our cohort. Single markers are not powerful enough to achieve a highly accurate and discriminative capacity of SRLs response categorization in such heterogeneous disease as acromegaly. Thus, a multi-molecular approach was used in our study and different results were obtained in different clinical scenarios. As a consequence, the molecular combination obtained to identify SRLs response was not the same when evaluating a patient with a tumor with extrasellar growth, or an aged subject, or indeed if the case under consideration is a man or a woman. In this regard, one of the conclusions of our study is that in the future, acromegaly patients with specific clinical conditions will require specific decision trees with their corresponding panel of molecules for prediction of response to pharmacologic treatment. The other very important issue is the definition of the cut-off values for application to clinical practice; in the present study we have been able to define cut-off values for the different clinical scenarios with reliable ranges of accuracy that would ensure clinicians that the therapeutic recommendation will allow their patient to benefit from a safe and efficient personalized treatment. Furthermore, this is a complex question that is not minor, as different molecules participate in the panels we constructed and there are no absolute cut-off values but dynamic values readable calculated when the equations are formulated.

The present study has some limitations in this regard, being the most important the relatively low number of cases; however, our results provide a proof-of-concept for the use of data mining strategies in the management of acromegaly patients. Thus, a constraint for implementation of personalized medicine at the moment, whether derived from classic or novel methods, is the necessity of validation of the proposed algorithms with other cohorts. However, by using data mining, the intrinsic nature of the mathematical analysis performs a continuous internal validation process, thus conferring reliability and robustness; despite this, an external validation by an international consortium, capable of establishing a large cohort of acromegaly patients would be welcome. Moreover, the inclusion of other biomarkers not yet identified may improve accuracy thus warranting further discovery investigation. Also, only SRLs response has been studied in the present study as it is the recommended first line treatment, but additional studies including other therapeutic molecules such as pasireotide would be possible if a cohort with sufficient treated patients would be available. In spite of the limitations, results provide a proof-of-concept for the use of data mining strategies in the management of acromegaly patients.

We are close to having personalized medicine and tailored treatments available for individual acromegaly patients. Data mining and modelling is a necessary instrument required to reach the goal of personalized medicine for patients and their physicians.

Conclusions

1. Among the different biomarkers previously reported related to the mechanism of action of SRLs only E-cadherin, *SSTR2* and Ki-67 have been validated as markers of response to first-generation SRLs of patients not cured by surgery, being E-cadherin the best predictor. The measurement of E-cadherin by IHC may be easily implemented in the clinical routine in pathology departments, to assist endocrinologists.
2. EMT is a process that some somatotropinomas suffer and provides a partial answer to the SRLs resistance; in particular, *RORC* expression in pre-surgically SRLs treated patients and *SNAIL1* expression regardless of SRLs pretreatment may be used to predict first-generation SRLs response of patients not cured by surgery.
3. Surgical debulking should be considered in macroadenomas not just for ameliorating potential mass effect but also because it may help to enhance SRLs response after surgery. In addition, high levels of *RORC* together with low Ki-67 in patients pretreated with SRLs may identify patients that would benefit from SRLs therapy after debulking surgery.
4. The use of data mining strategies opens a door to more precise personalized medicine for acromegaly patients. As a proof-of-concept we have developed two algorithms using based on the extrasellar growth of the tumor, sex, age and the expression of E-cadherin, *GHRL*, *IN1-GHRL*, *DRD2*, *SSTR5* and *PEBP1*.

8. Future perspectives

This work provides some answers while new questions arise. First, regarding SRLs response biomarkers, we validated some previously reported biomarkers and discarded others; however, the lack of enough precision to predict SRLs response with the previously reported biomarkers makes us wonder if there are other biomarkers of response to SRLs not yet discovered in acromegaly. Since it is a rare disease there are no large genome-wide studies. So, it is necessary to perform genome-wide studies to search for new biomarkers and to improve our understanding of the process of tumorigenesis of GH-producing cells.

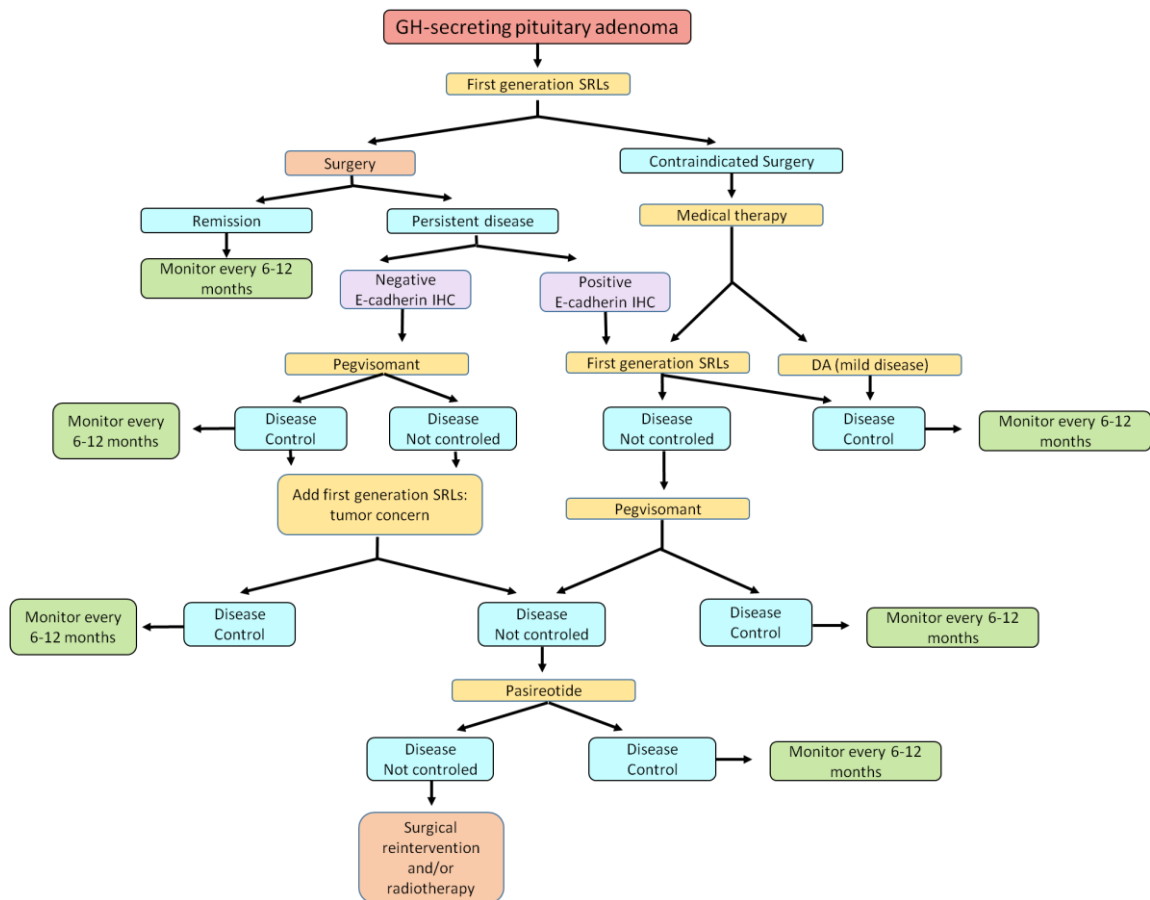
Regarding personalized medicine in acromegaly, we think that this work opens two scenarios: one suitable for the present and another one for the future. Nowadays, it would be already possible to begin a personalized treatment in any hospital through the implementation of E-cadherin IHC, which we found as the best predictor of response to SRLs by using classical statistics (Study 1). As our results show, E-cadherin IHC in acromegaly patients is very suitable for two main reasons: first, it discriminates patients that will not normalize IGF-1 levels with SRLs monotherapy; and second, it is an unambiguous marker that does not require a subjective score like an H-score as the no detection of E-cadherin indicates no response to SRLs. As some expert pathologists in acromegaly suggest (279), the pathologist plays a critical role in the era of precision medicine in diseases such as acromegaly. It is also worth to mention that, based on the results from Study 2 and 3, *RORC* IHC could be also an interesting biomarker for patients pre-surgically treated with SRLs that should be explored.

The other scenario that this study opens is the future application of precision medicine in acromegaly. For the different reasons indicated below, we think that this future should be based on highly quantitative and low-input methods, such as those based on RNA instead of IHC (the most widely-used technique in pathology departments), which would allow to maximize the benefits of the modeling approaches that we performed in this thesis (Study 4): (i) the tumor is usually really small allowing a small number of sections for IHC; (ii) RNA, if measured with a robust and reproducible technology, provides a numeric quantification that is not based on the subjective interpretation of a human-being as occurs in IHC; (iii) this approach will allow the creation of molecular panels composed of several markers that can be measured at once; (iv) the measurement of the upcoming tumors can be used to redefine and correct the models that classify the patients, allowing a continuous validation and modeling process that will provide more precise models.

Taking all of this into account, we propose two treatment algorithms for acromegaly. The first one adding E-cadherin IHC would be easily applicable in every hospital and the second using RNA measurements by RT-qPCR. In both algorithms, we recommend the use of preoperative SRLs since the latest and more complete metanalyses concluded that they produce a favorable impact on surgical cure rate at short-term (129). Furthermore, we only recommend pasireotide as the last treatment option because it showed only a 37% biochemical control ratio in patients not responding to first generation SRLs (280) while Pegvisomant shows a better biochemical control ratio, higher than 60% (281).

A negative E-cadherin IHC after the first surgery would allow distinguishing a subset of patients that would not normalize IGF-1 levels with only SRLs, so we propose to treat these patients with pegvisomant and maybe add SRLs if clinicians are concerned about tumor growth (Figure 33).

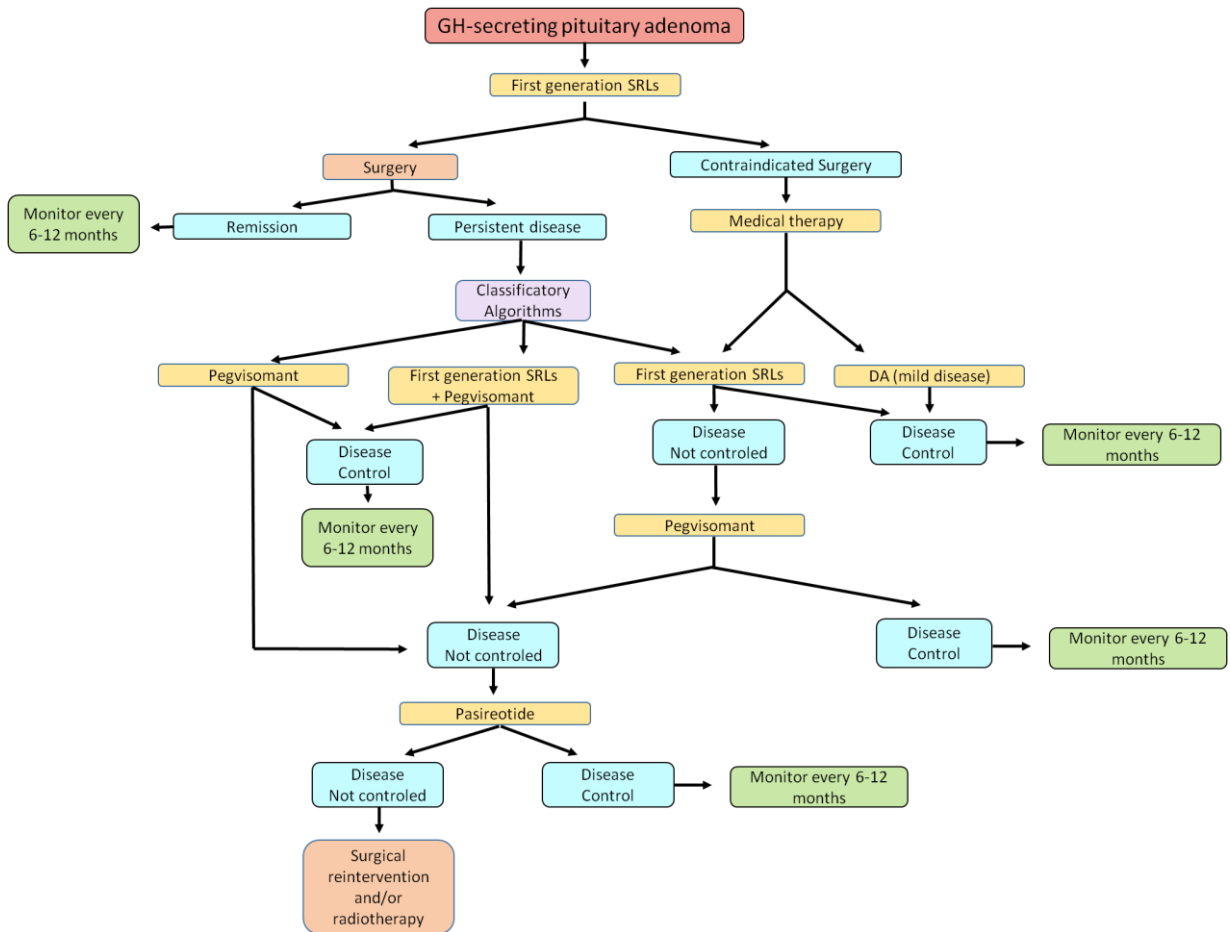
Figure 33.



Proposed treatment algorithm in acromegaly adding E-cadherin IHC as SRLs respond test.

The other algorithm developed, that remains as a proof-of-concept, would include the appliance of the algorithm based on mRNA resulting of the data mining. This algorithm would facilitate the medical treatment choice for every clinician treating acromegaly patients (Figure 34).

Figure 34.



Proposed treatment algorithm in acromegaly adding the resulting algorithms of the data mining analysis.

9. Bibliography

1. Drouin J. Chapter 1 - Pituitary Development. In: Melmed SBT-TP (Fourth E, editor. The Pituitary (Fourth Edition) [Internet]. 4th ed. Academic Press; 2017. p. 3–22. Available from: <http://www.sciencedirect.com/science/article/pii/B9780128041697000015>
2. Amar AP, Weiss MH. Pituitary anatomy and physiology. *Neurosurg Clin N Am* [Internet]. 2003 Jan;14(1):11–23. Available from: <https://linkinghub.elsevier.com/retrieve/pii/S1042368002000177>
3. Bichet DG. Chapter 8 - The Posterior Pituitary. In: Melmed SBT-TP (Fourth E, editor. Academic Press; 2017. p. 251–88. Available from: <http://www.sciencedirect.com/science/article/pii/B9780128041697000088>
4. Horvath E, Kovacs K, Lloyd R V. Pars intermedia of the human pituitary revisited: Morphologic aspects and frequency of hyperplasia of POMC-peptide immunoreactive cells. *Endocr Pathol* [Internet]. 1999 Mar;10(1):55–64. Available from: <http://link.springer.com/10.1007/BF02738816>
5. Melmed S. Pituitary-Tumor Endocrinopathies. Longo DL, editor. *N Engl J Med* [Internet]. 2020 Mar 5;382(10):937–50. Available from: <http://www.nejm.org/doi/10.1056/NEJMra1810772>
6. Andersen B, Rosenfeld MG. POU Domain Factors in the Neuroendocrine System: Lessons from Developmental Biology Provide Insights into Human Disease*. *Endocr Rev* [Internet]. 2001 Feb 1;22(1):2–35. Available from: <https://academic.oup.com/edrv/article/22/1/2/2423863>
7. Rhodes SJ, Chen R, DiMattia GE, Scully KM, Kalla KA, Lin SC, et al. A tissue-specific enhancer confers Pit-1-dependent morphogen inducibility and autoregulation on the pit-1 gene. *Genes Dev* [Internet]. 1993 Jun 1;7(6):913–32. Available from: <http://www.genesdev.org/cgi/doi/10.1101/gad.7.6.913>
8. Zhu X, Zhang J, Tollkuhn J, Ohsawa R, Bresnick EH, Guillemot F, et al. Sustained Notch signaling in progenitors is required for sequential emergence of distinct cell lineages during organogenesis. *Genes Dev* [Internet]. 2006 Oct 1;20(19):2739–53. Available from: <http://www.genesdev.org/cgi/doi/10.1101/gad.1444706>
9. MILLER WL, EBERHARDT NL. Structure and Evolution of the Growth Hormone Gene Family. *Endocr Rev* [Internet]. 1983 Apr;4(2):97–130. Available from: <https://academic.oup.com/edrv/article-lookup/doi/10.1210/edrv-4-2-97>
10. Chen EY, Liao Y-C, Smith DH, Barrera-Saldaña HA, Gelinás RE, Seeburg PH. The human growth hormone locus: Nucleotide sequence, biology, and evolution. *Genomics* [Internet]. 1989 May;4(4):479–97. Available from: <https://linkinghub.elsevier.com/retrieve/pii/0888754389902711>
11. Ryther RCC, Flynt AS, Harris BD, Phillips JA, Patton JG. GH1 Splicing Is Regulated by Multiple Enhancers Whose Mutation Produces a Dominant-Negative GH Isoform That Can Be Degraded by Allele-Specific Small Interfering RNA (siRNA). *Endocrinology* [Internet]. 2004 Jun 1;145(6):2988–96. Available from: <https://academic.oup.com/endo/article/145/6/2988/2878726>
12. Bonert VS, Melmed S. Chapter 4 - Growth Hormone. In: Melmed SBT-TP (Fourth E, editor. The Pituitary (Fourth Edition) [Internet]. 4th ed. Academic Press; 2017. p. 85–127. Available from: <http://www.sciencedirect.com/science/article/pii/B9780128041697000040>

13. Müller TD, Nogueiras R, Andermann ML, Andrews ZB, Anker SD, Argente J, et al. Ghrelin. *Mol Metab* [Internet]. 2015 Jun;4(6):437–60. Available from: <https://linkinghub.elsevier.com/retrieve/pii/S2212877815000605>
14. Gnanapavan S, Kola B, Bustin SA, Morris DG, McGee P, Fairclough P, et al. The Tissue Distribution of the mRNA of Ghrelin and Subtypes of Its Receptor, GHS-R, in Humans. *J Clin Endocrinol Metab* [Internet]. 2002 Jun;87(6):2988–2988. Available from: <https://academic.oup.com/jcem/article-lookup/doi/10.1210/jcem.87.6.8739>
15. Kojima M, Hosoda H, Date Y, Nakazato M, Matsuo H, Kangawa K. Ghrelin is a growth-hormone-releasing acylated peptide from stomach. *Nature* [Internet]. 1999 Dec;402(6762):656–60. Available from: <http://www.nature.com/articles/45230>
16. Takaya K, Ariyasu H, Kanamoto N, Iwakura H, Yoshimoto A, Harada M, et al. Ghrelin Strongly Stimulates Growth Hormone Release in Humans. *J Clin Endocrinol Metab* [Internet]. 2000 Dec;85(12):4908–11. Available from: <https://academic.oup.com/jcem/article-lookup/doi/10.1210/jcem.85.12.7167>
17. Tatemoto K, Mutt V. Isolation and characterization of the intestinal peptide porcine PHI (PHI-27), a new member of the glucagon--secretin family. *Proc Natl Acad Sci* [Internet]. 1981 Nov 1;78(11):6603–7. Available from: <http://www.pnas.org/cgi/doi/10.1073/pnas.78.11.6603>
18. Gaylinn BD. Growth hormone releasing hormone receptor. *Receptors Channels* [Internet]. 2002;8(3–4):155–62. Available from: <http://www.ncbi.nlm.nih.gov/pubmed/12529933>
19. Barinaga M, Bilezikjian LM, Vale WW, Rosenfeld MG, Evans RM. Independent effects of growth hormone releasing factor on growth hormone release and gene transcription. *Nature* [Internet]. 1985 Mar;314(6008):279–81. Available from: <http://www.nature.com/articles/314279a0>
20. Reichlin S. Somatostatin. *N Engl J Med* [Internet]. 1983 Dec 15;309(24):1495–501. Available from: <http://www.nejm.org/doi/abs/10.1056/NEJM198312153092406>
21. Koerker DJ, Ruch W, Chideckel E, Palmer J, Goodner CJ, Ensinnck J, et al. Somatostatin: Hypothalamic Inhibitor of the Endocrine Pancreas. *Science* (80-) [Internet]. 1974 Apr 26;184(4135):482–4. Available from: <https://www.sciencemag.org/lookup/doi/10.1126/science.184.4135.482>
22. Hoyer D, Bell GI, Berelowitz M, Epelbaum J, Feniuk W, Humphrey PPA, et al. Classification and nomenclature of somatostatin receptors. *Trends Pharmacol Sci* [Internet]. 1995 Mar;16(3):86–8. Available from: <https://linkinghub.elsevier.com/retrieve/pii/S0165614700889889>
23. Berelowitz M, Szabo M, Frohman L, Firestone S, Chu L, Hintz R. Somatomedin-C mediates growth hormone negative feedback by effects on both the hypothalamus and the pituitary. *Science* (80-) [Internet]. 1981 Jun 12;212(4500):1279–81. Available from: <https://www.sciencemag.org/lookup/doi/10.1126/science.6262917>
24. SHEPPARD MC, KRONHEIM S, PIMSTONE BL. STIMULATION BY GROWTH HORMONE OF SOMATOSTATIN RELEASE FROM THE RAT HYPOTHALAMUS IN VITRO. *Clin Endocrinol (Oxf)* [Internet]. 1978 Dec;9(6):583–6. Available from: <http://doi.wiley.com/10.1111/j.1365-2265.1978.tb01518.x>
25. Rosenthal SM, Hulse JA, Kaplan SL, Grumbach MM. Exogenous growth hormone inhibits

- growth hormone-releasing factor-induced growth hormone secretion in normal men. *J Clin Invest* [Internet]. 1986 Jan 1;77(1):176–80. Available from: <http://www.jci.org/articles/view/112273>
26. ROSS RJM, BORGES F, GROSSMAN A, SMITH R, NGAHFOONG L, REES LH, et al. GROWTH HORMONE PRETREATMENT IN MAN BLOCKS THE RESPONSE TO GROWTH HORMONE-RELEASING HORMONE; EVIDENCE FOR A DIRECT EFFECT OF GROWTH HORMONE. *Clin Endocrinol (Oxf)* [Internet]. 1987 Jan;26(1):117–23. Available from: <http://doi.wiley.com/10.1111/j.1365-2265.1987.tb03645.x>
 27. Peterfreund RA, Vale WW. Somatostatin Analogs Inhibit Somatostatin Secretion from Cultured Hypothalamus Cells. *Neuroendocrinology* [Internet]. 1984;39(5):397–402. Available from: <https://www.karger.com/Article/FullText/124011>
 28. BILEZIKJIAN LM, SEIFERT H, VALE W. Desensitization to Growth Hormone-Releasing Factor (GRF) Is Associated with Down-Regulation of GRF-Binding Sites*. *Endocrinology* [Internet]. 1986 May;118(5):2045–52. Available from: <https://academic.oup.com/endo/article-lookup/doi/10.1210/endo-118-5-2045>
 29. Coutant R, Bouhours-Nouet N. Endocrine Control and Regulation of Growth Hormone: An Overview. In: *Handbook of Growth and Growth Monitoring in Health and Disease* [Internet]. New York, NY: Springer New York; 2012. p. 73–92. Available from: http://link.springer.com/10.1007/978-1-4419-1795-9_5
 30. Carter-Su C, Schwartz J, Argetsinger LS. Growth hormone signaling pathways. *Growth Horm IGF Res* [Internet]. Churchill Livingstone; 2016 Jun 1 [cited 2020 Jul 13];28:11–5. Available from: <https://pubmed.ncbi.nlm.nih.gov/26421979/>
 31. Brooks AJ, Dai W, O’Mara ML, Abankwa D, Chhabra Y, Pelekanos RA, et al. Mechanism of activation of protein kinase JAK2 by the growth hormone receptor. *Science (80-)* [Internet]. American Association for the Advancement of Science; 2014 [cited 2020 Jul 13];344(6185). Available from: <https://pubmed.ncbi.nlm.nih.gov/24833397/>
 32. Melmed S, Yamashita S, Yamasaki H, Fagin J, Namba H, Yamamoto H, et al. IGF-I receptor signalling: lessons from the somatotroph. *Recent Prog Horm Res* [Internet]. 1996;51:189-215-6. Available from: <http://www.ncbi.nlm.nih.gov/pubmed/8701079>
 33. Mathews LS, Norstedt G, Palmiter RD. Regulation of insulin-like growth factor I gene expression by growth hormone. *Proc Natl Acad Sci U S A* [Internet]. National Academy of Sciences; 1986 Dec 1 [cited 2020 Jul 15];83(24):9343–7. Available from: <https://www.pnas.org/content/83/24/9343>
 34. Han VKM, D’Ercole AJ, Lund PK. Cellular localizaton of somatomedin (insulin-like growth factor) messenger RNA in the human fetus. *Science (80-)* [Internet]. Science; 1987 [cited 2020 Jul 15];236(4798):193–7. Available from: <https://pubmed.ncbi.nlm.nih.gov/3563497/>
 35. Clemmons DR. Multiple hormones stimulate the production of somatomedin by cultured human fibroblasts. *J Clin Endocrinol Metab* [Internet]. *J Clin Endocrinol Metab*; 1984 [cited 2020 Jul 15];58(5):850–6. Available from: <https://pubmed.ncbi.nlm.nih.gov/6368579/>
 36. Geffner ME, Bersch N, Cortez AB, And RCB, Golde DW. Growth-Promoting Actions of Parathyroid Hormone, Adrenocorticotrophic Hormone, and Thyroid-Stimulating Hormone: In Vitro Studies in Normal and Pygmy T-Lymphoblast Cell Lines. Vol. 37. 1995.

37. Underwood LE, Thissen EP, Ketelslegers JM. Nutritional regulation of the insulin-like growth factors. *Endocr Rev* [Internet]. *Endocr Rev*; 1994 [cited 2020 Jul 15];15(1):80–101. Available from: <https://pubmed.ncbi.nlm.nih.gov/8156941/>
38. JONES JI, CLEMMONS DR. Insulin-Like Growth Factors and Their Binding Proteins: Biological Actions*. *Endocr Rev* [Internet]. Oxford Academic; 1995 Feb 1 [cited 2020 Jul 15];16(1):3–34. Available from: <https://academic.oup.com/edrv/article-lookup/doi/10.1210/edrv-16-1-3>
39. Rajaram S, Baylink DJ, Mohan S. Insulin-Like Growth Factor-Binding Proteins in Serum and Other Biological Fluids: Regulation and Functions*. *Endocr Rev* [Internet]. The Endocrine Society; 1997 Dec 1 [cited 2020 Jul 15];18(6):801–31. Available from: <https://pubmed.ncbi.nlm.nih.gov/9408744/>
40. Gunawardane K, Krarup Hansen T, Sandahl Christiansen J, Lunde Jorgensen JO. Normal Physiology of Growth Hormone in Adults [Internet]. *Endotext*. MDText.com, Inc.; 2000 [cited 2020 Jul 15]. Available from: <http://www.ncbi.nlm.nih.gov/pubmed/25905284>
41. Moøller N, Joørgensen JOL. Effects of growth hormone on glucose, lipid, and protein metabolism in human subjects [Internet]. Vol. 30, *Endocrine Reviews*. Oxford Academic; 2009 [cited 2020 Jul 15]. p. 152–77. Available from: www.endo-society.org
42. Kawai M, Namba N, Mushiake S, Etani Y, Nishimura R, Makishima M, et al. Growth hormone stimulates adipogenesis of 3T3-L1 cells through activation of the Stat5A/5B-PPAR γ pathway. *J Mol Endocrinol* [Internet]. *J Mol Endocrinol*; 2007 Feb [cited 2020 Jul 15];38(1–2):19–34. Available from: <https://pubmed.ncbi.nlm.nih.gov/17242167/>
43. Yang S, Mulder H, Holm C, Edén S. Effects of growth hormone on the function of β -adrenoceptor subtypes in rat adipocytes. *Obes Res* [Internet]. North American Assoc. for the Study of Obesity; 2004 [cited 2020 Jul 15];12(2):330–9. Available from: <https://pubmed.ncbi.nlm.nih.gov/14981226/>
44. Pasarica M, Zachwieja JJ, DeJonge L, Redman S, Smith SR. Effect of growth hormone on body composition and visceral adiposity in middle-aged men with visceral obesity. *J Clin Endocrinol Metab* [Internet]. Endocrine Society; 2007 [cited 2020 Jul 15];92(11):4265–70. Available from: <https://pubmed.ncbi.nlm.nih.gov/17785361/>
45. Saltiel AR, Kahn CR. Insulin signalling and the regulation of glucose and lipid metabolism [Internet]. Vol. 414, *Nature*. *Nature*; 2001 [cited 2020 Jul 15]. p. 799–806. Available from: <https://pubmed.ncbi.nlm.nih.gov/11742412/>
46. Marie P. Sur deux cas d'acromégalie; hypertrophie singulière non congénitale des extrémités supérieures, inférieures et céphalique. *Rev Med Liege*. 1886;6:297–333.
47. Herder WW. Acromegaly and gigantism in the medical literature. Case descriptions in the era before and the early years after the initial publication of Pierre Marie (1886). *Pituitary* [Internet]. Springer; 2009 [cited 2020 Jul 15];12(3):236–44. Available from: <https://pubmed.ncbi.nlm.nih.gov/19111220/>
48. de Herder WW. The History of Acromegaly. *Neuroendocrinology* [Internet]. S. Karger AG; 2016 Feb 1 [cited 2020 Jul 15];103(1):7–17. Available from: <https://www.karger.com/Article/FullText/371808>
49. Benda C. Benda, Carl Beiträge zur normalen und pathologischen Histologie der menschlichen Hypophysis cerebri. *Arch f Anat u Phys, Phys Abt* [Internet]. 1900 [cited 2020 Jul 15];S:378. Available from: <https://www.medicusbooks.com/2->

Medizin/Neuroscience/Neuroanatomie/Benda-Carl-Beitraege-zur-normalen-und-pathologischen-Histologie-der-menschlichen-Hypophysis-cerebri-pp-1205-10-Frierich-Fran-Friedmann-Otto-Maas-Ueber-Exstipation-der-Hypophysis-cerebri-pp-

50. Cushing H. PARTIAL HYPOPHYSECTOMY FOR ACROMEGALY WITH REMARKS ON THE FUNCTION OF THE HYPOPHYSIS. *Ann Surg* [Internet]. 1909 [cited 2020 Jul 15];50(6):1002–7. Available from: https://journals.lww.com/annalsofsurgery/Citation/1909/12000/PARTIAL_HYPOPHYSECTOMY_FOR_ACROMEGALY___WITH.3.aspx
51. Cushing H. THE PITUITARY BODY AND ITS DISORDERS. CLINICAL STATES PRODUCED BY DISORDERS OF THE HYPOPHYSIS CEREBRI. *Am J Med Sci* [Internet]. 1912 [cited 2020 Jul 15];144(6):891. Available from: <https://insights.ovid.com/article/00000441-191212000-00019>
52. DAVIDOFF LM. STUDIES IN ACROMEGALY II. HISTORICAL NOTE*. *Endocrinology* [Internet]. Oxford Academic; 1926 Sep 1 [cited 2020 Jul 15];10(5):453–60. Available from: <https://academic.oup.com/endo/article-lookup/doi/10.1210/endo-10-5-453>
53. Lavrentaki A, Paluzzi A, Wass JAH, Karavitaki N. Epidemiology of acromegaly: review of population studies [Internet]. Vol. 20, *Pituitary*. Springer New York LLC; 2017 [cited 2020 Jul 15]. p. 4–9. Available from: [/pmc/articles/PMC5334410/?report=abstract](https://pubmed.ncbi.nlm.nih.gov/34410/)
54. Sesmilo G. Epidemiología de la acromegalia en España. *Endocrinol y Nutr* [Internet]. 2013 Oct;60(8):470–4. Available from: <https://linkinghub.elsevier.com/retrieve/pii/S1575092212003191>
55. Melmed S. Medical progress: Acromegaly. *N Engl J Med* [Internet]. 2006 Dec 14;355(24):2558–73. Available from: <http://www.ncbi.nlm.nih.gov/pubmed/17167139>
56. Colao A, Grasso LFS, Giustina A, Melmed S, Chanson P, Pereira AM, et al. Acromegaly. *Nat Rev Dis Prim* [Internet]. 2019 Dec 21;5(1):20. Available from: <http://www.nature.com/articles/s41572-019-0076-1>
57. Al-Brahim NYY, Asa SL. My approach to pathology of the pituitary gland. *J Clin Pathol* [Internet]. 2006 Apr 27;59(12):1245–53. Available from: <http://jcp.bmj.com/cgi/doi/10.1136/jcp.2005.031187>
58. Asa SL, Kovacs K. Pituitary pathology in acromegaly. Vol. 21, *Endocrinology and Metabolism Clinics of North America*. Elsevier; 1992. p. 553–74.
59. Akirov A, Asa SL, Amer L, Shimon I, Ezzat S. The Clinicopathological Spectrum of Acromegaly. *J Clin Med* [Internet]. MDPI AG; 2019 Nov 13 [cited 2020 Jul 15];8(11):1962. Available from: [/pmc/articles/PMC6912315/?report=abstract](https://pubmed.ncbi.nlm.nih.gov/34410/)
60. Scheithauer BW, Gaffey TA, Lloyd RV., Sebo TJ, Kovacs KT, Horvath E, et al. Pathobiology of Pituitary Adenomas and Carcinomas. *Neurosurgery* [Internet]. Oxford Academic; 2006 Aug 1 [cited 2020 Jul 15];59(2):341–53. Available from: <https://academic.oup.com/neurosurgery/article/59/2/341/2559287>
61. Stewart PM, Carey MP, Graham CT, Wright AD, London DR. Growth hormone secreting pituitary carcinoma: a case report and literature review. *Clin Endocrinol (Oxf)* [Internet]. John Wiley & Sons, Ltd; 1992 Aug 1 [cited 2020 Jul 15];37(2):189–94. Available from: <http://doi.wiley.com/10.1111/j.1365-2265.1992.tb02306.x>
62. Knosp E, Steiner E, Kitz K, Matula C. Pituitary Adenomas with Invasion of the Cavernous Sinus Space. *Neurosurgery* [Internet]. 1993 Oct;33(4):610–8. Available from:

<http://content.wkhealth.com/linkback/openurl?sid=WKPTLP:landingpage&an=00006123-199310000-00008>

63. Micko ASG, Wöhrer A, Wolfsberger S, Knosp E. Invasion of the cavernous sinus space in pituitary adenomas: endoscopic verification and its correlation with an MRI-based classification. *J Neurosurg* [Internet]. 2015 Apr;122(4):803–11. Available from: <https://thejns.org/view/journals/j-neurosurg/122/4/article-p803.xml>
64. Pedraza-Arévalo S, Gahete MD, Alors-Pérez E, Luque RM, Castaño JP. Multilayered heterogeneity as an intrinsic hallmark of neuroendocrine tumors. *Rev Endocr Metab Disord* [Internet]. 2018 Jun 6;19(2):179–92. Available from: <http://link.springer.com/10.1007/s11154-018-9465-0>
65. Cuevas-Ramos D, Carmichael JD, Cooper O, Bonert VS, Gertych A, Mamelak AN, et al. A Structural and Functional Acromegaly Classification. *J Clin Endocrinol Metab* [Internet]. 2015 Jan;100(1):122–31. Available from: <https://academic.oup.com/jcem/article-lookup/doi/10.1210/jc.2014-2468>
66. Hartman ML, Veldhuis JD, Vance ML, Faria ACS, Furlanetto RW, Thorner MO. Somatotropin pulse frequency and basal concentrations are increased in acromegaly and are reduced by successful therapy. *J Clin Endocrinol Metab* [Internet]. *J Clin Endocrinol Metab*; 1990 [cited 2020 Jul 15];70(5):1375–84. Available from: <https://pubmed.ncbi.nlm.nih.gov/2335577/>
67. Brabant G. Insulin-like growth factor-I: Marker for diagnosis of acromegaly and monitoring the efficacy of treatment. *Eur J Endocrinol Suppl*. 2003;148(2):15–20.
68. Katznelson L, Laws ER, Melmed S, Molitch ME, Murad MH, Utz A, et al. Acromegaly: an endocrine society clinical practice guideline. *J Clin Endocrinol Metab* [Internet]. 2014 Nov;99(11):3933–51. Available from: <http://www.ncbi.nlm.nih.gov/pubmed/25356808>
69. Reid TJ, Jin Z, Shen W, Reyes-Vidal CM, Fernandez JC, Bruce JN, et al. IGF-1 levels across the spectrum of normal to elevated in acromegaly: relationship to insulin sensitivity, markers of cardiovascular risk and body composition. *Pituitary* [Internet]. Springer New York LLC; 2015 Apr 24 [cited 2020 Jul 15];18(6):808–19. Available from: </pmc/articles/PMC4619193/?report=abstract>
70. Isotton AL, Wender MCO, Casagrande A, Rollin G, Czepielewski MA. Effects of oral and transdermal estrogen on IGF1, IGFBP3, IGFBP1, serum lipids, and glucose in patients with hypopituitarism during GH treatment: A randomized study. *Eur J Endocrinol* [Internet]. BioScientifica; 2012 Feb 1 [cited 2020 Jul 15];166(2):207–13. Available from: www.eje-online.org
71. Pokrajac A, Wark G, Ellis AR, Wear J, Wieringa GE, Trainer PJ. Variation in GH and IGF-I assays limits the applicability of international consensus criteria to local practice. *Clin Endocrinol (Oxf)* [Internet]. *Clin Endocrinol (Oxf)*; 2007 Jul [cited 2020 Jul 15];67(1):65–70. Available from: <https://pubmed.ncbi.nlm.nih.gov/17437512/>
72. Clemmons DR. Consensus statement on the standardization and evaluation of growth hormone and insulin-like growth factor assays. *Clin Chem* [Internet]. *Clin Chem*; 2011 Apr [cited 2020 Jul 15];57(4):555–9. Available from: <https://pubmed.ncbi.nlm.nih.gov/21285256/>
73. Zahr R, Fleseriu M. Updates in Diagnosis and Treatment of Acromegaly. *Eur Endocrinol* [Internet]. Touch Medical Media, Ltd.; 2018 [cited 2020 Jul 15];14(2):57. Available from: </pmc/articles/PMC6182922/?report=abstract>

74. Chanson P, Salenave S. Acromegaly. *Orphanet J Rare Dis* [Internet]. 2008 Jun 25;3:17. Available from: <http://www.ncbi.nlm.nih.gov/pubmed/18578866>
75. Drange MR, Fram NR, Herman-Bonert V, Melmed S. Pituitary Tumor Registry: A Novel Clinical Resource 1. *J Clin Endocrinol Metab* [Internet]. The Endocrine Society; 2000 Jan [cited 2020 Jul 15];85(1):168–74. Available from: <https://pubmed.ncbi.nlm.nih.gov/10634382/>
76. Molitch ME. Clinical manifestations of acromegaly. *Endocrinol Metab Clin North Am* [Internet]. 1992 Sep;21(3):597–614. Available from: <http://www.ncbi.nlm.nih.gov/pubmed/1521514>
77. NABARRO JDN. ACROMEGALY [Internet]. Vol. 26, *Clinical Endocrinology*. Clin Endocrinol (Oxf); 1987 [cited 2020 Jul 15]. p. 481–512. Available from: <https://pubmed.ncbi.nlm.nih.gov/3308190/>
78. Capatina C, Wass JAH. Acromegaly [Internet]. Vol. 226, *Journal of Endocrinology*. BioScientifica Ltd.; 2015 [cited 2020 Jul 15]. p. T141–60. Available from: <https://pubmed.ncbi.nlm.nih.gov/26136383/>
79. Mazziotti G, Biagioli E, Maffezzoni F, Spinello M, Serra V, Maroldi R, et al. Bone turnover, bone mineral density, and fracture risk in acromegaly: A meta-analysis [Internet]. Vol. 100, *Journal of Clinical Endocrinology and Metabolism*. Endocrine Society; 2015 [cited 2020 Jul 15]. p. 384–94. Available from: <https://pubmed.ncbi.nlm.nih.gov/25365312/>
80. Lieberman SA, Björkengren AG, Hoffman AR. Rheumatologic and skeletal changes in acromegaly. *Endocrinol Metab Clin North Am* [Internet]. 1992 Sep;21(3):615–31. Available from: <http://www.ncbi.nlm.nih.gov/pubmed/1521515>
81. Ben-Shlomo A, Melmed S. Skin manifestations in acromegaly. *Clin Dermatol*. Elsevier; 2006 Jul 1;24(4):256–9.
82. Berg C, Petersenn S, Lahner H, Herrmann BL, Buchfelder M, Droste M, et al. Cardiovascular risk factors in patients with uncontrolled and long-term acromegaly: Comparison with matched data from the general population and the effect of disease control. *J Clin Endocrinol Metab* [Internet]. Endocrine Society; 2010 [cited 2020 Jul 16];95(8):3648–56. Available from: <https://pubmed.ncbi.nlm.nih.gov/20463098/>
83. Sharma MD, Nguyen A V., Brown S, Robbins RJ. Cardiovascular Disease in Acromegaly [Internet]. Vol. 13, *Methodist DeBakey cardiovascular journal*. Methodist DeBakey Heart & Vascular Center; 2017 [cited 2020 Jul 16]. p. 64–7. Available from: </pmc/articles/PMC5512681/?report=abstract>
84. Sharma AN, Tan M, Amsterdam EA, Singh GD. Acromegalic cardiomyopathy: Epidemiology, diagnosis, and management. *Clin Cardiol* [Internet]. John Wiley and Sons Inc.; 2018 Mar 1 [cited 2020 Jul 16];41(3):419–25. Available from: <http://doi.wiley.com/10.1002/clc.22867>
85. Davi MV, Dalle Carbonare L, Giustina A, Ferrari M, Frigo A, Lo Cascio V, et al. Sleep apnoea syndrome is highly prevalent in acromegaly and only partially reversible after biochemical control of the disease. *Eur J Endocrinol* [Internet]. Eur J Endocrinol; 2008 Nov [cited 2020 Jul 16];159(5):533–40. Available from: <https://pubmed.ncbi.nlm.nih.gov/18765561/>
86. Attal P, Chanson P. Endocrine aspects of obstructive sleep apnea [Internet]. Vol. 95, *Journal of Clinical Endocrinology and Metabolism*. Endocrine Society; 2010 [cited 2020

- Jul 16]. p. 483–95. Available from: <https://academic.oup.com/jcem/article-abstract/95/2/483/2596448>
87. Crespo I, Valassi E, Webb SM. Update on quality of life in patients with acromegaly. *Pituitary* [Internet]. 2017 Feb 11;20(1):185–8. Available from: <http://link.springer.com/10.1007/s11102-016-0761-y>
 88. Chesnokova V, Zonis S, Zhou C, Recouvreux MV, Ben-Shlomo A, Araki T, et al. Growth hormone is permissive for neoplastic colon growth. *Proc Natl Acad Sci U S A* [Internet]. National Academy of Sciences; 2016 Jun 7 [cited 2020 Jul 16];113(23):E3250–9. Available from: www.pnas.org/cgi/doi/10.1073/pnas.1612785113Fig.6.GHinducesEMT,suppresses
 89. Hannon AM, Thompson CJ, Sherlock M. Diabetes in Patients With Acromegaly [Internet]. Vol. 17, *Current Diabetes Reports*. Current Medicine Group LLC 1; 2017 [cited 2020 Jul 16]. Available from: <https://pubmed.ncbi.nlm.nih.gov/28150161/>
 90. Melmed S, Bronstein MD, Chanson P, Klibanski A, Casanueva FF, Wass JAH, et al. A Consensus Statement on acromegaly therapeutic outcomes. *Nat Rev Endocrinol* [Internet]. 2018 Sep;14(9):552–61. Available from: <http://www.ncbi.nlm.nih.gov/pubmed/30050156>
 91. Fahlbusch R, Honegger J, Buchfelder M. Surgical management of acromegaly. *Endocrinol Metab Clin North Am* [Internet]. 1992 Sep;21(3):669–92. Available from: <http://www.ncbi.nlm.nih.gov/pubmed/1521518>
 92. Hazer DB, Işık S, Berker D, Güler S, Gürlek A, Yücel T, et al. Treatment of acromegaly by endoscopic transsphenoidal surgery: surgical experience in 214 cases and cure rates according to current consensus criteria. *J Neurosurg* [Internet]. 2013 Dec;119(6):1467–77. Available from: <https://thejns.org/view/journals/j-neurosurg/119/6/article-p1467.xml>
 93. Starke RM, Raper DMS, Payne SC, Vance ML, Oldfield EH, Jane JA. Endoscopic vs Microsurgical Transsphenoidal Surgery for Acromegaly: Outcomes in a Concurrent Series of Patients Using Modern Criteria For Remission. *J Clin Endocrinol Metab* [Internet]. 2013 Aug;98(8):3190–8. Available from: <https://academic.oup.com/jcem/article-lookup/doi/10.1210/jc.2013-1036>
 94. Ciric I, Ragin A, Baumgartner C, Pierce D. Complications of Transsphenoidal Surgery: Results of a National Survey, Review of the Literature, and Personal Experience. *Neurosurgery* [Internet]. 1997 Feb;40(2):225–37. Available from: <http://content.wkhealth.com/linkback/openurl?sid=WKPTLP:landingpage&an=00006123-199702000-00001>
 95. Bécclère A. Le traitement médical des tumeurs hypophysaires, du gigantisme et de l'acromégalie par la radiothérapie. *Bull Mem Soc Med Hop Paris*. 1909;27:274.
 96. Hannon MJ, Barkan AL, Drake WM. The Role of Radiotherapy in Acromegaly. *Neuroendocrinology* [Internet]. S. Karger AG; 2016 Feb 1 [cited 2020 Jul 16];103(1):42–9. Available from: <https://www.karger.com/Article/FullText/435776>
 97. Jenkins PJ, Bates P, Carson MN, Stewart PM, Wass JAH. Conventional Pituitary Irradiation Is Effective in Lowering Serum Growth Hormone and Insulin-Like Growth Factor-I in Patients with Acromegaly. *J Clin Endocrinol Metab* [Internet]. 2006 Apr;91(4):1239–45. Available from: <https://academic.oup.com/jcem/article-lookup/doi/10.1210/jc.2005-1616>

98. Minniti G, Jaffrain-Rea M-L, Osti M, Esposito V, Santoro A, Solda F, et al. The long-term efficacy of conventional radiotherapy in patients with GH-secreting pituitary adenomas. *Clin Endocrinol (Oxf)* [Internet]. 2005 Feb;62(2):210–6. Available from: <http://doi.wiley.com/10.1111/j.1365-2265.2005.02199.x>
99. Ayuk J, Clayton RN, Holder G, Sheppard MC, Stewart PM, Bates AS. Growth Hormone and Pituitary Radiotherapy, But Not Serum Insulin-Like Growth Factor-I Concentrations, Predict Excess Mortality in Patients with Acromegaly. *J Clin Endocrinol Metab* [Internet]. 2004 Apr;89(4):1613–7. Available from: <https://academic.oup.com/jcem/article-lookup/doi/10.1210/jc.2003-031584>
100. CHIODINI PG, LIUZZI A, BOTALLA L, CREMASCOLI G, SILVESTRINI F. Inhibitory Effect of Dopaminergic Stimulation on GH Release in Acromegaly. *J Clin Endocrinol Metab* [Internet]. 1974 Feb;38(2):200–6. Available from: <https://academic.oup.com/jcem/article-lookup/doi/10.1210/jcem-38-2-200>
101. Peillon F, Cesselin F, Zygelman N, Brandi A, Mauborgne A. [Effect of L dopa, dopamine and CB 154 on prolactin secretion from human pituitary adenomas in vitro (proceedings) (author's transl)]. *Ann Endocrinol (Paris)* [Internet]. 1978;39(3):255–7. Available from: <http://www.ncbi.nlm.nih.gov/pubmed/718128>
102. BRESSION D, BRANDI AM, NOUSBAUM A, LE DAFNIET M, RACADOT J, PEILLON F. Evidence of Dopamine Receptors in Human Growth Hormone (GH)-Secreting Adenomas with Concomitant Study of Dopamine Inhibition of GH Secretion in a Perfusion System*. *J Clin Endocrinol Metab* [Internet]. 1982 Sep;55(3):589–93. Available from: <https://academic.oup.com/jcem/article-lookup/doi/10.1210/jcem-55-3-589>
103. Venegas-Moreno E, Vazquez-Borrego MC, Dios E, Gros-Herguido N, Flores-Martinez A, Rivero-Cortés E, et al. Association between dopamine and somatostatin receptor expression and pharmacological response to somatostatin analogues in acromegaly. *J Cell Mol Med* [Internet]. 2018 Mar;22(3):1640–9. Available from: <http://www.ncbi.nlm.nih.gov/pubmed/29266696>
104. Sandret L, Maison P, Chanson P. Place of Cabergoline in Acromegaly: A Meta-Analysis. *J Clin Endocrinol Metab* [Internet]. 2011 May;96(5):1327–35. Available from: <https://academic.oup.com/jcem/article-lookup/doi/10.1210/jc.2010-2443>
105. Kuhn E, Chanson P. Cabergoline in acromegaly. *Pituitary* [Internet]. 2017 Feb 26;20(1):121–8. Available from: <http://link.springer.com/10.1007/s11102-016-0782-6>
106. Taboada GF, Luque RM, Neto LV, Machado E de O, Sbaffi BC, Domingues RC, et al. Quantitative analysis of somatostatin receptor subtypes (1–5) gene expression levels in somatotropinomas and correlation to in vivo hormonal and tumor volume responses to treatment with octreotide LAR. *Eur J Endocrinol* [Internet]. 2008 Mar;158(3):295–303. Available from: <https://ej.e.bioscientifica.com/view/journals/eje/158/3/295.xml>
107. Bauer W, Briner U, Doepfner W, Haller R, Huguenin R, Marbach P, et al. SMS 201–995: A very potent and selective octapeptide analogue of somatostatin with prolonged action. *Life Sci* [Internet]. 1982 Sep;31(11):1133–40. Available from: <https://linkinghub.elsevier.com/retrieve/pii/002432058290087X>
108. Taylor JE, Bogden AE, Moreau J-P, Coy DH. In vitro and in vivo inhibition of human small cell lung carcinoma (NCI-H69) growth by a somatostatin analogue. *Biochem Biophys Res Commun* [Internet]. 1988 May;153(1):81–6. Available from: <https://linkinghub.elsevier.com/retrieve/pii/S0006291X88811926>

109. Ben-Shlomo A, Melmed S. Somatostatin agonists for treatment of acromegaly. *Mol Cell Endocrinol* [Internet]. 2008 May;286(1–2):192–8. Available from: <https://linkinghub.elsevier.com/retrieve/pii/S0303720707004339>
110. Murray RD, Melmed S. A Critical Analysis of Clinically Available Somatostatin Analog Formulations for Therapy of Acromegaly. *J Clin Endocrinol Metab* [Internet]. 2008 Aug 1;93(8):2957–68. Available from: <https://academic.oup.com/jcem/article/93/8/2957/2598353>
111. Mazziotti G, Giustina A. Effects of lanreotide SR and Autogel on tumor mass in patients with acromegaly: a systematic review. *Pituitary* [Internet]. 2010 Mar 3;13(1):60–7. Available from: <http://link.springer.com/10.1007/s11102-009-0169-z>
112. Melmed S, Sternberg R, Cook D, Klibanski A, Chanson P, Bonert V, et al. A Critical Analysis of Pituitary Tumor Shrinkage during Primary Medical Therapy in Acromegaly. *J Clin Endocrinol Metab* [Internet]. 2005 Jul;90(7):4405–10. Available from: <https://academic.oup.com/jcem/article-lookup/doi/10.1210/jc.2004-2466>
113. Cozzolino A, Feola T, Simonelli I, Puliani G, Pozza C, Giannetta E, et al. Somatostatin Analogs and Glucose Metabolism in Acromegaly: A Meta-Analysis of Prospective Interventional Studies. *J Clin Endocrinol Metab* [Internet]. 2018 Jun 1;103(6):2089–99. Available from: <https://academic.oup.com/jcem/article/103/6/2089/4951498>
114. Giustina A, Chanson P, Kleinberg D, Bronstein MD, Clemmons DR, Klibanski A, et al. Expert consensus document: A consensus on the medical treatment of acromegaly. *Nat Rev Endocrinol* [Internet]. 2014 Apr;10(4):243–8. Available from: <http://www.ncbi.nlm.nih.gov/pubmed/24566817>
115. Annamalai AK, Webb A, Kandasamy N, Elkhawad M, Moir S, Khan F, et al. A Comprehensive Study of Clinical, Biochemical, Radiological, Vascular, Cardiac, and Sleep Parameters in an Unselected Cohort of Patients With Acromegaly Undergoing Presurgical Somatostatin Receptor Ligand Therapy. *J Clin Endocrinol Metab* [Internet]. 2013 Mar 1;98(3):1040–50. Available from: <https://academic.oup.com/jcem/article/98/3/1040/2536648>
116. Paragliola RM, Corsello SM, Salvatori R. Somatostatin receptor ligands in acromegaly: clinical response and factors predicting resistance. *Pituitary* [Internet]. 2017 Feb 24;20(1):109–15. Available from: <http://link.springer.com/10.1007/s11102-016-0768-4>
117. Colao A, Auriemma RS, Pivonello R, Kasuki L, Gadelha MR. Interpreting biochemical control response rates with first-generation somatostatin analogues in acromegaly. *Pituitary* [Internet]. 2016 Jun;19(3):235–47. Available from: <http://www.ncbi.nlm.nih.gov/pubmed/26519143>
118. Jaquet P, Gunz G, Saveanu A, Dufour H, Taylor J, Dong J, et al. Efficacy of chimeric molecules directed towards multiple somatostatin and dopamine receptors on inhibition of GH and prolactin secretion from GH-secreting pituitary adenomas classified as partially responsive to somatostatin analog therapy. *Eur J Endocrinol* [Internet]. 2005 Jul;153(1):135–41. Available from: <https://ej.e.bioscientifica.com/view/journals/eje/153/1/1530135.xml>
119. Colao A, Auriemma RS, Lombardi G, Pivonello R. Resistance to Somatostatin Analogs in Acromegaly. *Endocr Rev* [Internet]. 2011 Apr 1;32(2):247–71. Available from: <https://academic.oup.com/edrv/article/32/2/247/2354760>
120. Puig-Domingo M, Resmini E, Gomez-Anson B, Nicolau J, Mora M, Palomera E, et al.

- Magnetic resonance imaging as a predictor of response to somatostatin analogs in acromegaly after surgical failure. *J Clin Endocrinol Metab* [Internet]. 2010 Nov;95(11):4973–8. Available from: <http://www.ncbi.nlm.nih.gov/pubmed/20739382>
121. Colao A, Attanasio R, Pivonello R, Cappabianca P, Cavallo LM, Lasio G, et al. Partial Surgical Removal of Growth Hormone-Secreting Pituitary Tumors Enhances the Response to Somatostatin Analogs in Acromegaly. *J Clin Endocrinol Metab* [Internet]. 2006 Jan;91(1):85–92. Available from: <https://academic.oup.com/jcem/article-lookup/doi/10.1210/jc.2005-1208>
 122. Karavitaki N, Turner HE, Adams CBT, Cudlip S, Byrne J V., Fazal-Sanderson V, et al. Surgical debulking of pituitary macroadenomas causing acromegaly improves control by lanreotide. *Clin Endocrinol (Oxf)* [Internet]. 2008 Jun;68(6):970–5. Available from: <http://doi.wiley.com/10.1111/j.1365-2265.2007.03139.x>
 123. Fahlbusch R, Kleinberg D, Biller B, Bonert V, Buchfelder M, Cappabianca P, et al. Surgical debulking of pituitary adenomas improves responsiveness to octreotide lar in the treatment of acromegaly. *Pituitary* [Internet]. 2017 Dec 19;20(6):668–75. Available from: <http://link.springer.com/10.1007/s11102-017-0832-8>
 124. Petrossians P, Borges-Martins L, Espinoza C, Daly A, Betea D, Valdes-Socin H, et al. Gross total resection or debulking of pituitary adenomas improves hormonal control of acromegaly by somatostatin analogs. *Eur J Endocrinol* [Internet]. 2005 Jan;152(1):61–6. Available from: <https://eje.bioscientifica.com/view/journals/eje/152/1/1520061.xml>
 125. Jallad RS, Musolino NR, Kodaira S, Cescato VA, Bronstein MD. Does partial surgical tumour removal influence the response to octreotide-LAR in acromegalic patients previously resistant to the somatostatin analogue? *Clin Endocrinol (Oxf)* [Internet]. 2007 Aug;67(2):310–5. Available from: <http://doi.wiley.com/10.1111/j.1365-2265.2007.02885.x>
 126. Wass J. Debulking of pituitary adenomas improves hormonal control of acromegaly by somatostatin analogues. *Eur J Endocrinol* [Internet]. 2005 May;152(5):693–4. Available from: <https://eje.bioscientifica.com/view/journals/eje/152/5/1520693.xml>
 127. Buchfelder M, Schlaffer S-M. The surgical treatment of acromegaly. *Pituitary* [Internet]. 2017 Feb 21;20(1):76–83. Available from: <http://link.springer.com/10.1007/s11102-016-0765-7>
 128. Abreu C, Guinto G, Mercado M. Surgical-pharmacological interactions in the treatment of acromegaly. *Expert Rev Endocrinol Metab* [Internet]. 2019 Jan 2;14(1):35–42. Available from: <https://www.tandfonline.com/doi/full/10.1080/17446651.2019.1559729>
 129. Yang C, Li G, Jiang S, Bao X, Wang R. Preoperative Somatostatin Analogues in Patients with Newly-diagnosed Acromegaly: A Systematic Review and Meta-analysis of Comparative Studies. *Sci Rep* [Internet]. 2019 Dec 1;9(1):14070. Available from: <http://www.nature.com/articles/s41598-019-50639-6>
 130. Colao A, Bronstein MD, Freda P, Gu F, Shen C-C, Gadelha M, et al. Pasireotide Versus Octreotide in Acromegaly: A Head-to-Head Superiority Study. *J Clin Endocrinol Metab* [Internet]. 2014 Mar 1;99(3):791–9. Available from: <https://academic.oup.com/jcem/article/99/3/791/2537491>
 131. Gadelha MR, Bronstein MD, Brue T, Coculescu M, Fleseriu M, Guitelman M, et al. Pasireotide versus continued treatment with octreotide or lanreotide in patients with

- inadequately controlled acromegaly (PAOLA): a randomised, phase 3 trial. *Lancet Diabetes Endocrinol* [Internet]. 2014 Nov;2(11):875–84. Available from: <https://linkinghub.elsevier.com/retrieve/pii/S221385871470169X>
132. Coopmans EC, Muhammad A, van der Lely AJ, Janssen JAMJL, Neggers SJMM. How to Position Pasireotide LAR Treatment in Acromegaly. *J Clin Endocrinol Metab* [Internet]. 2019 Jun 1;104(6):1978–88. Available from: <https://academic.oup.com/jcem/article/104/6/1978/5270380>
 133. McKeage K. Pasireotide in Acromegaly: A Review. *Drugs* [Internet]. 2015 Jun 28;75(9):1039–48. Available from: <http://link.springer.com/10.1007/s40265-015-0413-y>
 134. Lasolle H, Ferriere A, Vasiljevic A, Eimer S, Nunes M-L, Tabarin A. Pasireotide-LAR in acromegaly patients treated with a combination therapy: a real-life study. *Endocr Connect* [Internet]. 2019 Oct;8(10):1383–94. Available from: <https://ec.bioscientifica.com/view/journals/ec/8/10/EC-19-0332.xml>
 135. Kopchick J. Discovery and mechanism of action of pegvisomant. *Eur J Endocrinol* [Internet]. 2003 Apr 1;S21–5. Available from: https://ej.e.bioscientifica.com/view/journals/eje/148/Suppl_2/S21.xml
 136. Chen WY, Wight DC, Wagner TE, Kopchick JJ. Expression of a mutated bovine growth hormone gene suppresses growth of transgenic mice. *Proc Natl Acad Sci* [Internet]. 1990 Jul 1;87(13):5061–5. Available from: <http://www.pnas.org/cgi/doi/10.1073/pnas.87.13.5061>
 137. Trainer PJ, Drake WM, Katznelson L, Freda PU, Herman-Bonert V, van der Lely AJ, et al. Treatment of Acromegaly with the Growth Hormone–Receptor Antagonist Pegvisomant. *N Engl J Med* [Internet]. 2000 Apr 20;342(16):1171–7. Available from: <http://www.nejm.org/doi/abs/10.1056/NEJM200004203421604>
 138. Buchfelder M, van der Lely A-J, Biller BMK, Webb SM, Brue T, Strasburger CJ, et al. Long-term treatment with pegvisomant: observations from 2090 acromegaly patients in ACROSTUDY. *Eur J Endocrinol* [Internet]. 2018 Dec;419–27. Available from: <https://ej.e.bioscientifica.com/view/journals/eje/179/6/EJE-18-0616.xml>
 139. Higham CE, Chung TT, Lawrance J, Drake WM, Trainer PJ. Long-term experience of pegvisomant therapy as a treatment for acromegaly. *Clin Endocrinol (Oxf)* [Internet]. 2009 Jul;71(1):86–91. Available from: <http://doi.wiley.com/10.1111/j.1365-2265.2008.03469.x>
 140. van der Lely AJ, Biller BMK, Brue T, Buchfelder M, Ghigo E, Gomez R, et al. Long-Term Safety of Pegvisomant in Patients with Acromegaly: Comprehensive Review of 1288 Subjects in ACROSTUDY. *J Clin Endocrinol Metab* [Internet]. 2012 May;97(5):1589–97. Available from: <https://academic.oup.com/jcem/article-lookup/doi/10.1210/jc.2011-2508>
 141. Sievers C, Baur DM, Schwanke A, Buchfelder M, Droste M, Mann K, et al. Prediction of therapy response in acromegalic patients under pegvisomant therapy within the German ACROSTUDY cohort. *Pituitary* [Internet]. 2015 Dec 30;18(6):916–23. Available from: <http://link.springer.com/10.1007/s11102-015-0673-2>
 142. Neggers SJMM, van der Lely AJ. Combination treatment with somatostatin analogues and pegvisomant in acromegaly. *Growth Horm IGF Res* [Internet]. 2011 Jun;21(3):129–33. Available from: <https://linkinghub.elsevier.com/retrieve/pii/S1096637411000207>

143. Giustina A, Barkan A, Beckers A, Biermasz N, Biller BMK, Boguszewski C, et al. A Consensus on the Diagnosis and Treatment of Acromegaly Comorbidities: An Update. *J Clin Endocrinol Metab* [Internet]. 2020 Apr 1;105(4):e937–46. Available from: <https://academic.oup.com/jcem/article/105/4/e937/5586717>
144. Puig Domingo M. Treatment of acromegaly in the era of personalized and predictive medicine. *Clin Endocrinol (Oxf)* [Internet]. 2015 Jul;83(1):3–14. Available from: <http://www.ncbi.nlm.nih.gov/pubmed/25640882>
145. Kasuki L, Wildemberg LE, Gadelha MR. MANAGEMENT OF ENDOCRINE DISEASE: Personalized medicine in the treatment of acromegaly. *Eur J Endocrinol* [Internet]. 2018 Mar;178(3):R89–100. Available from: <http://www.ncbi.nlm.nih.gov/pubmed/29339530>
146. Puig-Domingo M, Marazuela M. Precision medicine in the treatment of acromegaly. *Minerva Endocrinol* [Internet]. 2019 May;44(2). Available from: <https://www.minervamedica.it/index2.php?show=R07Y2019N02A0169>
147. Picò A. Acromegaly in the era of precision medicine. *Minerva Endocrinol* [Internet]. 2019 May;44(2). Available from: <https://www.minervamedica.it/index2.php?show=R07Y2019N02A0105>
148. Eden Engstrom B, Burman P, Karlsson FA. Men with acromegaly need higher doses of octreotide than women. *Clin Endocrinol (Oxf)* [Internet]. 2002 Jan;56(1):73–7. Available from: <http://doi.wiley.com/10.1046/j.0300-0664.2001.01440.x>
149. Colao A, Amato G, Pedroncelli AM, Baldelli R, Grottoli S, Gasco V, et al. Gender- and age-related differences in the endocrine parameters of acromegaly. *J Endocrinol Invest* [Internet]. 2002 Jun 22;25(6):532–8. Available from: <http://link.springer.com/10.1007/BF03345496>
150. Colao A, Attanasio R, Pivonello R, Cappabianca P, Cavallo LM, Lasio G, et al. Partial Surgical Removal of Growth Hormone-Secreting Pituitary Tumors Enhances the Response to Somatostatin Analogs in Acromegaly. *J Clin Endocrinol Metab*. 2006 Jan;91(1):85–92.
151. Bhayana S, Booth GL, Asa SL, Kovacs K, Ezzat S. The Implication of Somatotroph Adenoma Phenotype to Somatostatin Analog Responsiveness in Acromegaly. *J Clin Endocrinol Metab* [Internet]. 2005 Nov;90(11):6290–5. Available from: <https://academic.oup.com/jcem/article-lookup/doi/10.1210/jc.2005-0998>
152. Kiseljak-Vassiliades K, Carlson NE, Borges MT, Kleinschmidt-DeMasters BK, Lillehei KO, Kerr JM, et al. Growth hormone tumor histological subtypes predict response to surgical and medical therapy. *Endocrine* [Internet]. 2015 May;49(1):231–41. Available from: <http://www.ncbi.nlm.nih.gov/pubmed/25129651>
153. Fougner SL, Casar-Borota O, Heck A, Berg JP, Bollerslev J. Adenoma granulation pattern correlates with clinical variables and effect of somatostatin analogue treatment in a large series of patients with acromegaly. *Clin Endocrinol (Oxf)*. 2012 Jan;76(1):96–102.
154. Heck A, Emblem KE, Casar-Borota O, Bollerslev J, Ringstad G. Quantitative analyses of T2-weighted MRI as a potential marker for response to somatostatin analogs in newly diagnosed acromegaly. *Endocrine* [Internet]. 2016 May 16;52(2):333–43. Available from: <http://link.springer.com/10.1007/s12020-015-0766-8>
155. Kasuki L, Wildemberg LEA, Neto LV, Marcondes J, Takiya CM, Gadelha MR. Ki-67 is a predictor of acromegaly control with octreotide LAR independent of SSTR2 status and relates to cytokeratin pattern. *Eur J Endocrinol* [Internet]. 2013 Aug;169(2):217–23.

Available from: <http://www.ncbi.nlm.nih.gov/pubmed/23749849>

156. Florio T. Molecular mechanisms of the antiproliferative activity of somatostatin receptors (SSTRs) in neuroendocrine tumors. *Front Biosci* [Internet]. 2008;13(13):806. Available from: <http://www.bioscience.org/2008/v13/af/2722/list.htm>
157. Suliman M, Jenkins R, Ross R, Powell T, Battersby R, Cullen DR. Long-term treatment of acromegaly with the somatostatin analogue SR-lanreotide. *J Endocrinol Invest* [Internet]. 1999 Jun 11;22(6):409–18. Available from: <http://link.springer.com/10.1007/BF03343583>
158. Gadelha MR, Wildemberg LE, Bronstein MD, Gatto F, Ferone D. Somatostatin receptor ligands in the treatment of acromegaly. *Pituitary* [Internet]. 2017 Feb;20(1):100–8. Available from: <http://www.ncbi.nlm.nih.gov/pubmed/28176162>
159. Casar-Borota O, Heck A, Schulz S, Nesland JM, Ramm-Petersen J, Lekva T, et al. Expression of SSTR2a, but not of SSTRs 1, 3, or 5 in Somatotroph Adenomas Assessed by Monoclonal Antibodies Was Reduced by Octreotide and Correlated With the Acute and Long-Term Effects of Octreotide. *J Clin Endocrinol Metab* [Internet]. 2013 Nov;98(11):E1730–9. Available from: <https://academic.oup.com/jcem/article-lookup/doi/10.1210/jc.2013-2145>
160. Gatto F, Feelders RA, van der Pas R, Kros JM, Waaijers M, Sprij-Mooij D, et al. Immunoreactivity Score Using an Anti-sst2A Receptor Monoclonal Antibody Strongly Predicts the Biochemical Response to Adjuvant Treatment with Somatostatin Analogs in Acromegaly. *J Clin Endocrinol Metab* [Internet]. 2013 Jan;98(1):E66–71. Available from: <https://academic.oup.com/jcem/article-lookup/doi/10.1210/jc.2012-2609>
161. Wildemberg LEA, Vieira Neto L, Costa DF, Nasciutti LE, Takiya CM, Alves LM, et al. Validation of immunohistochemistry for somatostatin receptor subtype 2A in human somatotropinomas: comparison between quantitative real time RT-PCR and immunohistochemistry. *J Endocrinol Invest* [Internet]. 2012 Jun;35(6):580–4. Available from: <http://www.ncbi.nlm.nih.gov/pubmed/21897115>
162. Taboada GF, Luque RM, Bastos W, Guimarães RFC, Marcondes JB, Chimelli LMC, et al. Quantitative analysis of somatostatin receptor subtype (SSTR1-5) gene expression levels in somatotropinomas and non-functioning pituitary adenomas. *Eur J Endocrinol* [Internet]. 2007 Jan;156(1):65–74. Available from: <http://www.ncbi.nlm.nih.gov/pubmed/17218727>
163. Durán-Prado M, Gahete MD, Martínez-Fuentes AJ, Luque RM, Quintero A, Webb SM, et al. Identification and Characterization of Two Novel Truncated but Functional Isoforms of the Somatostatin Receptor Subtype 5 Differentially Present in Pituitary Tumors. *J Clin Endocrinol Metab* [Internet]. 2009 Jul 1;94(7):2634–43. Available from: <https://academic.oup.com/jcem/article/94/7/2634/2597487>
164. Luque RM, Ibáñez-Costa A, Neto LV, Taboada GF, Hormaechea-Agulla D, Kasuki L, et al. Truncated somatostatin receptor variant sst5TMD4 confers aggressive features (proliferation, invasion and reduced octreotide response) to somatotropinomas. *Cancer Lett* [Internet]. 2015 Apr 10;359(2):299–306. Available from: <http://www.ncbi.nlm.nih.gov/pubmed/25637790>
165. Baragli A, Alturaihi H, Watt HL, Abdallah A, Kumar U. Heterooligomerization of human dopamine receptor 2 and somatostatin receptor 2. Co-immunoprecipitation and fluorescence resonance energy transfer analysis. *Cell Signal* [Internet]. Cell Signal; 2007 Nov [cited 2020 Oct 12];19(11):2304–16. Available from:

<https://pubmed.ncbi.nlm.nih.gov/17706924/>

166. Rocheville M, Lange DC, Kumar U, Patel SC, Patel RC, Patel YC. Receptors for dopamine and somatostatin: Formation of hetero-oligomers with enhanced functional activity. *Science* (80-) [Internet]. *Science*; 2000 Apr 7 [cited 2020 Oct 12];288(5463):154–7. Available from: <https://pubmed.ncbi.nlm.nih.gov/10753124/>
167. Zatelli MC, Piccin D, Tagliati F, Bottoni A, Ambrosio MR, Margutti A, et al. Dopamine receptor subtype 2 and somatostatin receptor subtype 5 expression influences somatostatin analogs effects on human somatotroph pituitary adenomas in vitro. *J Mol Endocrinol* [Internet]. *BioScientifica*; 2005 Oct [cited 2020 Oct 12];35(2):333–41. Available from: www.endocrinology-journals.org
168. Neto LV, Machado EDO, Luque RM, Taboada GF, Marcondes JB, Chimelli LMC, et al. Expression analysis of dopamine receptor subtypes in normal human pituitaries, nonfunctioning pituitary adenomas and somatotropinomas, and the association between dopamine and somatostatin receptors with clinical response to octreotide-LAR in acromegaly. *J Clin Endocrinol Metab* [Internet]. *Endocrine Society*; 2009 [cited 2020 Oct 12];94(6):1931–7. Available from: <https://pubmed.ncbi.nlm.nih.gov/19293270/>
169. Coelho MCA, Vasquez ML, Wildemberg LE, Vázquez-Borrego MC, Bitana L, Camacho AH da S, et al. Molecular evidence and clinical importance of β -arrestins expression in patients with acromegaly. *J Cell Mol Med* [Internet]. 2018 Apr;22(4):2110–6. Available from: <http://www.ncbi.nlm.nih.gov/pubmed/29377493>
170. Gatto F, Biermasz NR, Feelders RA, Kros JM, Dogan F, van der Lely A-J, et al. Low beta-arrestin expression correlates with the responsiveness to long-term somatostatin analog treatment in acromegaly. *Eur J Endocrinol* [Internet]. 2016 May;174(5):651–62. Available from: <http://www.ncbi.nlm.nih.gov/pubmed/26888629>
171. Fougner SL, Bollerslev J, Latif F, Hald JK, Lund T, Ramm-Petersen J, et al. Low levels of raf kinase inhibitory protein in growth hormone-secreting pituitary adenomas correlate with poor response to octreotide treatment. *J Clin Endocrinol Metab* [Internet]. 2008 Apr;93(4):1211–6. Available from: <http://www.ncbi.nlm.nih.gov/pubmed/18230656>
172. Chahal HS, Trivellin G, Leontiou CA, Albani N, Fowkes RC, Tahir A, et al. Somatostatin analogs modulate AIP in somatotroph adenomas: the role of the ZAC1 pathway. *J Clin Endocrinol Metab* [Internet]. 2012 Aug;97(8):E1411–20. Available from: <http://www.ncbi.nlm.nih.gov/pubmed/22659247>
173. Barry S, Carlsen E, Marques P, Stiles CE, Gadaleta E, Berney DM, et al. Tumor microenvironment defines the invasive phenotype of AIP-mutation-positive pituitary tumors. *Oncogene* [Internet]. 2019 Jul 12;38(27):5381–95. Available from: <http://www.nature.com/articles/s41388-019-0779-5>
174. Ibáñez-Costa A, Korbonits M. AIP and the somatostatin system in pituitary tumours. *J Endocrinol* [Internet]. 2017 Dec;235(3):R101–16. Available from: <https://joe.bioscientifica.com/view/journals/joe/235/3/JOE-17-0254.xml>
175. Efsthadiadou ZA, Bargiota A, Chrisoulidou A, Kanakis G, Papanastasiou L, Theodoropoulou A, et al. Impact of gsp mutations in somatotroph pituitary adenomas on growth hormone response to somatostatin analogs: a meta-analysis. *Pituitary* [Internet]. 2015 Dec;18(6):861–7. Available from: <http://www.ncbi.nlm.nih.gov/pubmed/26115707>
176. Raehal KM, Bohn LM. β -Arrestins: Regulatory Role and Therapeutic Potential in Opioid and Cannabinoid Receptor-Mediated Analgesia. In 2014. p. 427–43. Available from:

http://link.springer.com/10.1007/978-3-642-41199-1_22

177. Trivellin G, Korbonits M. AIP and its interacting partners. *J Endocrinol* [Internet]. 2011 Aug;210(2):137–55. Available from: <https://joe.bioscientifica.com/view/journals/joe/210/2/137.xml>
178. Hernández-Ramírez LC, Gabrovska P, Dénes J, Stals K, Trivellin G, Tilley D, et al. Landscape of Familial Isolated and Young-Onset Pituitary Adenomas: Prospective Diagnosis in AIP Mutation Carriers. *J Clin Endocrinol Metab* [Internet]. 2015 Sep;100(9):E1242–54. Available from: <https://academic.oup.com/jcem/article-lookup/doi/10.1210/jc.2015-1869>
179. Gadelha MR, Kasuki L, Korbonits M. Novel pathway for somatostatin analogs in patients with acromegaly. *Trends Endocrinol Metab* [Internet]. 2013 May;24(5):238–46. Available from: <http://www.ncbi.nlm.nih.gov/pubmed/23270713>
180. Ibáñez-Costa A, Gahete MD, Rivero-Cortés E, Rincón-Fernández D, Nelson R, Beltrán M, et al. In1-ghrelin splicing variant is overexpressed in pituitary adenomas and increases their aggressive features. *Sci Rep* [Internet]. 2015 Mar 4;5:8714. Available from: <http://www.ncbi.nlm.nih.gov/pubmed/25737012>
181. Lekva T, Berg JP, Heck A, Lyngvi Fougner S, Olstad OK, Ringstad G, et al. Attenuated RORC expression in the presence of EMT progression in somatotroph adenomas following treatment with somatostatin analogs is associated with poor clinical recovery. *PLoS One* [Internet]. 2013;8(6):e66927. Available from: <http://www.ncbi.nlm.nih.gov/pubmed/23825587>
182. Lekva T, Berg JP, Fougner SL, Olstad OK, Ueland T, Bollerslev J. Gene expression profiling identifies ESRP1 as a potential regulator of epithelial mesenchymal transition in somatotroph adenomas from a large cohort of patients with acromegaly. *J Clin Endocrinol Metab* [Internet]. 2012 Aug;97(8):E1506-14. Available from: <http://www.ncbi.nlm.nih.gov/pubmed/22585092>
183. Fougner SL, Lekva T, Borota OC, Hald JK, Bollerslev J, Berg JP. The expression of E-cadherin in somatotroph pituitary adenomas is related to tumor size, invasiveness, and somatostatin analog response. *J Clin Endocrinol Metab* [Internet]. 2010 May;95(5):2334–42. Available from: <http://www.ncbi.nlm.nih.gov/pubmed/20335450>
184. van Roy F, Berx G. The cell-cell adhesion molecule E-cadherin. *Cell Mol Life Sci* [Internet]. 2008 Dec 23;65(23):3756–88. Available from: <http://link.springer.com/10.1007/s00018-008-8281-1>
185. Mendonsa AM, Na T-Y, Gumbiner BM. E-cadherin in contact inhibition and cancer. *Oncogene* [Internet]. 2018;37(35):4769–80. Available from: <http://www.ncbi.nlm.nih.gov/pubmed/29780167>
186. Nieto MA, Huang RY-J, Jackson RA, Thiery JP. EMT: 2016. *Cell* [Internet]. 2016 Jun;166(1):21–45. Available from: <https://linkinghub.elsevier.com/retrieve/pii/S0092867416307966>
187. Lekva T, Berg JP, Lyle R, Heck A, Ringstad G, Olstad OK, et al. Epithelial Splicing Regulator Protein 1 and Alternative Splicing in Somatotroph Adenomas. *Endocrinology* [Internet]. 2013 Sep;154(9):3331–43. Available from: <https://academic.oup.com/endo/article-lookup/doi/10.1210/en.2013-1051>
188. Venegas-Moreno E, Flores-Martinez A, Dios E, Vazquez-Borrego MC, Ibáñez-Costa A,

- Madrazo-Atutxa A, et al. E-cadherin expression is associated with somatostatin analogue response in acromegaly. *J Cell Mol Med* [Internet]. 2019 May 6;23(5):3088–96. Available from: <https://onlinelibrary.wiley.com/doi/abs/10.1111/jcmm.13851>
189. National Research Council (US) Committee on A Framework for Developing a New Taxonomy. *Toward Precision Medicine* [Internet]. Washington, D.C.: National Academies Press; 2011. Available from: <http://www.nap.edu/catalog/13284>
 190. Lesko LJ. Personalized Medicine: Elusive Dream or Imminent Reality? *Clin Pharmacol Ther* [Internet]. 2007 Jun;81(6):807–16. Available from: <http://doi.wiley.com/10.1038/sj.clpt.6100204>
 191. Aljawarneh S, Anguera A, Atwood JW, Lara JA, Lizcano D. Particularities of data mining in medicine: lessons learned from patient medical time series data analysis. *EURASIP J Wirel Commun Netw* [Internet]. 2019 Dec 28;2019(1):260. Available from: <https://jwcn-urasipjournals.springeropen.com/articles/10.1186/s13638-019-1582-2>
 192. Luque RM, Ibáñez-Costa A, Sánchez-Tejada L, Rivero-Cortés E, Robledo M, Madrazo-Atutxa A, et al. El Registro Molecular de Adenomas Hipofisarios (REMAH): una apuesta de futuro de la Endocrinología española por la medicina individualizada y la investigación traslacional. *Endocrinol y Nutr* [Internet]. 2016 Jun;63(6):274–84. Available from: <https://linkinghub.elsevier.com/retrieve/pii/S1575092216300171>
 193. Mallona I, Díez-Villanueva A, Martín B, Peinado MA. Chainy: an universal tool for standardized relative quantification in real-time PCR. *Bioinformatics* [Internet]. 2017 May 1;33(9):1411–3. Available from: <http://www.ncbi.nlm.nih.gov/pubmed/28453678>
 194. Vandesompele J, De Preter K, Pattyn F, Poppe B, Van Roy N, De Paepe A, et al. Accurate normalization of real-time quantitative RT-PCR data by geometric averaging of multiple internal control genes. *Genome Biol* [Internet]. 2002 Jun 18;3(7):RESEARCH0034. Available from: <http://www.ncbi.nlm.nih.gov/pubmed/12184808>
 195. Frommer M, McDonald LE, Millar DS, Collis CM, Watt F, Grigg GW, et al. A genomic sequencing protocol that yields a positive display of 5-methylcytosine residues in individual DNA strands. *Proc Natl Acad Sci* [Internet]. 1992 Mar 1;89(5):1827–31. Available from: <http://www.pnas.org/cgi/doi/10.1073/pnas.89.5.1827>
 196. Mallona I, Díez-Villanueva A, Peinado MA. Methylation plotter: a web tool for dynamic visualization of DNA methylation data. *Source Code Biol Med* [Internet]. 2014 Dec 7;9(1):11. Available from: <https://scfbm.biomedcentral.com/articles/10.1186/1751-0473-9-11>
 197. Bakhtiar Y, Hirano H, Arita K, Yunoue S, Fujio S, Tominaga A, et al. Relationship between cytokeratin staining patterns and clinico-pathological features in somatotropinoma. *Eur J Endocrinol* [Internet]. 2010 Oct;163(4):531–9. Available from: <https://ej.e.bioscientifica.com/view/journals/eje/163/4/531.xml>
 198. Franck SE, Gatto F, van der Lely AJ, Janssen JAMJL, Dallenga AHG, Nagtegaal AP, et al. Somatostatin Receptor Expression in GH-Secreting Pituitary Adenomas Treated with Long-Acting Somatostatin Analogues in Combination with Pegvisomant. *Neuroendocrinology* [Internet]. 2017;105(1):44–53. Available from: <http://www.ncbi.nlm.nih.gov/pubmed/27455094>
 199. Valls R, Pujol A, Artigas L, Mas JM. ANAXOMICS' methodologies -Understanding the complexity of biological processes-. White Pap. 2013;

200. Guyon I, Nikravesh M, Gunn S, Zadeh LA, editors. Feature Extraction [Internet]. Berlin, Heidelberg: Springer Berlin Heidelberg; 2006. (Studies in Fuzziness and Soft Computing; vol. 207). Available from: <http://link.springer.com/10.1007/978-3-540-35488-8>
201. Gorban AN, Zinovyev A. PRINCIPAL MANIFOLDS AND GRAPHS IN PRACTICE: FROM MOLECULAR BIOLOGY TO DYNAMICAL SYSTEMS. *Int J Neural Syst* [Internet]. 2010 Jun 30;20(3):219–32. Available from: <https://www.worldscientific.com/doi/abs/10.1142/S0129065710002383>
202. Coomans D, Massart DL. Alternative k-nearest neighbour rules in supervised pattern recognition. *Anal Chim Acta* [Internet]. 1982;136:15–27. Available from: <https://linkinghub.elsevier.com/retrieve/pii/S0003267001953590>
203. Wood SN. Fast stable direct fitting and smoothness selection for generalized additive models. *J R Stat Soc Ser B (Statistical Methodol)* [Internet]. 2008 Jul;70(3):495–518. Available from: <http://doi.wiley.com/10.1111/j.1467-9868.2007.00646.x>
204. Breiman L, Friedman J, Stone CJ, Olshen RA. Classification and Regression Trees. 1st ed. Belmont: Chapman and Hall/CRC; 1984. 368 p.
205. Cortes C, Vapnik V. Support-vector networks. *Mach Learn* [Internet]. 1995 Sep;20(3):273–97. Available from: <http://link.springer.com/10.1007/BF00994018>
206. Haykin SO. Neural Networks and Learning Machines. Pearson, editor. 2008. 936 p.
207. Fukunaga K. Introduction to Statistical Pattern Recognition [Internet]. 2nd ed. Academic Press; 2013. 592 p. Available from: <https://www.elsevier.com/books/introduction-to-statistical-pattern-recognition/fukunaga/978-0-08-047865-4>
208. Madsen H, P.Thyregod. Introduction to General and Generalized Linear Models. *Journal of Applied Statistics - J APPL STAT*. 2011.
209. Ng AY. Feature selection, L1 vs. L2 regularization, and rotational invariance. In: Twenty-first international conference on Machine learning - ICML '04 [Internet]. New York, New York, USA: ACM Press; 2004. p. 78. Available from: <http://portal.acm.org/citation.cfm?doid=1015330.1015435>
210. Russell S, Norvig P. Artificial Intelligence: A Modern Approach [Internet]. Third. Upper Saddle River, NJ: Prentice Hall; 2010. (Series in Artificial Intelligence). Available from: <http://aima.cs.berkeley.edu/>
211. Tibshirani R. Regression shrinkage and selection via the lasso: a retrospective. *J R Stat Soc Ser B (Statistical Methodol)* [Internet]. 2011 Jun;73(3):273–82. Available from: <http://doi.wiley.com/10.1111/j.1467-9868.2011.00771.x>
212. Chang Y-W, Hsieh C-J, Chang K-W, Lin C-J, Ringgaard M. Training and testing low-degree polynomial data mappings via linear SVM. *J Mach Learn Res*. 2010;11:1471–90.
213. De Bièvre P. The 2012 International Vocabulary of Metrology: “VIM”. *Accredit Qual Assur* [Internet]. 2012;17(2):231–2. Available from: <https://doi.org/10.1007/s00769-012-0885-3>
214. Boughorbel S, Jarray F, El-Anbari M. Optimal classifier for imbalanced data using Matthews Correlation Coefficient metric. Zou Q, editor. *PLoS One* [Internet]. 2017 Jun 2;12(6):e0177678. Available from: <https://dx.plos.org/10.1371/journal.pone.0177678>
215. Fawcett T. An introduction to ROC analysis. *Pattern Recognit Lett* [Internet]. 2006 Jun;27(8):861–74. Available from:

<https://linkinghub.elsevier.com/retrieve/pii/S016786550500303X>

216. Pearson K. LIII. On lines and planes of closest fit to systems of points in space. London, Edinburgh, Dublin Philos Mag J Sci [Internet]. 1901 Nov 8;2(11):559–72. Available from: <https://www.tandfonline.com/doi/full/10.1080/14786440109462720>
217. Laurens van der Maaten, Geoffrey E. H. Visualizing Data using t-SNE. J Mach Learn Res [Internet]. 2008;164(2210):10. Available from: <http://www.jmlr.org/papers/volume9/vandermaaten08a/vandermaaten08a.pdf>
218. Borg I, Groenen PJF. Modern Multidimensional Scaling [Internet]. New York, NY: Springer New York; 2005. (Springer Series in Statistics). Available from: <http://link.springer.com/10.1007/0-387-28981-X>
219. Donoho DL, Grimes C. Hessian eigenmaps: Locally linear embedding techniques for high-dimensional data. Proc Natl Acad Sci [Internet]. 2003 May 13;100(10):5591–6. Available from: <http://www.pnas.org/cgi/doi/10.1073/pnas.1031596100>
220. Choi H, Choi S. Robust kernel Isomap. Pattern Recognit [Internet]. 2007 Mar;40(3):853–62. Available from: <https://linkinghub.elsevier.com/retrieve/pii/S0031320306001804>
221. McFarland HR, Richards DSP. Exact Misclassification Probabilities for Plug-In Normal Quadratic Discriminant Functions. J Multivar Anal [Internet]. 2002 Aug;82(2):299–330. Available from: <https://linkinghub.elsevier.com/retrieve/pii/S0047259X01920342>
222. Wang J. Geometric Structure of High-Dimensional Data and Dimensionality Reduction [Internet]. Berlin, Heidelberg: Springer Berlin Heidelberg; 2011. Available from: <http://link.springer.com/10.1007/978-3-642-27497-8>
223. Lerner B, Guterman H, Aladjem M, Dinstant I, Romem Y. On pattern classification with Sammon’s nonlinear mapping an experimental study. Pattern Recognit [Internet]. 1998 Apr;31(4):371–81. Available from: <https://linkinghub.elsevier.com/retrieve/pii/S0031320397000642>
224. Balasubramanian M. The Isomap Algorithm and Topological Stability. Science (80-) [Internet]. 2002 Jan 4;295(5552):7a–7. Available from: <http://www.sciencemag.org/cgi/doi/10.1126/science.295.5552.7a>
225. Belkin M, Niyogi P. Laplacian Eigenmaps for Dimensionality Reduction and Data Representation. Neural Comput [Internet]. 2003 Jun;15(6):1373–96. Available from: <http://www.mitpressjournals.org/doi/10.1162/089976603321780317>
226. Li P, Chen S. A review on Gaussian Process Latent Variable Models. CAAI Trans Intell Technol [Internet]. 2016 Oct;1(4):366–76. Available from: <https://linkinghub.elsevier.com/retrieve/pii/S2468232216300828>
227. Schölkopf B, Smola A, Müller K-R. Nonlinear Component Analysis as a Kernel Eigenvalue Problem. Neural Comput [Internet]. 1998 Jul;10(5):1299–319. Available from: <http://www.mitpressjournals.org/doi/10.1162/089976698300017467>
228. Isomura T, Toyozumi T. A Local Learning Rule for Independent Component Analysis. Sci Rep [Internet]. 2016 Sep 21;6(1):28073. Available from: <http://www.nature.com/articles/srep28073>
229. Tandon R, Sra S. Sparse nonnegative matrix approximation: new formulations and algorithms. Tech Rep - Max Planck Inst Biol Cybern. 2010;193.
230. Minka TP. Automatic Choice of Dimensionality for PCA. In: Leen TK, Dietterich TG, Tresp

- V, editors. *Advances in Neural Information Processing Systems 13* [Internet]. MIT Press; 2001. p. 598–604. Available from: <http://papers.nips.cc/paper/1853-automatic-choice-of-dimensionality-for-pca.pdf>
231. Tipping ME, Bishop CM. Probabilistic Principal Component Analysis. *J R Stat Soc Ser B (Statistical Methodol* [Internet]. 1999 Aug;61(3):611–22. Available from: <http://doi.wiley.com/10.1111/1467-9868.00196>
 232. Zhang Z, Zha H. Principal Manifolds and Nonlinear Dimension Reduction via Local Tangent Space Alignment. *SIAM J Sci Comput*. 2002;26:313–38.
 233. Davison AC, Hinkley D V. *Bootstrap methods and their application* [Internet]. Cambridge: Cambridge University Press; 1997. Available from: <http://ebooks.cambridge.org/ref/id/CBO9780511802843>
 234. Efron B. Second Thoughts on the Bootstrap. *Stat Sci*. 2003;18(2):135–40.
 235. Wang R, Tang K. Feature Selection for Maximizing the Area Under the ROC Curve. In: *2009 IEEE International Conference on Data Mining Workshops* [Internet]. IEEE; 2009. p. 400–5. Available from: <http://ieeexplore.ieee.org/document/5360438/>
 236. Xuan G, Zhu X, Chai P, Zhang Z, Shi YQ, Fu D. Feature Selection Based on the Bhattacharyya Distance. In: *Proceedings of the 18th International Conference on Pattern Recognition - Volume 03* [Internet]. Washington, DC, USA: IEEE Computer Society; 2006. p. 1232–5. (ICPR '06). Available from: <http://dx.doi.org/10.1109/ICPR.2006.558>
 237. Christin C, Hoefsloot HCJ, Smilde AK, Hoekman B, Suits F, Bischoff R, et al. A Critical Assessment of Feature Selection Methods for Biomarker Discovery in Clinical Proteomics. *Mol Cell Proteomics* [Internet]. 2013 Jan;12(1):263–76. Available from: <http://www.mcponline.org/lookup/doi/10.1074/mcp.M112.022566>
 238. Auffarth B, Lopez M, Cerquides J. Comparison of Redundancy and Relevance Measures for Feature Selection in Tissue Classification of CT images. 2010.
 239. Manning CD, Raghavan P, Schütze H. *Introduction to Information Retrieval* [Internet]. Cambridge: Cambridge University Press; 2008. Available from: <http://ebooks.cambridge.org/ref/id/CBO9780511809071>
 240. Ververidis D, Kotropoulos C. Fast and accurate sequential floating forward feature selection with the Bayes classifier applied to speech emotion recognition. *Signal Processing* [Internet]. 2008 Dec;88(12):2956–70. Available from: <https://linkinghub.elsevier.com/retrieve/pii/S0165168408002120>
 241. Guyon I, Weston J, Barnhill S, Vapnik V. Gene Selection for Cancer Classification using Support Vector Machines. *Mach Learn* [Internet]. 2002;46(1):389–422. Available from: <https://doi.org/10.1023/A:1012487302797>
 242. Tin Kam Ho. Random decision forests. In: *Proceedings of 3rd International Conference on Document Analysis and Recognition* [Internet]. IEEE Comput. Soc. Press; 1995. p. 278–82. Available from: <http://ieeexplore.ieee.org/document/598994/>
 243. Chow C, Liu C. Approximating discrete probability distributions with dependence trees. *IEEE Trans Inf Theory* [Internet]. 1968 May;14(3):462–7. Available from: <http://ieeexplore.ieee.org/document/1054142/>
 244. Kira K, Rendell LA. A Practical Approach to Feature Selection. In: *Machine Learning Proceedings 1992* [Internet]. Elsevier; 1992. p. 249–56. Available from:

<https://linkinghub.elsevier.com/retrieve/pii/B9781558602472500371>

245. Burnett M. Blocking Brute Force Attacks [Internet]. UVA Computer Science, University of Virginia (UVA).; 2007. Available from: http://www.cs.virginia.edu/~cadmin/gen_support/brute_force.php
246. Pedregosa F, Varoquaux G, Gramfort A, Michel V, Thirion B, Grisel O, et al. Scikit-learn: Machine Learning in Python. *J Mach Learn Res* [Internet]. JMLR.org; 2011;12:2825–30. Available from: <http://dl.acm.org/citation.cfm?id=1953048.2078195>
247. Hanchuan Peng, Fuhui Long, Ding C. Feature selection based on mutual information criteria of max-dependency, max-relevance, and min-redundancy. *IEEE Trans Pattern Anal Mach Intell* [Internet]. 2005 Aug;27(8):1226–38. Available from: <http://ieeexplore.ieee.org/document/1453511/>
248. Zou H, Hastie T. Regularization and variable selection via the elastic net. *J R Stat Soc Ser B (Statistical Methodol)* [Internet]. 2005 Apr;67(2):301–20. Available from: <http://doi.wiley.com/10.1111/j.1467-9868.2005.00503.x>
249. Rodríguez-Girondo M, Salo P, Burzykowski T, Perola M, Houwing-Duistermaat J, Mertens B. Sequential double cross-validation for assessment of added predictive ability in high-dimensional omic applications. 2016 Jan 29; Available from: <http://arxiv.org/abs/1601.08197>
250. Efron B, Tibshirani R. *An Introduction to the Bootstrap*. Macmillan Publishers Limited. All rights reserved; 1993.
251. Kohavi R. A Study of Cross-Validation and Bootstrap for Accuracy Estimation and Model Selection. In Morgan Kaufmann; 1995. p. 1137–43.
252. Berx G, van Roy F. Involvement of Members of the Cadherin Superfamily in Cancer. *Cold Spring Harb Perspect Biol* [Internet]. 2009 Dec 1;1(6):a003129–a003129. Available from: <http://cshperspectives.cshlp.org/lookup/doi/10.1101/cshperspect.a003129>
253. Puig-Domingo M, Gil J, Sampedro Nuñez M, Jordà M, Webb SM, Serra G, et al. Molecular profiling for acromegaly treatment: a validation study. *Endocr Relat Cancer* [Internet]. 2020 Apr; Available from: <https://erc.bioscientifica.com/view/journals/erc/aop/erc-18-0565/erc-18-0565.xml>
254. Pastushenko I, Blanpain C. EMT Transition States during Tumor Progression and Metastasis. *Trends Cell Biol* [Internet]. 2019 Mar;29(3):212–26. Available from: <https://linkinghub.elsevier.com/retrieve/pii/S0962892418302010>
255. Lamouille S, Xu J, Derynck R. Molecular mechanisms of epithelial–mesenchymal transition. *Nat Rev Mol Cell Biol* [Internet]. 2014 Mar 21;15(3):178–96. Available from: <http://www.nature.com/articles/nrm3758>
256. Puig-Domingo M, Gil J, Sampedro M, Webb SM, Serra G, Salinas I, et al. Molecular profiling for assistance to pharmacological treatment of acromegaly. *Endocr Abstr* [Internet]. 2018 May 8; Available from: <http://www.endocrine-abstracts.org/ea/0056/ea0056oc13.3.htm>
257. Rotondo F, Di Ieva A, Kovacs K, Cusimano MD, Syro L V, Diamandis EP, et al. Human kallikrein 10 in surgically removed human pituitary adenomas. *Hormones (Athens)* [Internet]. 2014;14(2):272–9. Available from: <http://www.ncbi.nlm.nih.gov/pubmed/25553760>

258. Liu W, Xie L, He M, Shen M, Zhu J, Yang Y, et al. Expression of Somatostatin Receptor 2 in Somatotropinoma Correlated with the Short-Term Efficacy of Somatostatin Analogues. *Int J Endocrinol* [Internet]. 2017;2017:9606985. Available from: <http://www.ncbi.nlm.nih.gov/pubmed/28396686>
259. Hunter P. The reproducibility “crisis.” *EMBO Rep* [Internet]. 2017 Sep 9;18(9):1493–6. Available from: <https://onlinelibrary.wiley.com/doi/abs/10.15252/embr.201744876>
260. Pfaffl MW. A new mathematical model for relative quantification in real-time RT-PCR. *Nucleic Acids Res* [Internet]. 2001 May 1;29(9):45e–45. Available from: <https://academic.oup.com/nar/article-lookup/doi/10.1093/nar/29.9.e45>
261. Yoshida S, Kato T, Kato Y. EMT Involved in Migration of Stem/Progenitor Cells for Pituitary Development and Regeneration. *J Clin Med* [Internet]. 2016 Apr 6;5(4):43. Available from: <http://www.mdpi.com/2077-0383/5/4/43>
262. Pérez Millán MI, Brinkmeier ML, Mortensen AH, Camper SA. PROP1 triggers epithelial-mesenchymal transition-like process in pituitary stem cells. *Elife* [Internet]. 2016 Jun 28;5. Available from: <https://elifesciences.org/articles/14470>
263. Brabletz T, Kalluri R, Nieto MA, Weinberg RA. EMT in cancer. *Nat Rev Cancer* [Internet]. 2018 Feb 12;18(2):128–34. Available from: <http://www.nature.com/articles/nrc.2017.118>
264. Jia W, Zhu J, Martin TA, Jiang A, Sanders AJ, Jiang WG. Epithelial-mesenchymal Transition (EMT) Markers in Human Pituitary Adenomas Indicate a Clinical Course. *Anticancer Res* [Internet]. 2015 May;35(5):2635–43. Available from: <http://www.ncbi.nlm.nih.gov/pubmed/25964539>
265. Evang JA, Berg JP, Casar-Borota O, Lekva T, Kringen MK, Ramm-Pettersen J, et al. Reduced levels of E-cadherin correlate with progression of corticotroph pituitary tumours. *Clin Endocrinol (Oxf)* [Internet]. 2011 Dec;75(6):811–8. Available from: <http://doi.wiley.com/10.1111/j.1365-2265.2011.04109.x>
266. Qian ZR, Sano T, Yoshimoto K, Asa SL, Yamada S, Mizusawa N, et al. Tumor-specific downregulation and methylation of the CDH13 (H-cadherin) and CDH1 (E-cadherin) genes correlate with aggressiveness of human pituitary adenomas. *Mod Pathol* [Internet]. 2007 Dec 14;20(12):1269–77. Available from: <http://www.nature.com/articles/3800965>
267. Sano T, Rong QZ, Kagawa N, Yamada S. Down-Regulation of E-Cadherin and Catenins in Human Pituitary Growth Hormone-Producing Adenomas. In: *Molecular Pathology of the Pituitary* [Internet]. Basel: KARGER; 2004. p. 127–32. Available from: <https://www.karger.com/Article/FullText/79041>
268. Zhou Y, Zhang X, Klibanski A. Genetic and epigenetic mutations of tumor suppressive genes in sporadic pituitary adenoma. *Mol Cell Endocrinol* [Internet]. 2014 Apr;386(1–2):16–33. Available from: <https://linkinghub.elsevier.com/retrieve/pii/S0303720713003687>
269. Warnecke PM, Stirzaker C, Song J, Grunau C, Melki JR, Clark SJ. Identification and resolution of artifacts in bisulfite sequencing. *Methods* [Internet]. 2002 Jun;27(2):101–7. Available from: <https://linkinghub.elsevier.com/retrieve/pii/S1046202302000609>
270. Yang J, Antin P, Berx G, Blanpain C, Brabletz T, Bronner M, et al. Guidelines and definitions for research on epithelial–mesenchymal transition. *Nat Rev Mol Cell Biol* [Internet]. 2020

Apr 16; Available from: <http://www.nature.com/articles/s41580-020-0237-9>

271. Wang Y, Shi J, Chai K, Ying X, Zhou BP. The Role of Snail in EMT and Tumorigenesis. *Curr Cancer Drug Targets* [Internet]. 2013 Nov;13(9):963–72. Available from: <http://www.ncbi.nlm.nih.gov/pubmed/24168186>
272. Sun, Z; Unutmaz, D; Zou YR; Sunshine, MJ; Pierani, A; Brenner-Morton, S; Mebius, RE; Littman D. Requirement for ROR γ in Thymocyte Survival and Lymphoid Organ Development. *Science* (80-) [Internet]. 2000 Jun 30;288(5475):2369–73. Available from: <https://www.sciencemag.org/lookup/doi/10.1126/science.288.5475.2369>
273. Eberl G, Marmon S, Sunshine M-J, Rennert PD, Choi Y, Littman DR. An essential function for the nuclear receptor ROR γ t in the generation of fetal lymphoid tissue inducer cells. *Nat Immunol* [Internet]. 2004 Jan 21;5(1):64–73. Available from: <http://www.nature.com/articles/ni1022>
274. Akashi M, Takumi T. The orphan nuclear receptor ROR α regulates circadian transcription of the mammalian core-clock Bmal1. *Nat Struct Mol Biol* [Internet]. 2005 May 10;12(5):441–8. Available from: <http://www.nature.com/articles/nsmb925>
275. Ortiz MA, Piedrafita FJ, Pfahl M, Maki R. TOR: a new orphan receptor expressed in the thymus that can modulate retinoid and thyroid hormone signals. *Mol Endocrinol* [Internet]. 1995 Dec;9(12):1679–91. Available from: <https://academic.oup.com/mend/article-lookup/doi/10.1210/mend.9.12.8614404>
276. Cai D, Wang J, Gao B, Li J, Wu F, Zou JX, et al. ROR γ is a targetable master regulator of cholesterol biosynthesis in a cancer subtype. *Nat Commun* [Internet]. 2019 Dec 11;10(1):4621. Available from: <http://www.nature.com/articles/s41467-019-12529-3>
277. Kim SM, Choi JE, Hur W, Kim J-H, Hong SW, Lee EB, et al. RAR-Related Orphan Receptor Gamma (ROR- γ) Mediates Epithelial-Mesenchymal Transition Of Hepatocytes During Hepatic Fibrosis. *J Cell Biochem* [Internet]. 2017 Aug;118(8):2026–36. Available from: <http://doi.wiley.com/10.1002/jcb.25776>
278. Silverstein JM, Roe ED, Munir KM, Fox JL, Emir B, Kouznetsova M, et al. USE OF ELECTRONIC HEALTH RECORDS TO CHARACTERIZE A RARE DISEASE IN THE U.S.: TREATMENT, COMORBIDITIES, AND FOLLOW-UP TRENDS AMONG PATIENTS WITH A CONFIRMED DIAGNOSIS OF ACROMEGALY. *Endocr Pract* [Internet]. 2018 Jun;24(6):517–26. Available from: <http://www.ncbi.nlm.nih.gov/pubmed/29624099>
279. Mete O, Asa SL. Structure, Function, and Morphology in the Classification of Pituitary Neuroendocrine Tumors: the Importance of Routine Analysis of Pituitary Transcription Factors. *Endocr Pathol* [Internet]. 2020 Aug 19; Available from: <http://link.springer.com/10.1007/s12022-020-09646-x>
280. Colao A, Bronstein MD, Brue T, De Marinis L, Fleseriu M, Guitelman M, et al. Pasireotide for acromegaly: long-term outcomes from an extension to the Phase III PAOLA study. *Eur J Endocrinol*. 2020 Jun;182(6):583.
281. Bernabeu I, Marazuela M. Pegvisomant: balance de 10 años. *Endocrinol y Nutr*. 2015 Oct;62(8):363–5.

10. Annex

10.1 Supplementary Tables

Supplementary Table S1

All the significant predictive models found using the whole cohort for the analysis based on 1, 2 or 3 features

Number of features	Variables Names	CR+PR vs NR		CR vs NR		PR vs NR		CR vs PR	
		crosVal-Balanced ACC	crosVal-pValue	crosVal-Balanced ACC	crosVal-pValue	crosVal-Balanced ACC	crosVal-pValue	crosVal-Balanced ACC	crosVal-pValue
1	E-cadherin	62.61%	0.027	73.08%	0.001	-	-	65.84%	0.028
1	GHRL	67.26%	0.002	-	-	-	-	-	-
1	PEBP1	-	-	-	-	-	-	69.68%	0.004
1	DRD2 long isoform	-	-	69.23%	0.006	-	-	-	-
2	SSTR2 + AIP	62.25%	0.022	-	-	-	-	-	-
2	SSTR2 + SSTR5	62.25%	0.022	-	-	64.71%	0.006	-	-
2	E-cadherin + AIP	66.50%	0.002	75.00%	1.95E-04	-	-	-	-
2	SSTR2 + E-cadherin	69.95%	0.001	73.08%	0.001	-	-	-	-
2	PEBP1 + E-cadherin	-	-	71.15%	0.002	-	-	62.78%	0.028
2	SSTR5 + PEBP1	-	-	-	-	-	-	68.67%	0.004
2	E-cadherin + IN1GHRL	-	-	69.23%	0.006	-	-	68.78%	0.011
2	PLAGL1 + E-cadherin	-	-	73.08%	0.001	-	-	-	-
2	SSTR2 + Ki-67	-	-	-	-	67.87%	0.020	-	-
2	SSTR2 + ARRB1	-	-	-	-	67.76%	0.012	-	-
2	SSTR2 + IN1GHRL	-	-	63.46%	0.037	67.65%	0.002	-	-
3	ARRB1 + PLAGL1 + E-cadherin	63.42%	0.011	-	-	-	-	-	-
3	SSTR2 + PEBP1 + E-cadherin	66.46%	0.006	63.46%	0.047	-	-	-	-
3	SSTR2 + E-cadherin + AIP	67.26%	0.002	75.00%	1.95E-04	-	-	-	-
3	SSTR2 + SSTR5 + E-cadherin	68.02%	0.002	-	-	-	-	-	-
3	SSTR2 + DRD2short + E-cadherin	68.38%	0.002	-	-	-	-	-	-
3	SSTR5 + ARRB1 + PEBP1	-	-	-	-	-	-	64.82%	0.031
3	PEBP1 + E-cadherin + IN1GHRL	-	-	-	-	-	-	67.76%	0.012
3	PLAGL1 + PEBP1 + E-cadherin	-	-	67.31%	0.008	-	-	-	-
3	DRD2 short isoform + PEBP1 + E-cadherin	-	-	69.23%	0.004	-	-	-	-
3	DRD2 short and long isoform + E-cadherin	-	-	71.15%	0.002	-	-	-	-
3	SSTR2 + CDH1Ecad + IN1GHRL	-	-	75.00%	0.000	-	-	-	-
3	SSTR2 + SSTR5 + ARRB1	-	-	-	-	69.68%	0.004	-	-
3	SSTR2 + SSTR5 + PEBP1	-	-	-	-	67.76%	0.012	65.72%	0.011
3	SSTR2 + SSTR5 + DRD2 short isoform	-	-	-	-	63.80%	0.031	-	-
3	SSTR5 + ARRB1 + Ki-67	-	-	-	-	63.80%	0.031	-	-
3	SSTR2 + SSTR5 + IN1GHRL	-	-	-	-	62.78%	0.028	-	-

Supplementary Table S2

Cohort description: Number of patients for every comparison analyzed.

Population description			SRL response			
			CR	PR	CR+PR	NR
General population			26	17	43	26
Fragmented population	<i>Presurgical SRL</i>	NO	6	3	9	7
		YES	20	13	33	19
	<i>Extrasellar Growth</i>	NO	12	6	18	1
		YES	11	9	20	19
	<i>Sinus Invasion</i>	NO	18	8	26	7
		YES	5	7	12	10
	<i>Gender</i>	Female	14	11	25	10
		Male	12	6	18	16
	<i>GNAS</i>	WT	10	9	19	14
		Mutated	5	5	10	5

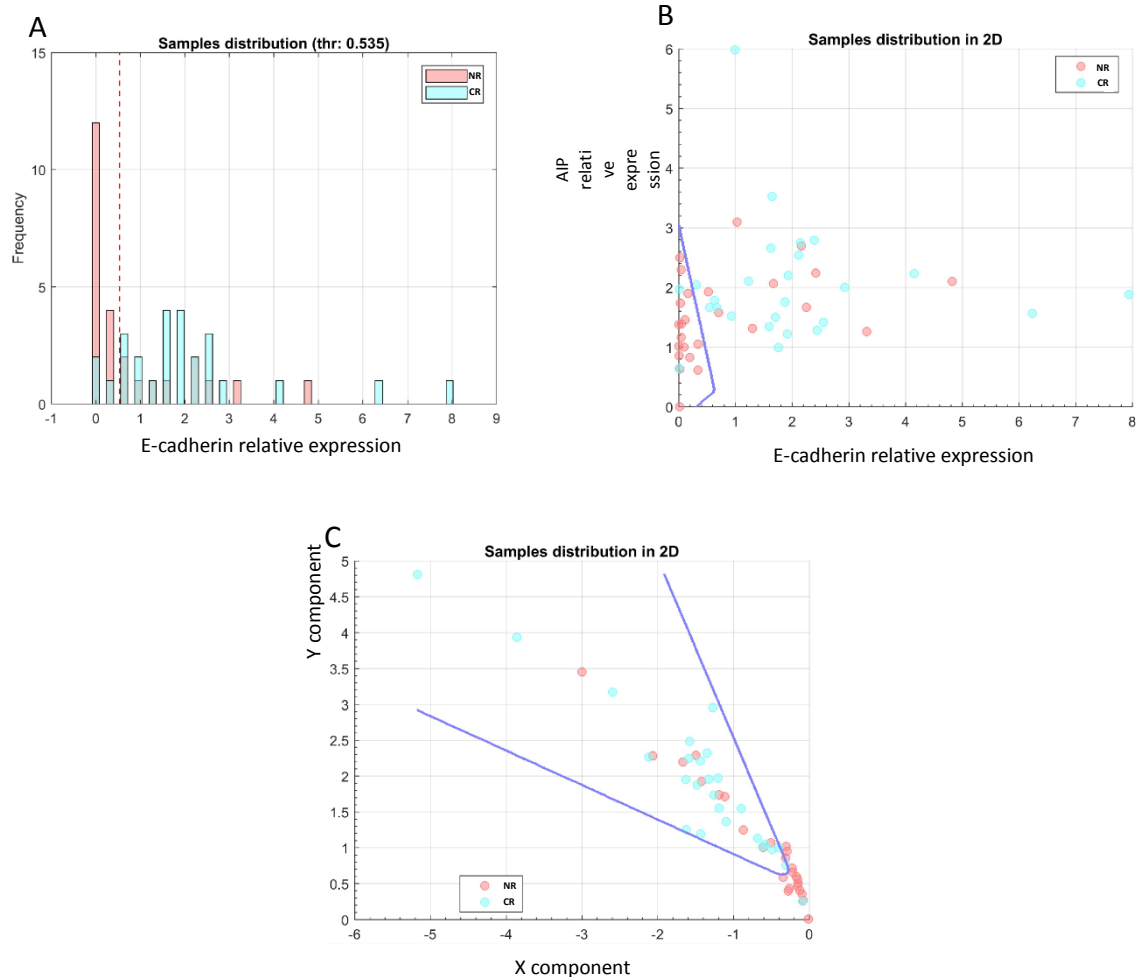
Supplementary Table S3

All the significant predictive models found using the fragmented populations for the analysis

Number of features	Fragmentation subgroup	Variables Names	CR +PR vs NR		CR vs NR		PR vs NR		CR vs PR	
			crosVal-Balanced ACC	crosVal-pValue	crosVal-Balanced ACC	crosVal-pValue	crosVal-Balanced ACC	crosVal-pValue	crosVal-Balanced ACC	crosVal-pValue
3	NO SRL PRESURGERY	PLAGL1 + PEBP1 + E-cadherin	88.89%	0.003	100.00%	0.001	-	-	-	-
2	NO SRL PRESURGERY	SSTR2 + E-cadherin	-	-	-	-	-	-	100.00%	0.012
3	NO SRL PRESURGERY	Age + SSTR2 + E-cadherin	-	-	100.00%	0.001	-	-	-	-
2	NO SRL PRESURGERY	Age + SSTR2	-	-	92.86%	0.004	-	-	-	-
3	NO SRL PRESURGERY	Age + SSTR2 + SSTR5	-	-	92.86%	0.004	-	-	-	-
3	SRL PRESURGERY	SSTR5 + DRD2 long isoform + E-cadherin	70.65%	0.001	-	-	-	-	-	-
2	SRL PRESURGERY	PEBP1 + IN1GHRL	-	-	-	-	-	-	76.92%	0.000
1	SRL PRESURGERY	PEBP1	-	-	-	-	-	-	73.08%	0.002
2	SRL PRESURGERY	PEBP1 + AIP	-	-	-	-	-	-	73.27%	0.008
2	SRL PRESURGERY	SSTR5 + AIP	-	-	-	-	-	-	69.23%	0.005
2	SRL PRESURGERY	SSTR5 + PEBP1	-	-	-	-	74.29%	0.003	70.58%	0.008
3	SRL PRESURGERY	SSTR2 + PEBP1 + IN1GHRL	-	-	-	-	-	-	70.58%	0.008
3	SRL PRESURGERY	PLAGL1 + E-cadherin + IN1GHRL	-	-	76.97%	0.001	-	-	-	-
2	SRL PRESURGERY	DRD2 long isoform + E-cadherin	-	-	71.32%	0.005	-	-	-	-
2	SRL PRESURGERY	PLAGL1 + E-cadherin	-	-	72.11%	0.005	-	-	-	-
3	SRL PRESURGERY	DRD2 short and long isoform + PLAGL1	-	-	71.97%	0.007	-	-	-	-
2	NO EXTRASELLAR GROWTH	SSTR5 + PEBP1	-	-	-	-	-	-	87.50%	0.004
1	EXTRASELLAR GROWTH	GHRL	71.32%	0.005	-	-	-	-	-	-
3	EXTRASELLAR GROWTH	SSTR5 + E-cadherin + IN1GHRL	-	-	-	-	-	-	79.80%	0.012
3	EXTRASELLAR GROWTH	SSTR2 + GHRL + IN1GHRL	-	-	70.10%	0.016	-	-	-	-
3	EXTRASELLAR GROWTH	Age + SSTR2 + ARRB1	-	-	-	-	72.22%	0.006	-	-
2	EXTRASELLAR GROWTH	SSTR2 + ARRB1	-	-	-	-	72.22%	0.006	-	-
1	NO SINUS INVASION	E-cadherin	69.51%	0.023	-	-	-	-	-	-
1	NO SINUS INVASION	SSTR2	69.51%	0.023	-	-	-	-	-	-
3	NO SINUS INVASION	SSTR2 + ARRB1 + KLK10	-	-	81.75%	0.007	-	-	-	-
3	NO SINUS INVASION	SSTR2 + PEBP1 + E-cadherin	-	-	-	-	-	-	72.22%	0.020

Number of features	Fragmentation subgroup	Variables Names	CR +PR vs NR		CR vs NR		PR vs NR		CR vs PR	
			crosVal-Balanced ACC	crosVal-pValue	crosVal-Balanced ACC	crosVal-pValue	crosVal-Balanced ACC	crosVal-pValue	crosVal-Balanced ACC	crosVal-pValue
2	NO SINUS INVASION	Ki-67 + IN1GHRL	-	-	-	-	85.71%	0.007	-	-
3	NO SINUS INVASION	Age + Ki-67 + IN1GHRL	-	-	-	-	85.71%	0.007	-	-
3	NO SINUS INVASION	SSTR2 + IN1GHRL + KLK10	-	-	-	-	86.61%	0.009	-	-
1	SINUS INVASION	AIP	77.50%	0.015	-	-	-	-	-	-
3	SINUS INVASION	PEBP1 + IN1GHRL + AIP	-	-	85.00%	0.017	-	-	-	-
2	FEMALES	PEBP1 + GHRL	73.78%	0.74%	-	-	-	-	-	-
2	FEMALES	SSTR2 + PEBP1	-	-	-	-	-	-	74.68%	0.016
3	FEMALES	PEBP1 + E-cadherin + AIP	-	-	79.76%	0.005	-	-	-	-
3	FEMALES	SSTR2 + ARRB1 + PLAGL1	-	-	-	-	85.35%	0.003	-	-
3	FEMALES	SSTR2 + PLAGL1 + GHRL	-	-	-	-	85.35%	0.003	-	-
3	FEMALES	SSTR2 + SSTR5 + PLAGL1	-	-	-	-	84.34%	0.003	-	-
2	MALES	Age + E-cadherin	80.83%	0.08%	81.82%	0.001	-	-	-	-
2	MALES	PLAGL1 + E-cadherin	77.29%	0.31%	-	-	-	-	-	-
3	MALES	DRD2 short and long isoforms + E-cadherin	-	-	-	-	-	-	80.00%	0.018
3	MALES	Age + PLAGL1 + E-cadherin	-	-	85.45%	0.000	-	-	-	-
2	MALES	ARRB1 + E-cadherin	-	-	80.91%	0.003	-	-	-	-
2	MALES	E-cadherin + IN1GHRL	-	-	79.70%	0.003	-	-	-	-
3	MALES	ARRB1 + E-cadherin + IN1GHRL	-	-	77.58%	0.008	-	-	-	-
3	GNAS WT	SSTR2 + DRD2 long isoform + ARRB1	77.07%	0.25%	-	-	-	-	-	-
2	GNAS WT	PEBP1 + E-cadherin + AIP	-	-	-	-	-	-	84.44%	0.004
3	GNAS WT	SSTR2 + PEBP1 + E-cadherin	-	-	-	-	-	-	83.89%	0.005
3	GNAS WT	SSTR5 + E-cadherin + Ki-67	-	-	-	-	-	-	84.44%	0.004
2	GNAS WT	DRD2 long isoform + ARRB1	-	-	71.43%	0.028	-	-	-	-
2	GNAS WT	SSTR2 + DRD2 long isoform	-	-	71.43%	0.028	-	-	-	-
3	GNAS WT	Age + SSTR2 + SSTR5	-	-	71.43%	0.028	-	-	-	-
3	GNAS WT	SSTR2 + DRD2 long isoform + IN1GHRL	-	-	71.43%	0.028	-	-	-	-
2	GNAS WT	SSTR5 + ARRB1	-	-	-	-	72.22%	0.014	-	-
3	GNAS MUT	PLAGL1 + E-cadherin + Ki-67	-	-	90.00%	0.024	-	-	-	-

Supplementary Figure S1



Supplementary Figure S2. Representation of different possible models resulting from the data mining analysis in the whole cohort. (A) Sampling distribution graph representing the distribution of CR and NR patients for E-cadherin expression. When the classifier contains only one variable we used a variable brute force technique. The discriminant function is a constant that is determined as the threshold value that separates samples from the two groups with the best accuracy (marked by dotted red line). (B) Sampling distribution graph in 2D representing the distribution of CR and NR patients for the expression of *AIP* and E-cadherin. The blue line is the mathematical function defined by the values of the classifier, a mathematical function that separates NR from CR patients. As this classifier is composed of two variables, each dimension of the graph stands for one variable. The variables were selected by the Lasso method and the model performed according to Multilayer perceptron (MLP) methodology. (C) Sampling distribution graph in 2D representing the distribution of CR and NR patients for the expression of *SSTR2*, E-cadherin and *AIP*. As this classifier is composed of more than two variables, each dimension of the graph stands for the two main components after performing a principal component analysis (PCA). The blue line is the mathematical function that separates CR from NR patients. The variables were selected by the Wilcoxon method and the model performed according to Multilayer perceptron (MLP) methodology.

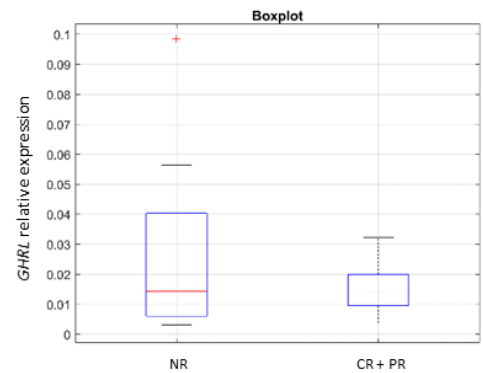
Supplementary Figure S2

A

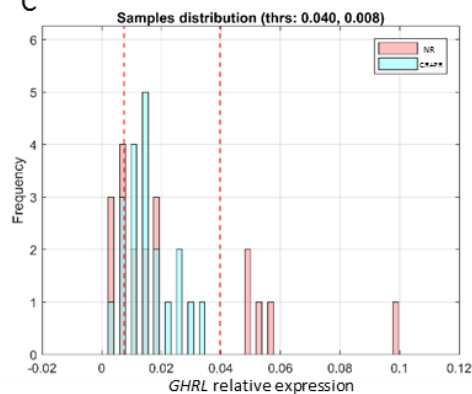
Selected Strategy

Feature Selection Method	One variable brute force
Base classifier	Optimal quadratic
Ensemble	<i>Not applied</i>
Cost function	Balanced accuracy
Validation	10 K-fold

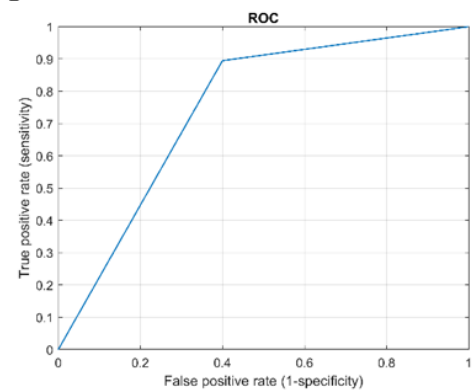
B



C



D



E

Samples separability test: Cross-validated

ACC	ACC p-value	TP	TN	FP	FN	PRE	SNS	SPC	Balanced ACC
71.79%	0.005	18	10	9	2	66.67	90.00	52.63	0.71

Samples separability test: without cross-validation

ACC	ACC p-value	TP	TN	FP	FN	PRE	SNS	SPC	Balanced ACC
76.92%	0.001	18	12	7	2	72.00	90.00	63.16	0.77

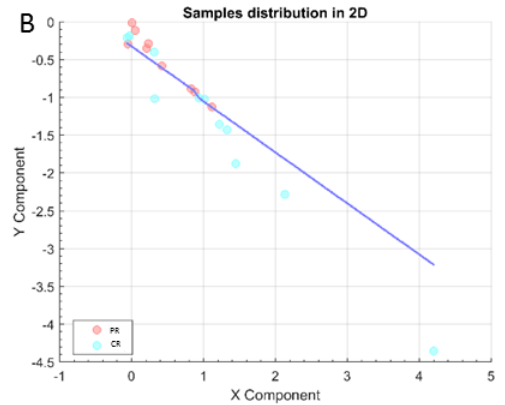
Supplementary Figure S2. GHRL model that discriminates between NR and CR+PR in patients with extrasellar growth. GHRL allowed the classification between NR and CR+PR in patients with extrasellar extension from our dataset. The details of the model subprocesses are presented in the table (A). The boxplot shows that there is not difference in the medians of GHRL expression ($p=0.92$) between NR and CR+PR patients but the distribution in each population is different (B), as we can clearly observe in the distribution graph of the samples (the dotted red lines indicates the best accuracy thresholds) (C). The Receiver Operating Characteristic (ROC) illustrates the performance of a our model as its discrimination threshold varies (D). Finally, the tables showing the performance in the sample separability tests allows for a clear evaluation of the model performing (E). Abbreviations: ACC (Accuracy), TP (True positives), TN (True negative), FP (False positive), FN (False Negative), PRE (Precision), SNS (Sensitivity), SPC (Specificity).

Supplementary Figure S3

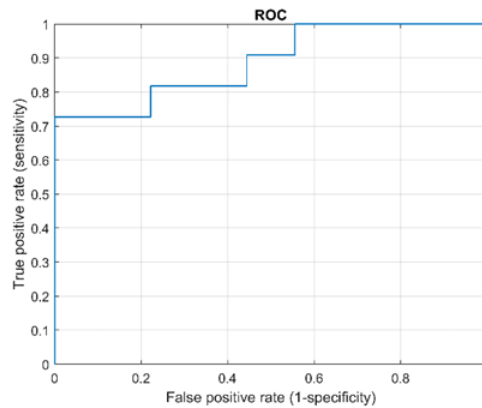
A

Selected Strategy

Feature Selection Method	Lasso
Base classifier	Generalized linear method (Binomial)
Ensemble	<i>Not applied</i>
Cost function	Balanced accuracy
Validation	10 K-fold



C



D

Samples separability test: Cross-validated

ACC	ACC p-value	TP	TN	FP	FN	PRE	SNS	SPC	Balanced ACC
80.00%	0.012	9	7	2	2	81.82	81.82	77.78	0.80

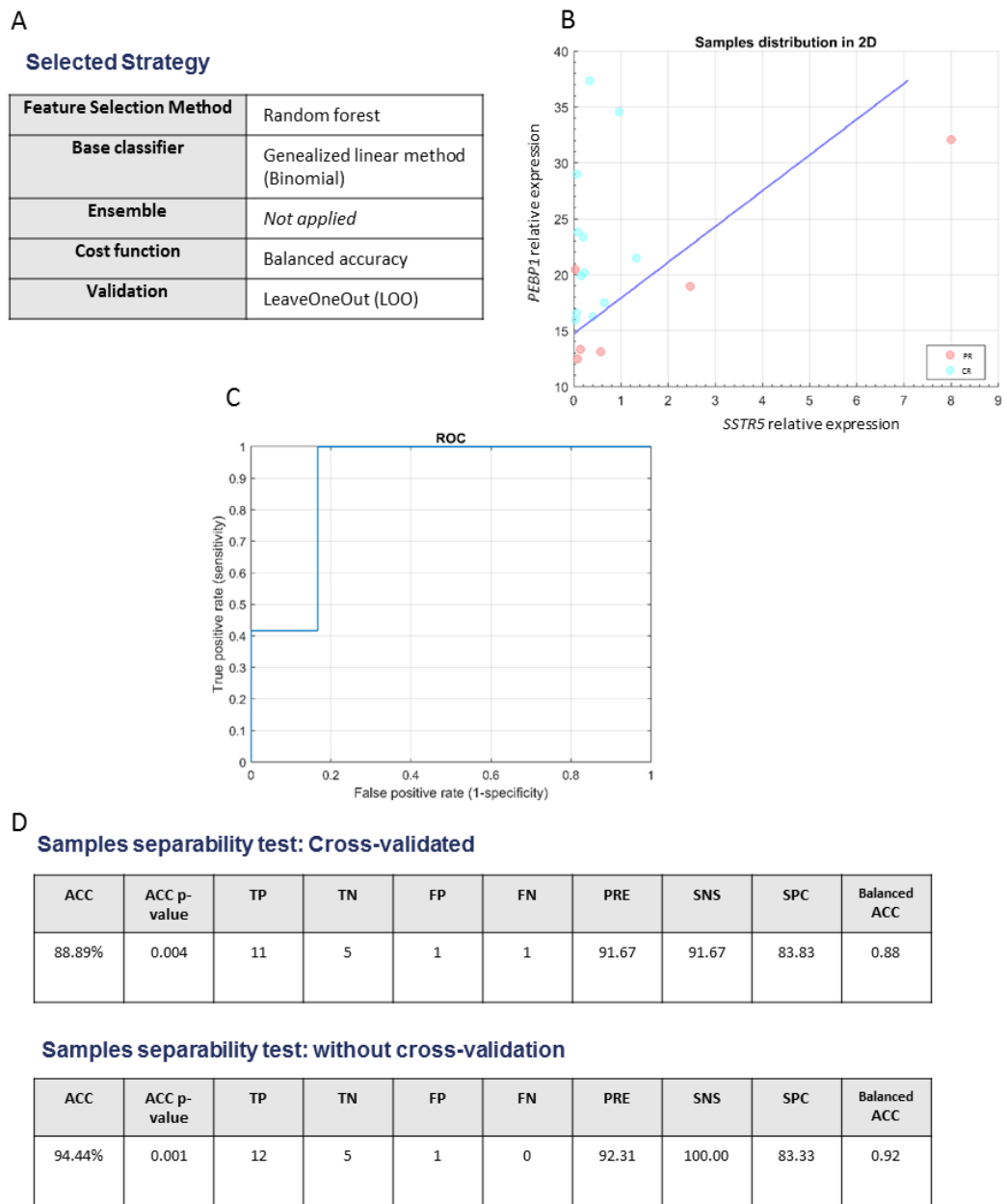
Samples separability test: without cross-validation

ACC	ACC p-value	TP	TN	FP	FN	PRE	SNS	SPC	Balanced ACC
75.00%	0.035	8	7	2	3	80.00	72.73	77.78	0.75

Supplementary Figure S3. E-cadherin + *SSTR5* + IN1-GHRL model that discriminates between CR and PR in patients with extrasellar growth. *E-cadherin*, *SSTR5* and *In1-GHRL* allowed the classification between PR and CR in patients with extrasellar extension in our dataset. The details of the model subprocesses are presented in the table (A). The graph represents the distribution of the samples in a 2D plot. The blue line is the mathematical function defined by the values of the classifier. X and Y components are obtained by means a Dimensionality Reduction Process (B). The Receiver Operating Characteristic (ROC) illustrates the performance of a our model as its discrimination threshold varies (C). Finally, the tables showing the performance in the sample separability tests allows for a clear evaluation of the model performing (D).

Abreviations: ACC (Accuracy), TP (True positives), TN (True negative), FP (False positive), FN (False Negative), PRE (Precision), SNS (Sensitivity), SPC (Specificity).

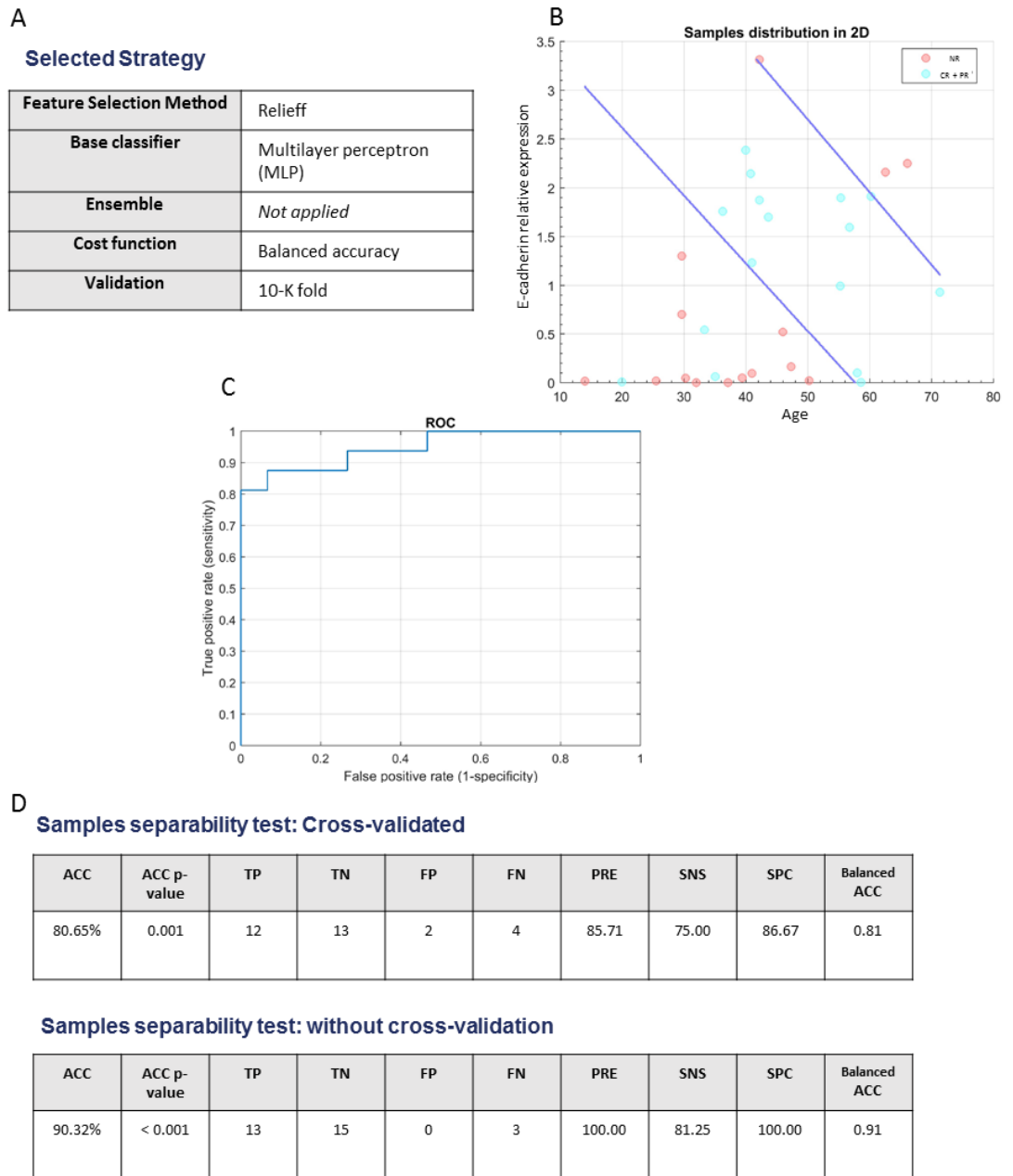
Supplementary Figure S4



Supplementary Figure S4. *SSTR5* + *PEBP1* model that discriminates between CR and PR in patients without extrasellar growth. *SSTR5* and *PEBP1* allowed the classification between PR and CR in patients without extrasellar extension in our dataset. The details of the model subprocesses are presented in the table (A). The graph represents the distribution of the samples in a 2D plot. The blue line is the mathematical function defined by the values of the classifier (B). The Receiver Operating Characteristic (ROC) illustrates the performance of our model as its discrimination threshold varies (C). Finally, the tables showing the performance in the sample separability tests allows for a clear evaluation of the model performing (D).

Abbreviations: ACC (Accuracy), TP (True positives), TN (True negative), FP (False positive), FN (False Negative), PRE (Precision), SNS (Sensitivity), SPC (Specificity).

Supplementary Figure S5



Supplementary Figure S5. Age + E-cadherin model that discriminates between NR and CR+PR in male patients. E-cadherin and the age of the patients allowed the classification between responders (CR + PR) and NR in male patients. The details of the model subprocesses are presented in the table (A). The graph represents the distribution of the samples in a 2D plot. The blue line is the mathematical function defined by the values of the classifier (B). The Receiver Operating Characteristic (ROC) illustrates the performance of our model as its discrimination threshold varies (C). Finally, the tables showing the performance in the sample separability tests allows for a clear evaluation of the model performing (D).

Abbreviations: ACC (Accuracy), TP (True positives), TN (True negative), FP (False positive), FN (False Negative), PRE (Precision), SNS (Sensitivity), SPC (Specificity).

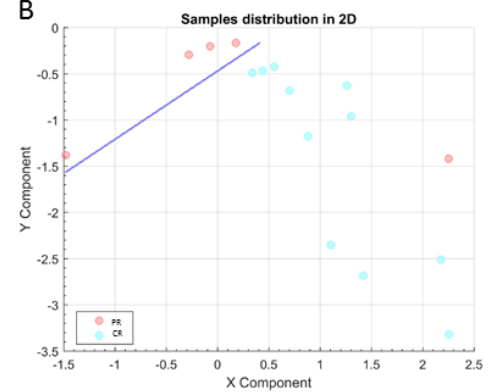
Supplementary Figure S6

A

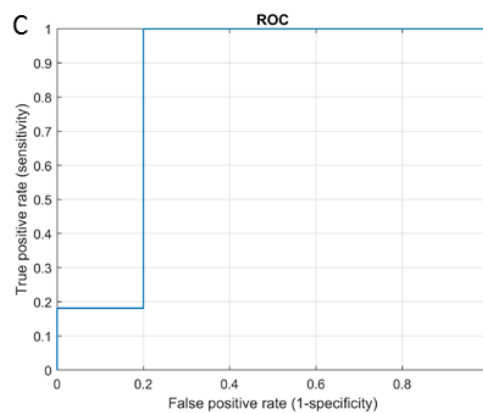
Selected Strategy

Feature Selection Method	Simple regression
Base classifier	Genealized linear method (Binomial)
Ensemble	<i>Not applied</i>
Cost function	Balanced accuracy
Validation	10 K-fold

B



C



D

Samples separability test: Cross-validated

ACC	ACC p-value	TP	TN	FP	FN	PRE	SNS	SPC	Balanced ACC
87.50%	0.018	11	3	2	0	84.62	100.00	60.00	0.80

Samples separability test: without cross-validation

ACC	ACC p-value	TP	TN	FP	FN	PRE	SNS	SPC	Balanced ACC
93.75%	0.003	11	4	1	0	91.67	100.00	80.00	0.90

Supplementary Figure S6. E-cadherin + DRD2 long and short isoform model that discriminates between CR and PR in male patients. *E-cadherin* and *DRD2* long and short isoform allowed the classification between PR and CR in male patients in our dataset. The details of the model subprocesses are presented in the table (A). The graph represents the distribution of the samples in a 2D plot. The blue line is the mathematical function defined by the values of the classifier. X and Y components are obtained by means a Dimensionality Reduction Process (B). The Receiver Operating Characteristic (ROC) illustrates the performance of a our model as its discrimination threshold varies (C). Finally, the tables showing the performance in the sample separability tests allows for a clear evaluation of the model performing (D).

Abbreviations: ACC (Accuracy), TP (True positives), TN (True negative), FP (False positive), FN (False Negative), PRE (Precision), SNS (Sensitivity), SPC (Specificity).

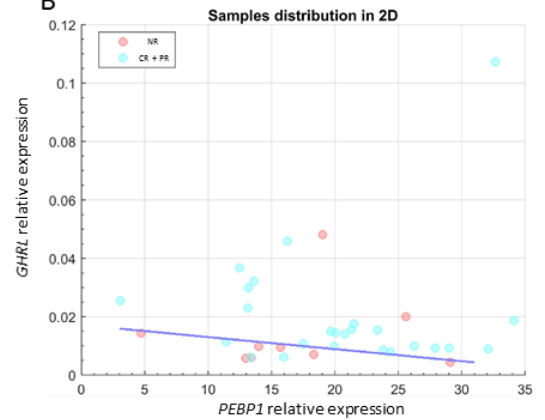
Supplementary Figure S7

A

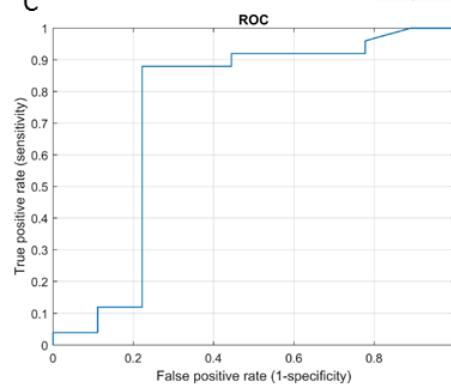
Selected Strategy

Feature Selection Method	Random generalized linear model
Base classifier	Multilayer perceptron (MLP)
Ensemble	<i>Not applied</i>
Cost function	Balanced accuracy
Validation	10 K-fold

B



C



D

Samples separability test: Cross-validated

ACC	ACC p-value	TP	TN	FP	FN	PRE	SNS	SPC	Balanced ACC
82.35%	0.007	23	5	4	2	85.19	92.00	55.65	0.74

Samples separability test: without cross-validation

ACC	ACC p-value	TP	TN	FP	FN	PRE	SNS	SPC	Balanced ACC
85.29%	0.001	22	7	2	3	91.67	88.00	77.78	0.83

Supplementary Figure S7. GHRL + PEBP1 model that discriminates between NR and CR+PR in female patients. GHRL and PEBP1 allowed the classification between responders (PR and CR) and NR in female patients. The details of the model subprocesses are presented in the table (A). The graph represents the distribution of the samples in a 2D plot. The blue line is the mathematical function defined by the values of the classifier (B). The Receiver Operating Characteristic (ROC) illustrates the performance of our model as its discrimination threshold varies (C). Finally, the tables showing the performance in the sample separability tests allows for a clear evaluation of the model performing (D).
 Abbreviations: ACC (Accuracy), TP (True positives), TN (True negative), FP (False positive), FN (False Negative), PRE (Precision), SNS (Sensitivity), SPC (Specificity).

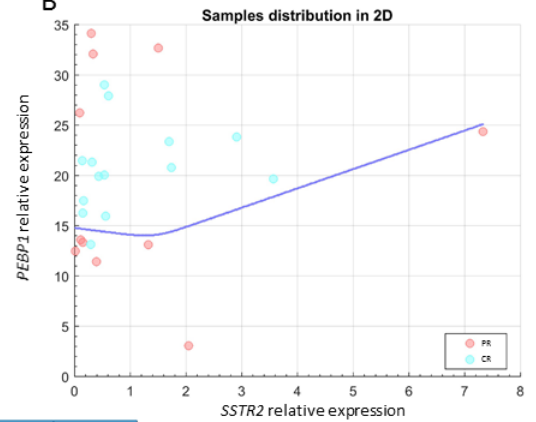
Supplementary Figure S8

A

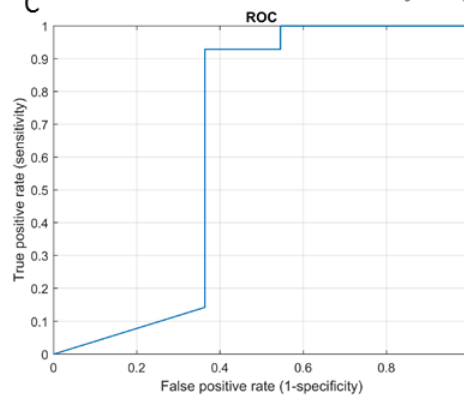
Selected Strategy

Feature Selection Method	Relieff
Base classifier	Multilayer perceptron (MLP)
Ensemble	<i>Not applied</i>
Cost function	Balanced accuracy
Validation	10 K-fold

B



C



D

Samples separability test: Cross-validated

ACC	ACC p-value	TP	TN	FP	FN	PRE	SNS	SPC	Balanced ACC
76.00%	0.016	12	7	4	2	75.00	85.71	63.64	0.75

Samples separability test: without cross-validation

ACC	ACC p-value	TP	TN	FP	FN	PRE	SNS	SPC	Balanced ACC
80.00%	0.004	13	7	4	1	76.47	92.86	63.64	0.78

Supplementary Figure S8. *SSTR2* + *PEBP1* model that discriminates between CR and PR in female patients. *SSTR2* and *PEBP1* allowed the classification between CR and PR in female patients. The details of the model subprocesses are presented in the table (A). The graph represents the distribution of the samples in a 2D plot. The blue line is the mathematical function defined by the values of the classifier (B). The Receiver Operating Characteristic (ROC) illustrates the performance of our model as its discrimination threshold varies (C). Finally, the tables showing the performance in the sample separability tests allows for a clear evaluation of the model performing (D).

Abbreviations: ACC (Accuracy), TP (True positives), TN (True negative), FP (False positive), FN (False Negative), PRE (Precision), SNS (Sensitivity), SPC (Specificity).

